https://doi.org/10.15388/vu.thesis.915
https://orcid.org/0000-0003-2082-8422

VILNIUS UNIVERSITY
STATE RESEARCH INSTITUTE CENTER FOR PHYSICAL SCIENCES AND TECHNOLOGY

Kasparas Kižys

Investigation of Bioelectrochemical Systems and Application in Yeast-Based Microbial Fuel Cells

DOCTORAL DISSERTATION

Natural Sciences,
Chemistry (N 003)

VILNIUS 2026

The dissertation was prepared from 2020 to 2025 at the State Research Institute, Center for Physical Sciences and Technology (lit. VMTI FTMC). The research was supported the by Research Council of Lithuania.

Scientific Supervisor – Dr. Inga Morkvėnaitė-Vilkončienė (VMTI Center For Physical Sciences And Technology, Natural Sciences Chemistry – N 003).
This doctoral dissertation will be defended in a public meeting of the

Dissertation Defence Panel:
Chairman – Prof. Habil. Dr. Rimantas Ramanauskas (State research institute Center for Physical Sciences and Technology, Natural Sciences, Chemistry – N 003).

Members:
Dr. Marcin Filipiak (Centre for Advanced Materials and Technologies CEZAMAT, Warsaw University of Technology, Warsaw, Natural Sciences, Chemistry – N 003);
Prof. dr. Jaunius Urbonavičius (Vilnius Gediminas technical university – Vilnius TECH, Natural Sciences, Chemistry – N 003);
Dr. Rokas Žalnėravičius (State research institute Center for Physical Sciences and Technology, Natural Sciences, Chemistry – N 003);
Dr. Šarūnas Žukauskas (State research institute Center for Physical Sciences and Technology, Natural Sciences, Chemistry – N 003).

The dissertation shall be defended at a public meeting of the Dissertation Defence Panel at 14:00 on 8th of May 2026 in lecture hall B128 at the State Research Institute, Center for Physical Sciences and Technology, Saulėtekio al. 3, Vilnius, Lithuania. Tel. +37061642060; kasparas.kizys@ftmc.lt

https://doi.org/10.15388/vu.thesis.915
https://orcid.org/0000-0003-2082-8422

VILNIAUS UNIVERSITETAS
VALSTYBINIS MOKSLINIŲ TYRIMŲ INSTITUTAS FIZINIŲ IR
TECHNOLOGIJOS MOKSLŲ CENTRAS

Kasparas Kižys

Bioelektrocheminių sistemų tyrimai ir taikymas mielių mikrobiniuose kuro elementuose

DAKTARO DISERTACIJA

Gamtos mokslo sritis,
Chemija (N 003)

VILNIUS 2026

Disertacija rengta 2020–2025 metais Valstybiniame mokslinių tyrimų institute Fizinių ir technologijos mokslų centre (VMTI FTMC). Mokslinius tyrimus rėmė Lietuvos mokslo taryba.

Mokslinė vadovė – dr. Inga Morkvėnaitė-Vilkončienė (VMTI Fizinių ir technologijos mokslų centras, gamtos moklsai, chemija – N 003).

Gynimo taryba:
Pirmininkas – prof. habil. dr. Rimantas Ramanauskas (Valstybinis mokslinių tyrimų institutas Fizinių ir technologijos mokslų centras, gamtos mokslai, chemija – N 003).

Nariai:
Dr. Marcin Filipiak (Centre for Advanced Materials and Technologies CEZAMAT, Warsaw University of Technology, Varšuva, gamtos mokslai, chemija – N 003);
Prof. dr. Jaunius Urbonavičius (Vilniaus Gedimino technikos universitetas – VilniusTECH, gamtos mokslai, chemija – N 003);
Dr. Rokas Žalnėravičius (Valstybinis mokslinių tyrimų institutas Fizinių ir technologijos mokslų centras, gamtos mokslai, chemija – N 003);
Dr. Šarūnas Žukauskas (Valstybinis mokslinių tyrimų institutas Fizinių ir technologijos mokslų centras, gamtos mokslai, chemija – N 003).

Disertacija bus ginama viešame Gynimo tarybos posėdyje 14:00 valandą, 2026 metų gegužės 8 dieną, B128 auditorijoje Valstybiniame mokslinių tyrimų institute Fizinių ir technologijos mokslų centre, Saulėtekio al. 3, Vilnius, Lietuva. Tel. +37061642060; kasparas.kizys@ftmc.lt

ABBREVIATIONS LIST

APAP	– acetaminophen
APTES	– γ-aminopropyltriethoxysilane
AuNPs	– gold nanoparticles
BC	– biocellulose
BioAu	– biogenic gold nanoparticles
CFU	– colony-forming unit
CMC	– carbomethyl cellulose
CNT	– carbon nanotubes
CPs	– conductive polymers
CV	– cyclic voltammetry
DPV	– differential pulse voltammetry
DSMZ	– Deutsche Sammlung von Mikroorganismen und Zellkulturen
EET	– extracellular electron transfer
FeMnNP	– iron-manganese nanoflowers
FeNP	– iron carbide nanoparticles
HDAC	– histone deacetylases
hmMSC	– human myocardium-derived mesenchymal stem cells
MB	– methylene blue
MFCs	– microbial biofuel cells
MD	– menadione
MWCNTs	– multi-walled carbon nanotubes
NADPH	– nicotinamide adenine dinucleotide phosphate (reduced)
NPs	– nanoparticles
OsRP	– osmium redox polymer

PANI – polyaniline

PCTE – polycarbonate track etch (membrane)

PD – power density

PEDOT:PSS – poly(3,4-ethylene dioxythiophene):poly(4-styrene sulfonate)

PEI – polyethylenimine

PMET – plasma membrane electron transfer

pPy – polypyrrole

PU – polyurethane

PQ – 9,10-phenanthrenequinone

QS – quorum sensing

ROS – reactive oxygen species

SAHA – suberoylanilide hydroxamic acid

SECM – scanning electrochemical microscopy

TEG – thermally expanded graphite

UME – ultramicroelectrode

TABLE OF CONTENTS

1. INTRODUCTION

The increasing demand for sustainable energy together with the urgent need for efficient wastewater treatment has stimulated the development of technologies capable of addressing both challenges simultaneously. [1] Microbial fuel cells (MFCs) represent one of the most promising approaches, as they enable the direct conversion of chemical energy stored in organic substrates into electricity under mild operating conditions. This dual functionality allows energy recovery from waste streams while reducing the environmental burden of wastewater, positioning MFCs as attractive components of circular bioeconomy systems. [2] However, despite intensive research, their large-scale application remains limited by low power density and insufficient long-term stability, which are primarily associated with inefficient extracellular electron transfer (EET).

EET efficiency in eukaryotic microorganisms is strongly restricted by the insulating properties of the cell wall and plasma membrane. As a consequence, electron transfer in yeast-based MFCs typically relies on soluble redox mediators. Although mediator-based systems can generate current, they introduce additional complexity, increase operational costs, and may negatively affect cell viability and system sustainability. Therefore, the development of a stable, conductive, and biocompatible interface of the microbial cell is a key challenge for improving the performance of yeast-based MFCs.

Unlike electroactive bacteria, *Saccharomyces cerevisiae* is non-pathogenic, genetically well characterized, tolerant to environmental fluctuations, and widely used in industrial biotechnology. Its robustness, simple cultivation, and ability to grow under both aerobic and anaerobic conditions make it a highly attractive organism for scalable and economically feasible bioelectrochemical systems. Nevertheless, its intrinsically low EET efficiency limits its direct application in high-performance MFCs. Overcoming this limitation requires engineering strategies that enable more efficient charge transfer without compromising cellular metabolism and viability.

One of the most promising approaches for improving EET involves the modification of the cell–electrode interface using conductive and biocompatible materials. Conductive polymers such as polypyrrole can be deposited extracellularly to form a semiconductive and redox-active layer that enhances electron transport while simultaneously improving microbial adhesion and biofilm stability. Gold nanoparticles, due to their high electrical conductivity, chemical stability, and nanoscale dimensions, can establish localized conductive pathways that facilitate direct electron transfer across otherwise poorly conductive cellular structures. The combination of these two

components offers a synergistic strategy for the formation of an efficient bioelectrochemical interface. However, the integrated effect of extracellular polypyrrole deposition and gold nanoparticle incorporation on yeast-based MFC performance, particularly under conditions relevant to real wastewater treatment, has not been sufficiently investigated.

In parallel with the development of MFC systems, the implementation of electrochemical techniques capable of probing redox processes at the level of single living cells is essential for establishing a direct link between biointerface architecture and electrochemical performance. Since macroscopic current generation in bioelectrochemical systems originates from intracellular redox balance, plasma membrane electron transport, and the local distribution of electroactive species, non-invasive and spatially resolved methodologies are required to obtain mechanistic insight under physiologically relevant conditions. Scanning electrochemical microscopy (SECM) provides such a possibility by enabling quantitative mapping of redox activity in the immediate vicinity of viable cells with micro- and nanoscale resolution while preserving cellular integrity. In this work, SECM was therefore employed as a methodological validation platform for the investigation of redox activity in human atrial mesenchymal stromal cells (hmMSCs), a well-defined model system exhibiting distinct metabolic states, in order to verify the sensitivity and selectivity of the technique toward biologically relevant redox variations and to establish an experimental and analytical framework for subsequent studies of microbial systems. The demonstrated ability of SECM to differentiate between cellular redox states confirms its function not only as an imaging tool but as a bioelectrochemical diagnostic approach that connects cellular physiology with electrochemical response and provides the mechanistic basis for evaluating and interpreting the performance of engineered conductive cell–electrode interfaces in yeast-based microbial fuel cells. For the practical implementation of MFC technology, system performance must be evaluated not only under controlled laboratory conditions but also in real and compositionally complex substrates. Wastewater sludge represents a highly relevant feedstock, as it contains both biodegradable organic matter and naturally occurring redox mediators that can support microbial metabolism and electron transfer. The integration of modified yeast-based MFCs into such environments is an essential step toward the development of scalable and environmentally sustainable energy recovery systems.

The novelty of this dissertation lies in the development of a dual biointerface engineering strategy for *Saccharomyces cerevisiae*-based

microbial fuel cells, combining extracellular polypyrrole deposition with gold nanoparticle incorporation in order to enhance charge transfer while maintaining biological viability. In addition, the performance of the modified systems is evaluated using real wastewater sludge, thereby bridging the gap between laboratory-scale studies and practical applications.

The aim of this dissertation is to enhance extracellular electron transfer in *Saccharomyces cerevisiae*-based microbial fuel cells by engineering a conductive and biocompatible cell–electrode interface using polypyrrole and gold nanoparticles, and to evaluate the performance of the modified systems under conditions relevant to real wastewater treatment. The work also demonstrates the applicability of SECM as a non-destructive electrochemical tool for the investigation of redox processes in living cells and bioelectrochemical systems.

The objectives of the work:

1. to evaluate the capability of SECM to detect differences in redox activity between healthy and pathological hmMSCs and to validate its application for bioelectrochemical investigations;
2. to develop extracellular polypyrrole deposition on yeast cells and assess its influence on direct electron transfer and cell viability;
3. to determine the effect of gold nanoparticle incorporation on charge transfer efficiency and MFC performance;
4. to investigate the operation of the modified yeast-based MFCs using wastewater sludge under both laboratory and real environmental conditions.

The defendable statements of this dissertation:

– SECM enables the differentiation of living cells based on their intracellular redox activity and plasma membrane electron transfer;
– extracellular deposition of polypyrrole forms a conductive and biocompatible interface that enhances direct electron transfer in yeast-based MFCs;
– the incorporation of gold nanoparticles creates additional conductive pathways that increase current generation and power density;
– the use of wastewater sludge as a substrate allows the modified systems to operate under conditions relevant to practical application without loss of performance.

2. LITERATURE REVIEW

2.1 SECM investigation principles

SECM is a comprehensive strategy that employs an ultramicroelectrode (UME) probe to investigate and observe the electrochemical processes with micro- to nanoscale resolution. [3] Although corrosion studies were the primary application, SECM is now widely employed to examine biological samples in vitro owing to its benign characteristics and capacity to study cells in their natural environment. [4–9] Through the quantification of diffusion gradients that surround cells which contain redox-active mediators, SECM provides insights into intracellular redox states and cell membrane electron transfer activity. [10–13] Consequently, SECM is adept at assessing intracellular redox states and plasma membrane electron transfer (PMET) across diverse cell types, including human atrium-derived mesenchymal stem cells (hmMSCs), under both physiological and pathological conditions, as well as therapeutic interventions, utilizing benign measurements through SECM feedback mode and employing a cell-impermeant FcCOOH as a mediator.

The UME, with a diameter in the micrometer range, is the most critical component of the SECM. It is frequently utilized as an operational electrode in an electrochemical cell. The UME can be relocated in three distinct manners – vertically and horizontally as per the sample surphase, and perpendicularly, in Z axis – with the present measurement recorded, and later illustrated, according to the coordinates. There is a four-electrode electrochemical cell using the UME as a mobile working electrode, with a reference electrode, a counter electrode, and the substrate serving as an additional working electrode. The bi-potentiostat interlinks all electrodes. A designated software application governs and documents the UME's motion and regulation, along with the current registration status. The steady-state diffusion-controlled current correlates with the concentration of the mediator [14]: $i_{T,\infty} = nFDC$, where n denotes the number of electrons participating in the reaction at the surface of the UME, F represents the Faraday constant (9.65×10^4 C/mol), D signifies the diffusion coefficient, C indicates the concentration of the mediator, and an refers to the radius of the UME. All SECM tests can be conducted at a fixed height between sample surphace and UME tip or maintained at constant distance between the two. In constant height mode, the UME is restricted to horizontal and vertical movement. In constant distance mode, the UME can traverse all three dimensions (x, y, and z) while maintaining a consistent distance from the sample. In this mode, the UME current is influenced by the distance of the UME from the surface of interest and the reactivity of the

chemicals adhered to the surface. To determine the ideal distance for the necessary resolution of SECM in continuous height mode measurement, the current-distance relationship can be assessed in feedback mode by placing the UME nearer to the surface of interest. Employing SECM theory, we could ascertain the distance between the UME and the sample. The ratio of UME current to steady-state current at a distance from an electrochemically active surface ($i_T/i_{T,\infty}$) can be utilized to determine the distance between the sample and the UME radius (d/a). This procedure, conversely, lacks precision and may result in the tip breaking or damaging the sample due to human error possibility. These constraints can be mitigated by employing a shear-force based constant-distance control [15]: the microelectrode oscillates at its resonance frequency with standard amplitudes of only a few nanometers, aided by a piezo-pusher [16]. A laser beam is concurrently concentrated on the extremity of the vibrating electrode, and the resultant Fresnel diffraction pattern is displayed on a bifurcated photodiode. The amplitude and phase data of the vibrating tip are acquired by magnifying the signal discrepancies from the split photodiode in relation to the modulation signal utilized by a lock-in amplifier. As the proximity between the tip and the sample diminishes, the augmented shear forces between the tip and the sample's surface result in a reduction in the vibration amplitude and a shift in phase. This can maintain a predetermined damping value associated with a constant distance of around 50 ± 100 nm through a software-controlled feedback loop. [16] An alternative method for measuring shear force involves affixing two piezoelectric plates to the scanning probe using mechanical means. [17] One plate induces vibrations in the SECM tip, while the other plate quantifies the intensity of these vibrations. As the shear forces at the sample's surface intensify, the vibration amplitude diminishes and the phase undergoes a shift. The alterations are observable by linking the detecting piezoelectric plate to a dual-phase analog lock-in amplifier. [17] A shear force-based methodology can function effectively at varying distances between the tip and the sample. Consequently, it can delineate comprehensive diffusion patterns near sources or sinks of redox-active compounds. [18] The integration of SECM with scanning probe techniques such as Atomic Force Microscopy (AFM) [19] and Scanning Ion Conductance Microscopy (SICM) [20], shear force methods [17,21,22], and impedance-based approaches [23] has facilitated enhanced control over the distance between the probe tip and the sample. The AFM tip functions as both a working electrode and a force sensor in the AFM-SECM methodology. [24,25] This technique enables the acquisition of optimal resolution and the assessment of various surface characteristics.

Feedback Types There are two categories of SECM feedback: negative feedback and positive feedback. The current is influenced solely by the concentration and diffusion of the redox species, independent of the surface. Should the current diminish as the UME approaches the surface of interest, the curve exhibits negative feedback behavior. This occurs when a surface functions as an insulator. As the UME approaches the surface, an increase in current indicates a positive feedback mechanism. This may occur when the UME approaches a conductive surface. Negative feedback in biological systems occurs only in the absence of a redox reaction when the UME approaches biological entities. The distance from the surface is the only factor that influences the current. As the ultramicroelectrode approaches a conducting surface of interest in positive feedback scanning electrochemical microscopy mode, the current increases. Moreover, the measured current in positive feedback mode may increase even when the conducting surface, evaluated by SECM, is not connected to the potentiostat. [26] In this scenario, the redox species generated on the UME participate in a reciprocal oxidation-reduction reaction on the conductive surface, so creating a self-sustaining "positive" feedback loop. [26] Consequently, the quantity of chemicals utilized by the UME increases near the conducting surface. However, this type of reversible redox activity is observable only when the ultramicroelectrode is positioned within 1 to 2 radii of the conductive surface.

2.2 Processes of cardio-vascular cells treatment

Cardiomyopathies are a group of heart disorders that are caused by problems with heart mechanics or electrical systems. They are usually characterized by an enlarged ventricle and poor performance. Fourteen Dilated cardiomyopathy (DCM) is the most common kind around the world and a major cause of heart failure and heart transplantation. [27] It is widely recognized that DCM linked to chronic heart failure represents a significant long-term consequence of myocarditis, often resulting from common viral infections and a range of internal and external toxic factors, including alcohol consumption, stress, and chemotherapeutic agents, among others. [28,29] Standard pharmacological interventions are crucial for the prevention of myocardial lesions; nevertheless, the treatment of DCM is challenging due to the disease's complexity, involving multiple molecular mechanisms that adversely affect cardiac tissue contraction and overall function. [29,30]

Contraction, electrical conductivity, and blood propulsion are the most important functions of cardiac tissue for keeping the heart healthy. [31] Mechanical problems usually lead to diastolic or systolic failure, whereas

electrical problems might affect the atria and cause arrhythmias that could be fatal. [32] These actions inside the heart muscle need a lot of energy, which comes mostly from breaking down fatty acids in mitochondria to make ATP. [33] When mitochondria don't have enough energy sources, heart cells use other things including glucose, lactate, ketone bodies, and amino acids. [34] Also, the NAD(H)/NADP(H) redox pools are very important for controlling the balance of redox reactions in cells and metabolic activities. [35] The reduction in metabolic flexibility in the heart is directly linked to an increased risk of heart failure and other pathological conditions. [34] Consequently, devising innovative strategies to augment energetic and redox potential in human cardiac cells, particularly those derived from dilated hearts, alongside approaches to evaluate these parameters, is imperative for advancing heart tissue regeneration.

The human heart has a very limited ability to heal itself after an injury, like a heart attack. [36] Unlike certain vertebrates, adult humans cannot efficiently regenerate lost cardiac muscle; instead, scar tissue replaces damaged areas, which can make the heart work less well and even lead to heart failure. Even while cardiomyocyte regeneration happens to a little extent, it is not enough to fix a big injury. It is very important that regenerated human myocardium-derived mesenchymal stromal cells (hmMSCs) are present in the heart. [37] Human mesenchymal stem cells (hmMSCs), also referred to as fibroblasts in cardiac research, comprise over 70% of normal adult cardiac tissue, surrounding cardiomyocytes, and play critical structural, paracrine, and functional functions in the control of heart rhythm and contraction. [38]

Heart regeneration is currently acknowledged as feasible via two principal strategies: (1) ex vivo synthesis of functional heart tissue for transplantation, and (2) stimulation of intrinsic healing processes. [36] As a result, targeted stimulation of the regenerative capacity in human heart hmMSCs has significant promise for improving recovery in injured cardiac tissue (ALCADIA study). [39,40] This study examines a distinctive epigenetic approach to activate human atrial hmMSCs and introduces a novel electrochemical method to assess their redox activity in vitro, with significant ramifications for heart tissue regeneration in vivo.

Recent research suggests that the broad-spectrum histone deacetylase (HDAC) inhibitor suberoylanilide hydroxamic acid (SAHA) may offer protection against myocardial ischemia/reperfusion injury by inhibiting the sodium-calcium exchanger. [41] In animal models, SAHA promotes autophagy, hence reducing cardiac fibrosis and infarct size. [42,43] Additionally, SAHA has shown that it can increase oxygen consu HDAC HDAC mption and mitochondrial performance in healthy and dilated ventricle-derived human

mesenchymal stem cells. [44] Still, the effects of SAHA on intracellular acetylation, mitochondrial membrane potential (MMP), NAD+ concentrations, intracellular redox state, and PMET status in human atrial hmMSCs – all have still not been assessed by non-invasive SECM feedback mode using a cell-impermeable FcCOOH mediator.

2.3 MFC Architecture and Operating Principles

Key MFC components and viewpoints are covered in this part. First, MFC design and fuel type will be given top priority; then improvements will take place and power outputs will be revealed.

Microbial fuel cells work by using the complex metabolic activities of microorganisms, which may produce electrons as a side effect of their biological operations. The electrons are then caught in an external circuit, where they become electrical current. Usually connected with the reduction of oxygen, the basic configuration consists of anode – the location of microbial oxidation processes – and cathode. Moreover, a membrane is essential for separating the two chambers and allowing ions to flow between them. Substrate metabolism generates electrons, which subsequently must pass the microbial membrane. This channel runs over an electrode interface before interacting with the external circuit. Commonly known as extracellular electron transfer, the mechanism of electron transfer is fundamental for the fundamental ideas guiding MFCs. This basic procedure greatly affects the working efficiency and performance of microbial fuel cells. Notwithstanding the wealth of studies gathered over the years, the broad commercial use of microbial fuel cells still presents major obstacles. The primary difficulties these systems have are their low power production and the inefficiencies resulting from electron transfer. The primary causes of our difficulties are inherent to the barrier characteristics of microbial cell membranes. These features impede the direct flow of electrons to the electrodes' surfaces, therefore preventing the formation of effective contact. The difficulty becomes more apparent in organisms like Saccharomyces cerevisiae that cannot create electrical impulses. The fact that the cell membrane contains naturally occurring redox-active proteins emphasizes this point even further. [45]

Several approaches have been suggested to meet these difficulties. The approaches cover a range of fundamental components, such as the use of synthetic redox mediators greatly helps electrons transfer. Within the field of genetic engineering, scientists are committed to synthesizing proteins displaying conductive characteristics. Furthermore, changed are the surface form and chemical characteristics of the electrodes. Enhancement of the electron transport routes depends much on CPs and nanostructures. Each one

of these ideas offers a diverse set of benefits along with some drawbacks that should be given thought. Although some methods may improve charge transfer rates, they might unintentionally compromise the viability of microorganisms or cause problems during process scaling-up.

With their exceptional electrical conductivity, great chemical stability, and favorable biocompatibility, gold nanoparticles (AuNPs) stand out from other conductive nanomaterials even in lesser amounts. [46] Their small scale allows close contact with the microbial surface, hence generating localized conductive connections. Interactions that take place commonly in the presence of insulating cell membranes help to enhance the occurrence of direct electron transfer (DET). Recent research indicates that whilst improving power density, AuNPs could lower internal resistance in MFC systems. The efficiency and performance of these energy systems might be much enhanced by this double impact. This improvement highlights the potential of AuNPs in maximizing the performance of MFCs, since it happens particularly without significantly slowing down microbial growth. [47,48]

Extensive polypyrrole (pPy) research has been conducted; it is identified as a conductive polymer. This material has many distinguishing properties: low conductivity, redox activity, and special fit with biological systems. Direct electrochemical polymerizing this molecule onto microbiological surfaces produces a semiconductive coating. This specific coating promotes the transmission of electrons between the redox centers of microorganisms and the electrode, therefore improving the general interaction and efficiency of the system. Additionally, pPy demonstrates numerous methods for enhancing microbial adhesion, providing cells in flow systems with a defense against shear stress. The importance of this specific characteristic cannot be emphasized as it is necessary for the establishment of stable biofilms on electrodes. AuNPs and pPy used together show a synergistic impact that improves their respective characteristics. Regarding microbial cell designs, pPy is particularly important as a stabilizer, which greatly increases the general stability and usefulness of these systems. This not only encourages effective electron transfer across their surfaces but also greatly helps these cells to be generally stable. Acting as "shortcuts," AuNPs improve the effective passage of electrons over thicker or less permeable sections of the cell wall, therefore acting as specialized channels with great conductivity. Particularly by means of a dual method in biointerface engineering, as reported in academic literature, recent developments in the evolution of MFCs have been defined by a noteworthy and creative approach.

This specific yeast species is an essential tool in many different scientific disciplines as it provides understanding of basic biological processes and

helps to enable a variety of biochemical reactions. [49–55] Many remarkably effective MFC systems depend on the presence of electrochemically active bacteria such as Shewanella oneidensis and Geobacter sulfurreducens. Usually needing both a particular kind of growth medium and stringent anaerobic conditions, these bacteria need optimum performance. Conversely, *Saccharomyces cerevisiae*, also known as baker's yeast, has a set of advantageous properties that make it particularly fit for scalable and reasonably priced uses in MFC. This specific fungus is well-known for both its non-pathogenic properties and well-established genetic profile. This choice shows an amazing degree of flexibility and a great capacity to resist different pH values and temperature circumstances. Besides, it is easily accessible for many industrial uses. An organism's ability to survive in both aerobic and anaerobic conditions depends much on its strong metabolic capacity. Its minimal complexity of culture makes it particularly suitable for many different applications. [56,57]

Anode and cathode chambers characterize MFCs. Anaerobic breakdown of organic substrates generates protons and electrons in the anode compartment among microorganisms. The reaction occurs under relatively moderate temperature and acidity conditions, which reduces the need for strong catalysts or the use of elevated temperatures during biomaterial and electrodes symbiosis. Because of their special characteristics, the MFCs are particularly well-suited to be incorporated into systems that prioritize the concepts of a circular bioeconomy, especially those designated for already existing water treatment infrastructure. While an external electrical circuit sends electrons from the anode to the cathode, producing electricity, protons cross a proton exchange membrane (PEM) separating the chambers. From electrons, protons, and molecular oxygen, a cathode oxygen reducing reaction (ORR) generates water. By means of this environmentally friendly bioelectrochemical process, MFCs can directly translate chemical energy into electrical energy.

Monosacharides such as glucose are the most oftenly used fuel sources in MFCs since, in ideal conditions, they offer 0.3 to 0.5 V per cell unit.[58] Glycolysis, respiration, and trans-plasma membrane electron transport proteins are thought to be the only electron transport processes in yeast. The electrons and protons produced during the oxidation of the substrate are directed to intracellular and extracellular electron acceptors. EET is made possible by soluble electron shuttles or membrane-bound electron shuttling compounds [59].

The cytoplasmic NADH is the most important intracellular electron carriers [60]. Glycolysis is the first step in carbohydrate oxidative degradation,

and the importance of glycolytic NADH in EET processes is undeniable. The proportion of NAD+/NADH in eukaryotic cells is around 700, which stimulates oxidation processes [61], whereas the ratio of NADP+/NADPH is only 0.005 and the reduced form NADPH is dominant [62]. The varying quantities are crucial for the distinct metabolic roles of NADH and NADPH. Because cytoplasmic NADPH is produced in the Pentose-Phosphate Pathway (PPP), which the main function is associated with anabolic processes (nucleotide production, DNA replication, and reproduction), direct NADPH involvement in EET would not be of a high priority. NADPH, on the other hand, may indirectly contribute to EET processes as a cofactor of reductase and hydrogenase enzymes. The biological function of EET is to maintain intracellular redox balance, i.e., to sustain an optimal NAD+/NADH ratio for catabolic processes to occur. By use of soluble electron shuttles or outer-membrane-bound metalloproteins, NADH re-oxidation in combination with an external electron acceptor (the biofuel cell anode) enhances substrate oxidation, hence supplying NAD+ and therefore enhancing energy generation in the form of ATP.

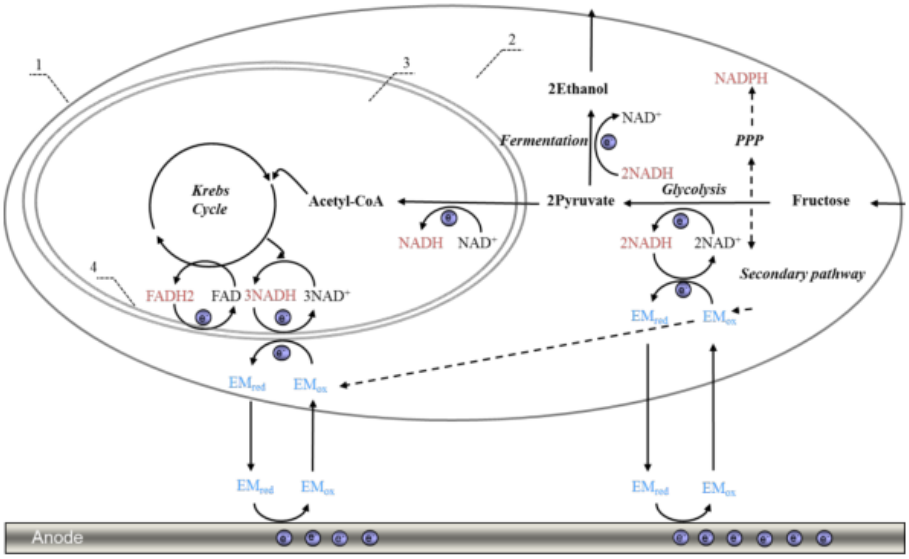

Figure 1. Extracellular electron transfer in yeast-based biofuel cell. The scheme presents the possible electron origin and electron transfer mechanism from the yeast to the anode in a batch-regime of cultivation, where 1 - yeast cell, 2 – cytoplasm, 3 – mitochondrion, 4 – inner mitochondrial membranes with mitochondrial respiratory chain components (complexes I-IV). The oxidized and reduced forms of the endogenous mediator are presented as EMox and EMred. Adapted from [63].

Other cytoplasmic catabolic processes, such as the lactate reaction cycle [64] and the purine catabolic pathway [65], are thought to contribute to the EET processes in addition to glycolysis. The processes associated with phosphate metabolism [66], which are an important part of cellular bioenergetics, also play a role in the current generation, balancing intracellular energy requirements and extracellular transfer. As a redox-neutral process, alcoholic fermentation (conversion of pyruvate to ethanol in anaerobic conditions) is not directly connected with an electron exchange. Despite the classical presumption that the biofuel cell anode should operate under strictly anaerobic conditions to eliminate the competition of oxygen as a terminal electron acceptor, several papers [60,67,68] reported higher current and power outputs obtained with yeast-based biofuel cells, operating in aerobic conditions. In aerobic conditions, a portion of extracellularly transferred electrons is produced in the mitochondrial matrix and diverted to the EMox via the respiratory chain complexes [69]. The proportion of extracellular electrons transferred in aerobic and anaerobic respiration reflects the degree of catabolic pathways implementation [60,69]. When mitochondrial functions are inhibited, the amount of electricity generated by the MFC drops by about 40%, reaching levels like those found in anaerobic conditions [69].

Although earlier research has focused on the addition of nanoparticles together with the use of CPs, the combined impacts of these two components have not yet been fully investigated. This is especially clear when one looks at the study of actual, practical wastewater samples gathered from relevant environments. Moreover, the effect of these changes on yeast viability – a crucial component for the continuous functioning of MFCs – is not well studied.

This work investigates the effectiveness of the reengineered MFC systems using differential pulse voltammetry (DPV), cyclic voltammetry (CV), and power density evaluations among other electrochemical techniques, as well as the power of SECM feedback mode in the biosensorical investigations of living cells. Experiments were conducted under simulated real-world scenarios as well as under controlled laboratory environments to evaluate the scalability and application of the suggested approach.

Anode material influences microbial adherence, surface reactivity, and electron transfer efficiency in turn influencing MFC performance. Recent studies find that anodes made of nanostructured carbon felt (CF) have the highest power densities. *Saccharomyces cerevisiae* biofilms respond best with CF anodes comprising gold nanoparticles[70] or nano-flowers[71] of manganese-iron oxide combinations (Table 1). Mannoproteins and glucans *S. cerevisiae*

secreted enable microbial cells to build a strong, conductive interface with electrodes coated in nanomaterials.

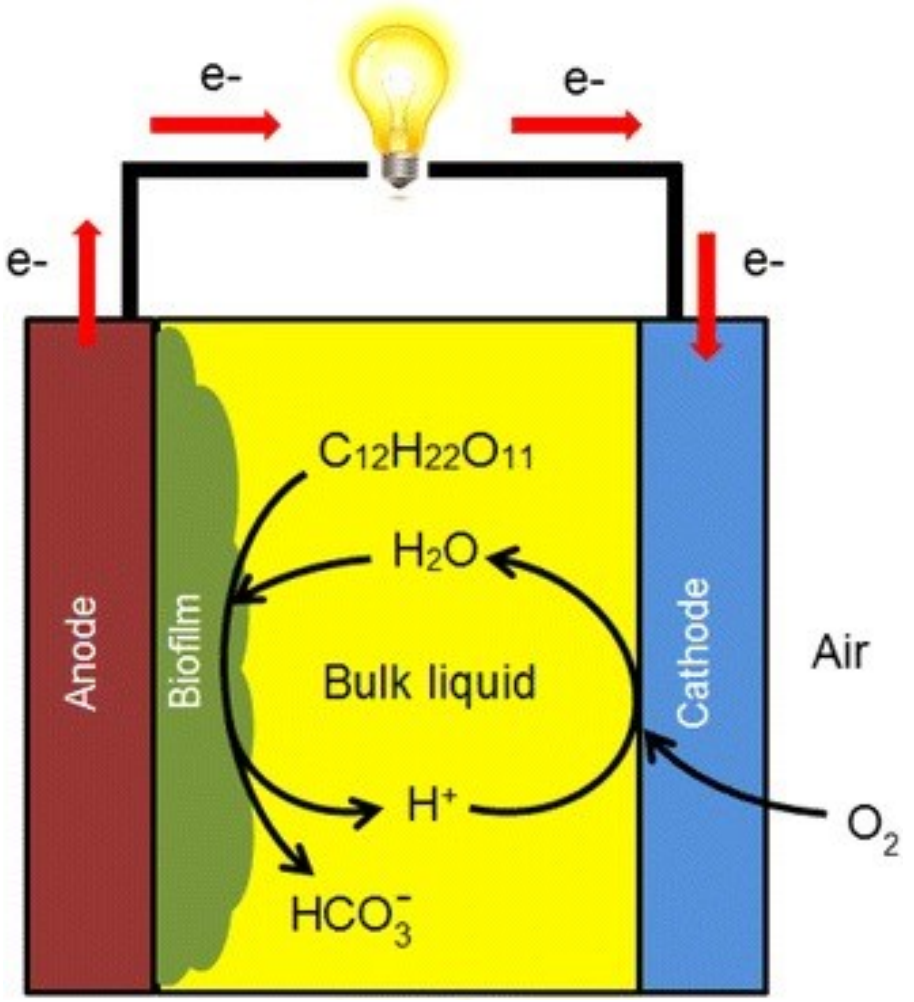

Figure 2. A representative scheme of a one-compartment aerobic microbial fuel cell. Adapted from [72]

These bio-nanocomposite surfaces increase DET-like behavior, an MFC system limit. The large specific surface area and microbial-friendly environment of carbon felt's three-dimensional porous architecture produce more current. Furthermore, allowing directional selective proton transfer, Nafion, a proton exchange membrane, stops oxygen from moving from the cathode to the anode, so preserving anaerobic conditions for microbial activity.

In MFCs, the cathode hosts the terminal electron-accepting reaction and therefore strongly influences the overall cell potential, power output, and operational stability. The most commonly applied cathodic process is the oxygen reduction reaction (ORR), particularly in air–cathode configurations. Under neutral conditions typical for biological systems, the preferred pathway is the four-electron reduction of oxygen to hydroxide ($O_2 + 2H_2O + 4e^- \rightarrow 4OH^-$), because it provides the highest thermodynamic efficiency and avoids the accumulation of reactive intermediates. However, on non-noble carbon materials the ORR is kinetically slow and often proceeds partially via a two-electron pathway, leading to peroxide formation. This results in increased overpotentials, reduced energy efficiency, and possible degradation of electrode materials and catalytic sites.

The catalytic properties of the cathode material are therefore critical. Platinum exhibits excellent ORR kinetics and selectivity toward the four-electron pathway and is commonly used as a benchmark catalyst. Due to its high cost, susceptibility to poisoning, and limited long-term stability in complex media, significant research has focused on alternative catalysts, including activated carbon, transition-metal–nitrogen–carbon (M–N–C) materials, metal oxides, and heteroatom-doped carbon structures. These materials aim to improve electron transfer kinetics, enhance oxygen adsorption, and reduce activation losses while maintaining chemical and mechanical stability.

In addition to catalyst limitations, mass transport represents a major constraint at the cathode. Oxygen solubility and diffusion in aqueous electrolytes are low, which can lead to concentration polarization, particularly at high current densities. Furthermore, the ORR in neutral media generates hydroxide ions, causing a local increase in pH near the cathode surface. Simultaneously, proton production at the anode leads to acidification. This pH gradient across the cell reduces the effective cathode potential and contributes to additional voltage losses.

Alternative cathodic reactions have also been explored to improve performance or enable specific applications. Soluble electron acceptors such as ferricyanide provide fast and reversible kinetics and are therefore frequently used in laboratory studies to evaluate anode performance, although they are not suitable for long-term or large-scale operation due to regeneration requirements. Other cathodic processes, including nitrate, sulfate, metal ion, or carbon dioxide reduction, allow MFCs to be integrated into wastewater treatment, resource recovery, or electrosynthesis systems, where the cathode

becomes a site of value-added chemical transformation rather than solely an electron sink.

Overall, the cathode is a key determinant of MFC performance because it defines the maximum achievable cell voltage, contributes substantially to internal resistance through activation and mass-transfer losses, and governs long-term system stability. Consequently, the development of efficient, selective, and durable cathodic materials and architectures is essential for improving the practical applicability of MFC technologies.

2.4 Integrated redox bioelectrochemical analysis and biointerface engineering in living systems

Microbial fuel cells (MFCs) operate under relatively mild temperature and pH conditions, which significantly reduces the requirement for harsh catalysts and energy-intensive processing during the formation of functional bioelectrode interfaces. This intrinsic compatibility with biological systems makes MFC technology particularly attractive for integration into circular bioeconomy frameworks, especially within existing wastewater treatment infrastructures where simultaneous waste remediation and energy recovery can be achieved. The central limitation of these systems, however, remains the efficiency of extracellular electron transfer (EET), which is strongly constrained by the insulating properties of biological membranes and the complexity of intracellular redox metabolism.

SECM has emerged as a powerful and non-invasive technique for investigating electrochemical activity at the micro- and nanoscale using UME probes. Originally developed for corrosion studies, SECM is now widely applied to biological systems because of its ability to probe living cells in their native environment without causing significant perturbation. [3–9] By quantifying diffusion gradients of redox mediators in the vicinity of the cell surface, SECM enables real-time assessment of intracellular redox balance and plasma membrane electron transfer (PMET) activity. [10–13] The feedback mode, particularly when combined with cell-impermeable mediators such as FcCOOH, allows selective monitoring of transmembrane electron fluxes and provides a direct functional readout of cellular metabolic state.

The importance of intracellular redox homeostasis is especially evident in highly energy-demanding tissues such as the myocardium. Cardiomyopathies represent a heterogeneous group of myocardial disorders characterized by structural and electrical dysfunction, with DCM being the most prevalent form and a leading cause of heart failure and transplantation worldwide.[27,73] DCM frequently develops as a long-term consequence of myocarditis and can be

triggered by viral infections, toxic agents, alcohol, chemotherapeutic drugs, or chronic stress. [28,29] Despite advances in pharmacological therapy, the multifactorial molecular mechanisms underlying DCM continue to limit treatment efficacy. [29,30]

Cardiac function depends on a continuous supply of ATP, primarily generated through mitochondrial fatty acid oxidation. [33] When metabolic flexibility is compromised, cardiomyocytes switch to alternative substrates such as glucose, lactate, ketone bodies, and amino acids, a transition that is closely linked to alterations in NAD(H)/NADP(H) redox pools and the progression toward heart failure.[34,35] Because the adult human heart has minimal regenerative capacity following injury, damaged myocardium is largely replaced by fibrotic scar tissue.[36] In this context, human myocardium-derived mesenchymal stromal cells (hmMSCs) play a critical structural and paracrine role, representing a major non-myocyte cell population that regulates cardiac electrophysiology, mechanical stability, and tissue remodeling.[37,38] Strategies aimed at enhancing the regenerative and metabolic potential of hmMSCs therefore represent a promising direction for cardiac repair. [36,39,40]

Epigenetic modulation has recently attracted attention as a means of improving mitochondrial function and cellular bioenergetics. The HDAC inhibitor SAHA has been shown to reduce myocardial ischemia–reperfusion injury, attenuate fibrosis, and promote autophagy in experimental models. [42,43] In hmMSCs derived from both healthy and dilated ventricles, SAHA increases oxygen consumption and mitochondrial activity. [44] Nevertheless, its influence on intracellular acetylation, mitochondrial membrane potential, NAD+ levels, and PMET activity in atrial hmMSCs has not been fully characterized using non-invasive electrochemical approaches.

SECM-based studies combined with flow cytometry have demonstrated that pathological hmMSCs exhibit lower intracellular acetylation, reduced mitochondrial membrane potential, decreased NAD+ content, and diminished redox activity compared to healthy cells. HDAC inhibition enhances acetylation and mitochondrial polarization in both cell types, although the restoration of redox capacity is more pronounced in healthy cells. These findings confirm that SECM provides a sensitive and bio-harmless platform for functional discrimination between physiological and pathological cellular states and for evaluating the metabolic effects of biologically active compounds.

The conceptual parallels between intracellular redox regulation in mammalian cells and EET processes in microbial electrochemical systems are

striking. In MFCs, metabolic oxidation of substrates generates electrons that must cross the microbial envelope and reach the anode. This step is the principal bottleneck in systems based on non-electrogenic organisms such as *Saccharomyces cerevisiae*, where direct electrical communication with the electrode is inefficient. [45] Various strategies have been proposed to overcome this limitation, including the use of synthetic mediators, genetic engineering of conductive proteins, and modification of electrode surfaces with conductive nanomaterials and polymers. Each approach improves charge transfer but may also affect cell viability or process scalability.

Gold nanoparticles (AuNPs) represent one of the most promising conductive nanomaterials because of their high electrical conductivity, chemical stability, and excellent biocompatibility. [46] Their nanoscale dimensions enable intimate contact with the microbial surface, creating localized conductive pathways that facilitate direct electron transfer and reduce internal resistance without significantly inhibiting microbial growth. [47,48] Conductive polymers such as polypyrrole (pPy) further enhance this effect by forming semiconductive coatings that improve cell adhesion, stabilize biofilms, and protect microorganisms from shear stress in flow systems. The synergistic combination of AuNPs and pPy creates a multifunctional biointerface in which the polymer matrix provides structural stability while embedded nanoparticles act as highly conductive electron transport shortcuts.

Saccharomyces cerevisiae is an attractive model organism for such studies because of its non-pathogenic nature, genetic accessibility, tolerance to a wide range of environmental conditions, and ability to grow under both aerobic and anaerobic regimes. [49–57] In yeast-based MFCs, EET is predominantly mediated by soluble redox shuttles such as quinones, which penetrate the cell membrane, oxidize intracellular NADH, and subsequently transfer electrons to external acceptors.[74] Cytosolic NADH produced during glycolysis represents the main intracellular electron source, while the high NAD+/NADH ratio favors continuous substrate oxidation.[59–61] In contrast, NADPH generated in the pentose phosphate pathway primarily supports anabolic metabolism and contributes indirectly to EET through reductase-dependent reactions. [62]

Additional catabolic pathways, including lactate metabolism, purine degradation, and phosphate-associated bioenergetic processes, also participate in extracellular current generation. [64–66] Although classical MFC design assumes strict anaerobic conditions to avoid competition with oxygen, several studies have reported higher power outputs in the presence of oxygen, where mitochondrial respiration contributes a significant fraction of the exported electrons. [60,67–69] Inhibition of mitochondrial function reduces current

generation by approximately 40%, highlighting the central role of respiratory metabolism in yeast-based EET.[69]

Despite extensive research on conductive nanomaterials and polymers, their combined effects on electron transfer efficiency, microbial viability, and performance in real wastewater matrices remain insufficiently explored. Addressing these gaps requires electrochemical techniques capable of correlating biointerface properties with functional redox activity in living systems. Differential pulse voltammetry, cyclic voltammetry, power density measurements, and SECM feedback mode together provide a comprehensive analytical framework for evaluating both the bioelectrochemical performance of engineered MFCs and the metabolic state of the participating cells under conditions that mimic real-world operation.

2.5 Redox Mediators in Yeast-based MFCs

In systems running on yeast, electron transport generally relies on redox mediator availability. Among the important examples of these mediators are quinones, especially 9,10-phenanthrenequinone, which is rather important in promoting this action. Examined mediator could pass the cell membrane, where they are essential for the oxidation of the intracellular redox cofactor NADH. [74] They then move via this process toward the anode's surface, therefore enabling the electron release and relay to ferricyanide, the second, hydrophylic mediator to pass the electrons further for a chain formation.

MFCs represent a novel approach to bioelectronic devices as they can generate power and clean polluted water. [75,76] A large amount of electric charge may be produced [77,78] in the metabolic redox reactions taking place within live microorganisms. Nevertheless, the cell membrane and cell wall restrict the ability of yeast cells to transfer the charge generated during metabolism to the anode. [79] Thus, it is essential to raise the electrical conductivity of the cell wall and/or membrane. Usually, modern microbial fuel cells provide a low current density and power output. [80] Still, using suitable redox mediators [79] increases the efficiency of charge transfer. The mediators used in MFCs should show the following characteristics:

1. Exhibit reversible redox activity within the operational voltage range.
2. Be non-toxic to microbial catalysts.
3. Penetrate cell membranes or bind outer-membrane redox proteins.
4. Have a redox potential matching microbial electron export and anode acceptance.
5. Remain stable and soluble in both oxidized and reduced forms.
6. Rapidly transfer electrons to the anode surface.[36,38]

Babanova et al. in 2011 identified thionin, methylene blue, and neutral red as effective artificial mediators for electron transfer in yeast-based MFC.[81] Electron transport between yeast cells and an electrode may be improved using a two-mediator redox system. When the first mediator is lipophilic, which helps it to interact with redox centers within the cell and pass across the cell membrane. Having hydrophilic characteristics, the second mediator may accept electrons from the lipophilic mediator (via redox cycling) and subsequently transfer them to the electrode.[79,82] One class of chemicals that show great lipophilic redox mediation are quinones. Nevertheless, depending on their chemical characteristics and the surrounding environment, there are certain negative effects connected with them, like toxicity and the possibility of structural damage or termination of microbial cells.[83–87]

Renowned lipophilic redox chemical substance 9,10-phenanthrenequinone (PQ) may pass cell membranes to enable intracellular redox cycling mechanisms.[88,89] Its limited water solubility, however, greatly limits its direct usage in MFCs, as it cannot efficiently transmit electrons to the anode under aquatic conditions. Developed to tackle this issue are dual-mediator systems including both lipophilic and hydrophilic redox mediators. [82] Whereas the lipophilic mediator (e.g., PQ or menadione) acts intracellularly, delivering electrons from within the cell to the membrane, the hydrophilic mediator (e.g., ferricyanide) allows charge transfer to the electrode in the extracellular environment. [90]

In previous studies, yeast cells – more especially, *S. cerevisiae* and baker's yeast (non-cultural mixed species) – have exhibited remarkable bioelectrocatalytic activity in MFCs, when redox and electrophile-mediated pathways were employed in a biological experiment based on yeast to assess cellular toxicity. Menadione (2-methyl-1,4-naphthoquinone, MD) [91,92] and PQ [93,94] have demonstrated good effectiveness as intracellular electron shuttles among the investigated redox molecules. After cellular reduction, where it interacts with the external mediator, menadione may re-diffuse across the membrane into the surrounding solution. [95,96] In our prior research, we demonstrated the potential use of PQ as a redox mediator to assess yeast viability [97–99]. It exhibited a significantly higher electrochemical signal than p-benzoquinone, 2,6-dichlorophenolindophenol sodium salt hydrate, and 10-phenanthroline-5,6-dione. According to the findings, it was anticipated that PQ could be an excellent choice for designing a yeast-based MFC to enhance the transfer of electrical charge across the yeast membrane and cell wall toward the electrode.

Reactive oxygen species (ROS), like hydrogen peroxide (H_2O_2) and superoxide (O^{-2}), have been linked to negative effects on quinones including

PQ and MD. The organism and its environment define the fluctuations in redox of the mediators' effects. Still, their redox activity and membrane permeability make them major advantages for the design of MFC. [100] Although their usage in controlled electrochemical settings is still advantageous, quinones have been demonstrated to produce adducts with nucleic acids.[101–104]

Experimental findings from our study showed that when grown at 30°C baker's yeast shows more resistance to PQ than MD.[105,106] Effective electron flow from yeast to the electrode was enhanced by the dual-mediator system – PQ and potassium ferricyanide. The MFC with immobilized MD on the anode and generated an open circuit voltage of 62 mV in the absence of glucose upon 23 mM ferricyanide. Baker's yeast and MD produced the maximum power output of 0.408 mW/m^2 at a voltage of 24 mV. The MFC showing the highest power output (22.2 mW/m^2) was obtained during isolated PQ testing with an open circuit voltage of 178 mV. These findings support the use of dual-mediator systems incorporating PQ and MD to improve electron transport in yeast-based MFCs and demonstrate their relevance for upcoming bioelectrochemical applications.

2.6 Conductive Polymer Integration Strategies

The references numbered [51,52,79,82,107] illustrate the potential application of PQ as a redox mediator for evaluating yeast viability, aligning with the framework of our experimental design. A MFC was constructed and evaluated utilizing PQ and yeast cells, with particular attention given to bakers' yeast and a pure strain of *S. cerevisiae* for the anode component. Our laboratory in 2021 study[106] demonstrated that bakers' yeast exhibits a greater resistance to PQ at a temperature of 30 °C in comparison to *S. cerevisiae* cells. The utilization of two redox mediators, specifically PQ and ferricyanide, demonstrates significant potential in facilitating the transfer of electrons from yeast to the electrode within the system. This study revealed that the anode of a MFC utilizing baker's yeast generated a power output of 22.2 mW/m^2, as measured during the experiments conducted. The cell exhibited an open circuit voltage measured at 178 mV, which corresponded with a power output reading of 56 mV. Particularly when used with CPs, the electrochemical sedimentation approach shows an effective way to enhance the properties of electrode surfaces. Devices using bioelectronics usually follow a certain approach in their design – using graphite rod electrodes as the main model for low scale measurements. [108] It seems advantageous to change and use a spectrum of electrical characteristics to reach the construction of a CP layer

that conforms with accepted physicochemical performance criteria. [109,110] The use of electrochemical methods as well as the exact computation of the working electrode potential necessary to start the polymerization process of the first monomer will be the main topics of this dissertation. Modifying the ideal electrochemical conditions required for the polymerization process [111] could consequently influence the physical characteristics of the resulting layers. This discussion encompasses the different variations in layer density, thickness, and the permeability of ions. Furthermore, various chemical constituents significantly affect the characteristics of the produced CP layers. Several essential factors must be considered, including the selection of solvents, the types of polymerizable monomers, the overall composition of the polymerization process, and the pH values required for the successful execution of the operation. Through the process of electrochemical polymerization, it is possible to create a sheet composed of a conductive polymer that possesses an impressive ability to encapsulate a wide range of physiologically active chemicals. This illustrates the adaptability and potential uses of this method across various biological contexts, as it encompasses not only proteins [112–115] and DNA [116,117] but also living cells and bacteria as the attainment of this result is significantly facilitated by the components present in the polymerization mixture.

The efficiency of bioelectronics-based devices is increased by methods of electrosedimentation by which conductive polymer layers merge into their frames.[118–120] The general efficiency of MFCs is influenced mainly by the rate of nutrients serving as microbial biofuels and their ability to enter the system. Sometimes it is permissible to use organic-based "spacers" to vary the porosity of the produced CP-based layer.[121] Linking many polymeric chains depends on these spacers, thereby influencing the overall properties of the material significantly. After these modifications, the efficiency of MFCs would be influenced by the conductivity of the layers generated from CPs contained in their composition. Moreover, discussed in the work are the layers of polyaniline (PANI)[116,122] and the impact of several synthesis factors on the electrical conductivity of polypyrrole (pPy) films[123] produced by electrochemical methods. Our group has simultaneously created a mathematical model[124] aimed to explain this phenomenon. Particularly in the electrochemical production of multi-layer electrodes composed of pPy, modern surroundings might profit from the insights gained from this knowledge.

A broad spectrum of bacteria[125,126] as well as live human cells including lymphocytes[127] and erythrocytes[128] may be used in biofuel cell development. Currently the rate of electron transport between microorganisms and the electrode is still little understood, due to the plethora of different EET

mechanisms that evolved through microbial adaptation. Thus, the alteration of bacteria intended for use in MFCs greatly affects the design and structural framework of these bioelectronic devices. A prevalent approach in this domain enables the modification of microorganisms via their essential metabolic pathways, which is vital to produce CPs. Showing significant advancement in this area of research, CPs provide enormous possibility to increase electron transfer efficiency across cell membrane/wall in microorganisms.[49,50,129,130] Studies reveal that certain microorganisms[49,76] – including stem cells[131,132] – keep their viability and metabolic activity in spite of cell surface modifications induced by CPs. Enhancements in biofuel cells that increase electrical current production may be essential for maintaining overall system stability. Using these modified microorganisms in biofuel cells provides important new insights as live cells keep their biocatalytic activity for a longer period[133] than polymer-modified enzymes[134,135]. Under this paradigm, a wide range of cell types[136] – including those generated from fungus[50,137] and bacteria[138] – were deftly combined into the formation of many polymers, most importantly CPs among their ranks. Focusing on the processes of charge transfer enabled by microorganisms across their cell membranes and walls might help to improve the efficiency of MFC. The chosen approach therefore relies on redox chemicals that effectively enable charge transfer. The redox actors could be terminated outside or within living cells before entering a full electrical chain with the electrodes. Supported by a lot of data, many studies – more especially, references[51–53,139,140] – show that the compounds, such as PQ, MD, or Potassium hexacyano ferrate, are acknowledged redox mediators. These main categories define redox mediators: (I) hydrophilic mediators, which are soluble in water; (II) lipophilic mediators, which are soluble in fats and oils; and (III) nanoparticles derived from several sources;[141,142] and (IV) there are redox polymer-based conducting matrices that are quite important for these reactions.[76,143,144] Redox mediators used cleverly in the design of biofuel cells have the ability to link cells and electrodes, therefore improving the charge transfer efficiency from the cell cytoplasm. Usually, hydrophilic mediators improve the efficiency of MFCs by means of their interactions with the trans-plasma redox system inside the cell.[145] The mediator is suggested to interact with the cytoplasmic redox enzymes. One of the most often seen events consists on the many membrane-bound cytochromes.[146] Redox-active entities are one way to define cytochromes; they might be functional groups, coenzymes, core components, or a mix of these many components.[147] Generally speaking, one may say that the hydrophilic domains of enzymes cannot pass over the membrane. Charges are transferred across the cell membrane with significant help from lipophilic mediators. Potential integration of redox mediators into the plasma membrane helps the charge to

be transferred from the internal components of the cell to the outside leaflet of the membrane to be efficient. Enhancement of charge transfer and migration processes depends much on the presence of redox-active functional groups in lipophilic mediators. One must understand that usually lipophilic mediators are used in tandem with their hydrophilic counterparts. Consequently, net charge transfer has clearly increased and now reaches a value of.[145]

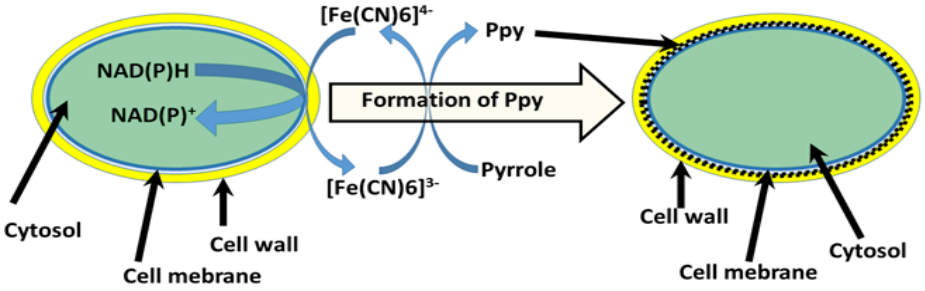

Figure 3. A schematic representation illustrates the synthesis of pPy within the cell wall of yeast. The redox enzymes situated within the plasma membrane play a crucial role in the oxidation of $[Fe(CN)_6]^{4-}$ to $[Fe(CN)_6]^{3-}$. This transformation serves as the starting point for a polymerization process involving pyrrole. [148]

2.7 Nanomaterials in Bioelectrochemical Systems

The MFC model, based on para-aminophenol, a pharmaceutical contaminant, and *Saprochaete dehoogii*, generates electricity and filters pharmaceutical waste, demonstrating bioenergy and environmental remedial properties. These devices can be temporarily used in smaller wastewater treatment systems due to their extraordinary operational stability over eight days. [149,150]By influencing microbial adhesion, surface reactivity, and electron transfer efficiency, the anode material influences the performance of MFCs. Recent work indicates that nanostructured materials on CF anodes maximize power densities. *Saccharomyces cerevisiae* biofilms together with manganese and iron oxide nanoflower structures or gold nanoparticles help CF anodes perform effectively. Extracellular polymeric compounds of *S. cerevisiae* stabilize and behave in microbial cells towards electrodes coated in nanomaterials. As *S. loihica* is known for its metal-reducing properties, the MFCs using *S. loihica* provide a nontoxic and ecologically sustainable method for the remediation of chromium and related contamination by means of chromium nanoparticles. [151] Sewage silt was purified and energy production from *Negativicutes* and *Gammaproteobacteria* was achieved using MFCs. [152] Rather than on the creation of MFCs fit for practical use, the study mostly focused on electrode surface alterations using varied materials as a framework

to improve device performance.[51,153–158] In those past examples, *S. cerevisiae* usually was the main model microorganism used.

Many nanomaterials are used in MFCs, which may be distinguished by their diverse kinds, diameters, and sources. The advancement of MFCs is significantly influenced by the incorporation of carbon-based nanomaterials and metallic nanoparticles, which enhance the charge transfer processes associated with redox enzymes.[51,159,160] The alteration is applying nanoparticles to the surface of the cells thereby establishing an electrical link between the cells and the electrodes.[161] Unlike changes done to electrodes, the cells are coupled to nanoparticles instead of being directly attached to the electrodes themselves.[162] One might categorize the above stated cell manipulation techniques as "conventional" approaches. There is a strong tendency for nanoparticle applications in biology [163], industrial chemistry [164], electrochemical sensing devices [165], and bioelectrochemistry [46]. Gold nanoparticles are known as good candidates for achieving higher charge transfer [166,167]. Among all possible applicable nanoparticles, 10 nm gold sphere nanoparticles were chosen for our research due to their low cytotoxicity when bigger size nanoparticles are used [168] at lower concentrations [169].

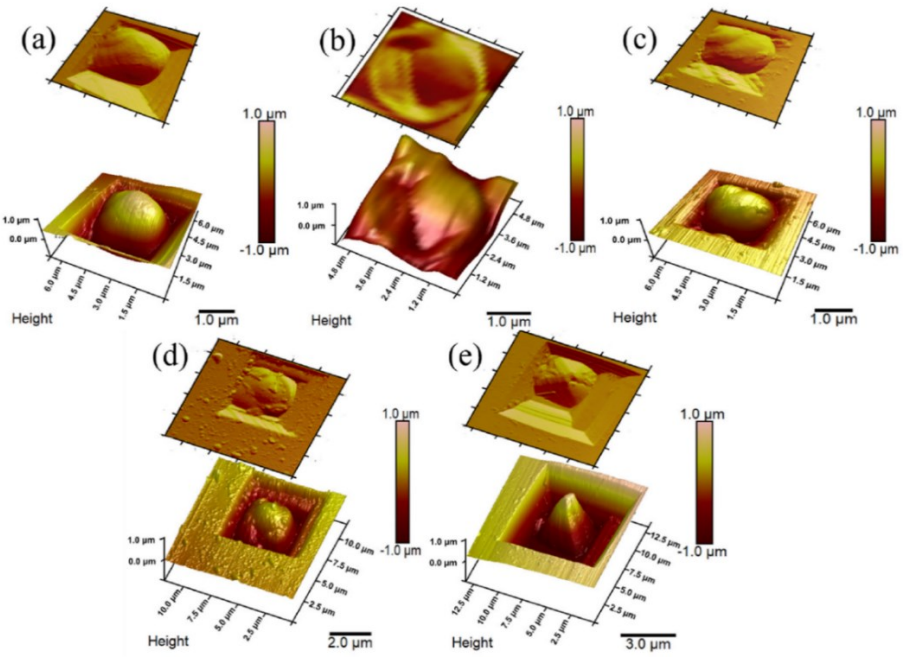

Figure 4. AFM images show: (a) an unmodified yeast cell; (b) an inactivated yeast cell; (c) a yeast cell modified with pPy at a concentration of 0.05 mM; (d) a yeast cell treated with pPy at a concentration of 0.1 mM; and (e) a yeast cell modified with pPy at a concentration of 0.3 mM. Originally from A. Zinovičius 2022 y. publication. [170]

2.8 Microbial Cell Surface Engineering

An important progress in the subject is the creation of polymeric self-encapsulation of cells, especially for biosensing and medicine uses.[130] One special benefit of *in situ* polymer matrices over other techniques is their availability. These entities may arise concurrently with cell culture or by means of different metabolic or chemical reactions inside the individual cells. Scholars in recent debates have been somewhat interested in pPy. By releasing innovative research targeted on the synthesis of bio-assisted pPy polymers, our research team achieved notable advancements in the area in 2016, hence advancing the discipline.[138] Studies show that certain species of *Streptomyces* bacteria have the amazing capacity to independently generate spherical pPy particles—all without requiring chemical treatments. The capacity of redox enzymes, including phenol-oxidase, to interact with their extracellular environment offers important new perspectives on the events seen in species of *Streptomyces*. pPy is one of the phenol-based monomers that polymerizes and calls for the presence of enzymes with the necessary capacity for this transformation. Studies suggest that phenol-oxidases may synthesis polypyrrole. Six days of development saw *Streptomyces spp.* bacteria effectively create hollow microspheres made of pPy. The hollow microspheres' diameters ran from 10 to 20 micrometers. The organic components in the developing medium seemed to affect the kinds of particles that showed up.

There is also proof that pPy may encapsulate *S. cerevisiae* yeast cells.[49,171] This technique cycles $[Fe(CN)_6]^{4-}/[Fe(CN)_6]^{3-}$, which acts as a redox mediator throughout the process. Yeast cells were used together with the potassium hexacyano ferrate. Figure 4 shows how, under careful reaction control, this approach helped to enable *in situ* synthesis of pPy. The influence of pPy on cell survival as well as its uses in other domains were discussed. The results provide new light on the many mechanisms that could control synthesis and thereby need attention. The mechanical properties of pPy covered cells are investigated in this work. This study examined pPy concentrations by nonradioactive isotopic monomer labeling combined with isotope ratio mass spectrometry. This specific molecule is essential for the building of an intercalating matrix inside the cell wall.[50,171] Ensuring the ongoing vitality of bacterial life after the modification procedure including pPy is crucial in the search of lasting microbial biofuel cells. Observations revealed that presence of yeast cell walls affected the structural distribution of pPy. This interaction changed the physical and chemical properties of the altered cells, hence improving their resistance to lysis enzymes particular to yeast.[50] A relationship between polypyrrole treatment and several elements

including cell survival, cell shape, size, and cell surface roughness is also researched.[170] Surface roughness and pyrrole content show an intriguing pattern wherein cell diameter decreases in line with increasing pyrrole concentration. Figure 4D shows the created tiny polymer clusters. At the minimal concentration of 0.05 M pyrrole, a slight alteration in the physiological condition of the cells was observed. Consequently, this specific concentration was selected for use in the MFC. The microbial fuel cell (MFC) demonstrated an output of 47.12 mW/m² and an open circuit potential of 390 mV. These values represent an increase of 8.32 mW/m² and 55 mV when compared to the control MFC.[170]

A spectrum of bacteria was investigated throughout this period: *Shewanella oneidensis* MR 1, *Ochrobacterium anthropic*, *Escherichia coli*, and *Streptococcus thermophiles*.[172] Iron nitride, especially iron (III) nitrate nonahydrate, was shown to help build a structure like pPy. The bacterial cells were submerged in a solution of iron (III) nitrate nonahydrate in the first step of bacterial cell preparation, therefore enabling the substance to be absorbed into their outer layers. Then pyrrole started the polymerization process for pPy. According to research results, bacterial cells survived, and it was noted that the coating had no appreciable effect on their multiplication. Moreover, with respect to the electrical characteristics, the use of the conductive polymer pPy has resulted in an amazing rise in power density, so attaining a 14.1-fold increase over the unmodified *Shewanella oneidensis*, with a power density of 147.9 μW/cm^2. The pPy method was used for self-encapsulation of microorganisms, subsequently its possible uses in MFC were investigated. That work is especially concentrating on the utilization of Asp*ergillus niger* and *Rhizoctonia sp*.[76,129,173]

Scanning electrochemical microscopy (SECM) was used to evaluate MFC.[130] Investigating the electrochemical characteristics of immobilized transformed cell cultures found a three-fold improvement over the control group and quite notable rise in current generation. The highest current noted was I_{max}=0.30 nA. By contrast, the cultures that experienced transformation showed a clear rise to reach a peak current of I_{max}=0.86 nA.[130] Examining the surface approach curve produced some rather interesting revelations. Furthermore, the findings of these investigations revealed many elements influencing charge transfer efficiency, a necessary condition to produce current in MFC. The aspects under discussion include: (I) the spatial interactions among the individual cells and the ultra-micro electrode employed in SECM; and (II) changes happening on the surfaces of bacteria. Then recorded is the nominal current output of 0.47 nA arising from the ultra-micro electrode placed 1.5 times higher above the test sample than the control sample.

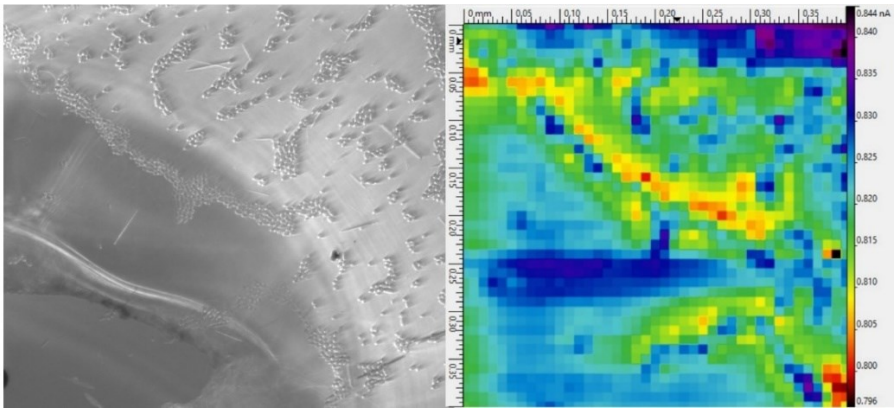

Figure 5. Example of the authors work with SECM. Optical microscope (on the left) image and SECM generation-collection (GC) mode generated image (on the right) side by side to represent specific cell agglomerates and their electrochemical activity. The images represent a real-time view of the same Petri dish.

Another work offers a thorough analysis of the effective alteration of White-rot fungus isolates belonging to the *Trametes spp* group enabled by the use of pPy.[130] The production of pPy inside the fungal hyphae is much influenced by the laccase enzyme, which is generated and released by *Trametes spp.* fungus into the surrounding growth conditions. An unprocessed enzyme extract helped pyrrole polymerization to proceed during cell development on a growth media.[174] Clearly, the synthesis of bio-assisted polymers during that era was unique and, to the best of our knowledge, one of the fundamental research that enabled the effective use of enzyme-assisted techniques in the manufacturing of CPs.[175–179] Later, as underlined in some studies,[49,50,129,130] the creation of polymer-based coatings in the framework of cell culture has taken front stage in research. Studies on cells altered using CPs reveal improved electron transfer process efficiency. This development helps these microorganisms be used in the domains of MFCs[76] and biosensors.[180,181]

Inside the context of bio-synthetic polymers, there is an interesting possibility to improve electron flow in fuel cell.[182] This achievement underlines not just the fresh contributions given to the area but also the important part live cell-induced polypyrrole synthesis performs in it. pPy was generated quite satisfactorily by suspending the K562 leukemia cell line and using the manufacturing technique detailed in our earlier work.[183] The pyrrole polymerization approach proposed by the scientists presents a different one from the one seen in Figure 4. This change might be explained by the effect of cell exudate molecules instead of dependent on the oxidoreductase systems

present in the plasma membrane. Furthermore, studies focused on comprehending the processes by which cancer cells die within the framework of pyrrole polymerization. This element serves as a "reverse pro-drug", therefore offering another use for the pyrrole polymerization process. In the framework of cell death, the deadly molecule pyrrole shows a propensity to polymerize, producing a biocompatible conductive polymer pPy.[184] Black in color, this polymer has special qualities that make it especially appropriate for use as an optical dead cell indicator.

2.9 Microbial Experimentation

It is interesting, nonetheless, that the Fe^{+3} state does not set off the polymerizing mechanism. Redox reactions involving Fe^{+2} and Fe^{+3} ions help to clearly decrease concentration, which starts the polymerization processes using non-toxic monomers. In cellular biology, it is crucial to highlight the significant accomplishments of cells, particularly regarding their abilities in metal reduction. Notable organisms such as *Cupriavidus metallidurans*, *Escherichia coli*, and *Clostridium sporogenes* have made considerable progress beyond the stage of Atom Transfer Radical Polymerization (ATRP) by employing a range of monomers, including poly(ethylene glycol methyl ether methacrylate), hydroxyethyl methacrylate, N-Hydroxyyl acrylamide, 2-Acrylamido-2-methyl-1-propanesulfonic sodium, and 2-(Methacryloyloxy) ethyl dimethyl-(3-sulfopropyl) ammonium hydroxide.[185] In this context, researchers have presented an innovative approach for the advancement of cell-assisted polymerization. Reduced to Fe^{+2} in a regulated manner, Fe^{+3} – which is unable of commencing polymerization – initiates the polymerization of monomers harmless to cells and participates in redox processes of Fe^{+2}/Fe^{+3}. They demonstrate an impressive ability to sustain their lifespan while preserving their functional capabilities.

Apart from pPy, many additional polymers are used for cell modification with a goal to improve their performance within especially developed MFC. In a same vein, *S. xiamenensis* were subjected to polydopamine (PDA) coating.[185] Particularly specific strains of bacteria may stick to PDA when biofilms develop on MFCs. Under aerobic circumstances and somewhat alkaline surroundings – more especially, at a pH of 8 – this process takes place by oxidative polymerization. Researchers reported in their results that PDA-modified, namely *S. xiamenensis* cells, bacteria showed a greatly increased power density of 452.8 mW/m^2. Compared to non-modified cells, this amazing output was 6.1 times more than that seen in the MFC system generating a power density of 74.7 mW/m^2. Moreover, the development of

conductive PDA additives happened in only three hours, which may be regarded as a rather quick procedure. Moreover, it seems that the change of bacteria had an insignificant effect on cell viability, thereby reducing only 2–3%. regularly covered with PDA, *Shewanella oneidensis* MR-1 is one of the most extensively used bacteria in the construction of MFCs. Yu et al.[186] found in their studies that while using the same bacterial strains to help the biomineralization of iron sulfide (FeS) nanoparticles, cell-assisted synthesis may be used to produce conductive PDA. The results revealed different interfaces connecting to a cell at different degrees of contact. As such, the electric and electrochemical characteristics show different changes. A remarkable output of up to 3.2 W/m^2 was obtained by the research showing that the interface of polysulfide reductase mineralized FeS nanoparticles greatly improved the efficiency of MFC anodes. Producing just 0.2 W/m^2, its performance was found to be 14.5 times higher than that of anodes altered with native *Shewanella oneidensis* cells. By comparison, anodes covered with PDA had a current density of over 0.6 A/m^2.

Researchers have shown another method by internalizing pre-synthesized carbon dots (CD) and carbon nanoparticles into *S. oneidensis* and *Shewanella xiamenensis,* respectively.[187,188] Both investigations revealed notable impacts of carbon dots (CD), which showed great degree of biocompatibility. Furthermore, via significant rise in internal ATP levels, CD might enhance metabolic activity. Given the circumstances, it was suggested that improved metabolic activities might produce unwanted reactive oxygen species. Still, it was not the current scenario. Moreover, the development of photoactive particles by CD helps lactate to be consumed, which generates current when exposed to light. Whereas the control group recorded a current density of 0.19 A/m^2, the greatest current density attained with *Shewanella oneidensis* MR-1, was 1.23 A/m^2. The greatest power density recorded in the MFC running CD in the meanwhile came out to be 0.491 W/m^2. Being 6.46 times more than the control, which used the identical non-modified microorganisms and reported a power density of 0.076 W/m^2, this number shows an amazing increase. *Shewanella xiamenensis* obtained a current density of 329.4 $\mu A/cm^2$ under certain lighting conditions and using lactate as the only carbon source. This amazing result shows 4.8 times increase above the 68.1 $\mu A/cm^2$ control test.

Osmium redox polymers find applicability in the construction of microbial fuel cells (MFCs), as suggested in the references.[157,189–192] By use of [Osmium (2,2'-bipyridine)(poly-vinylimidazole)10Cl]Cl, cells were efficiently immobilized and linked to the electrode surface.[193] For the bacterial cells of *Gluconobacter oxydans*, the pre-synthesized polymer was both a conductive binding matrix and a co-mediator. Drop coating techniques used on glassy

carbon paste electrodes helped to achieve the electrode designs. Together with an open circuit potential value of 176 mV, the researchers effectively obtained a maximum charge density of 15.079 mA/cm^2.

2.10 Challenges, Limitations, and Future Outlook

Here we reviewed and gave a summary of the newly developed technologies and approaches meant to raise the performance of MFCs. Many molecules - either directly into the structure of the cells or as a protective layer - were introduced to achieve this success. Three main categories define the technologies: engineering of cell surfaces, different approaches for internalization, and synthesis of biofilms. The production of polymeric coverings and the integration of polymers into live cells are two of the most amazing methods for cell modification. It is important to acknowledge that some limitations still exist even if a lot of evidence shows how alteration influences charge transfer.[76] Some modifications have a level of complexity that would cause challenges for real MFCs.[157,189–192] The main constraints are on the survival and multiplication of microorganisms as the newly produced cells in microbial fuel cells either inherit traits from their ancestors or undergo certain changes. When all the elements are considered, the negative effects already described greatly influence the lifetime and steady electrical generation of the MFCs. Given the circumstances, the changes made to the cell surface should have a synergistic impact with the other approaches covered in this study to improve the general power production from MFCs.

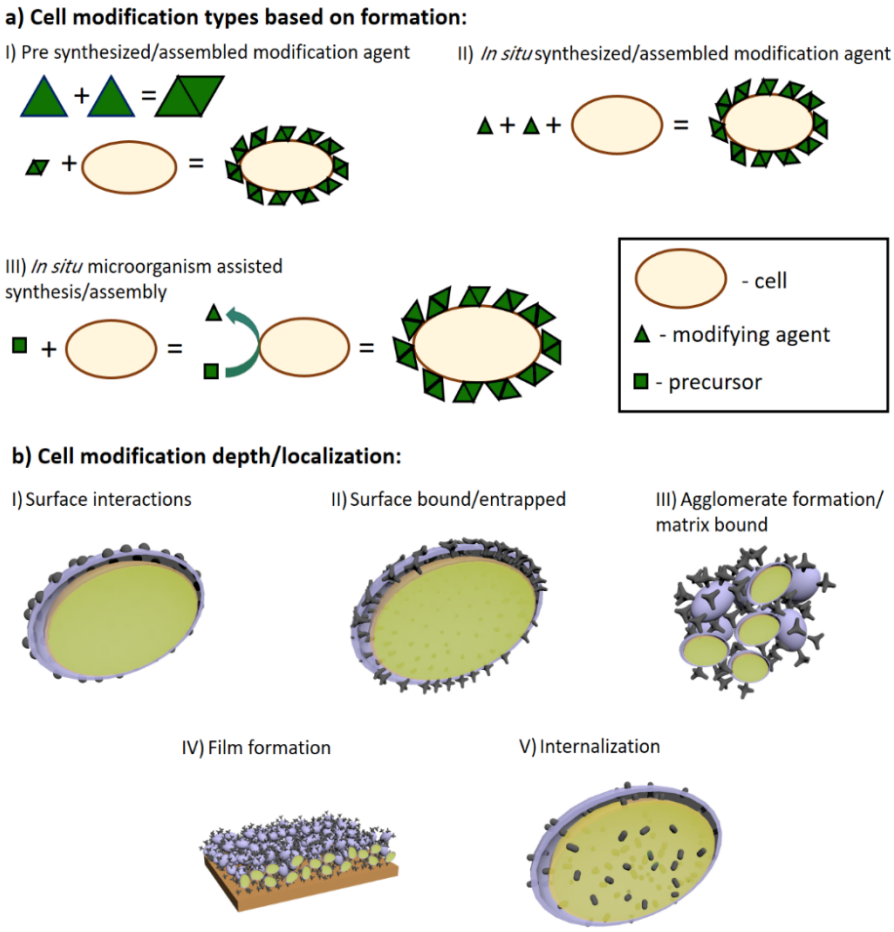

Figure 6. A schematic representation illustrating the modification of cells through the principle of agent formation (A). Cells can undergo modifications through various approaches: one method involves the use of pre-synthesized compounds (I), while another approach entails the assembly or synthesis of these compounds in situ, directly in the presence of living cells (II). There is a way in which the cells actively support or catalyze the synthesis and assembly of the modifying agent in situ, it is represented in (B) section: (I) adsorption and electrostatic interactions are among the many mechanisms that help one to grasp surface interactions; (II) the modifying agent could create complex, inseparable structures with cell walls or like entities or generate covalent connections; (III) the altering chemical might cause aggregates from its matrix and surrounding cells to develop; (IV) there is a clear inclination toward a higher organization of agglomerates on surfaces; (V) also there is internalizing of the altering agent. Adapted from [194]

Table 1. Description of the MFC anode modification method and performance. Abbreviations are provided below the table. This table provides a comprehensive overview of the MFC anode modification technique, exploring its various aspects and assessing its effectiveness in practical applications. The abbreviations can be found listed beneath the table. Adapted from [195] and expanded.

Anode	Anode material/ Electron donor	PD, mW/m^2	Ref.
Bacillus subtilis on aldrithiol monolayer and OsRP	Gold, Graphite/ Succinate	-	[157]
Saccharomyces cerevisiae on PQ and MWCNTs	Graphite/ Glucose	1.13	[51]
Saccharomyces cerevisiae	Carbon paper/ Glucose	3	[196]
Scedosporium dehoogii	CF/ APAP	6.5	[197]
Shewanella loihica on PANI and carbon nanotubes	APTES, ITO/ Sodium lactate	34.5	[198]
Scedosporium dehoogii	CF/ APAP, Lignin	50,16	[199]
Saccharomyces cerevisiae with CNTs	PU/ Glucose, MB	100	[153]
Thermincola ferriacetica	Graphite/ DSMZ	146	[200]
Saccharomyces cerevisiae on PEI and one of the QS molecules (phenylethanol, ryptophol and tyrosol).	CF/ Glucose	159* 156 135	[201]
Gammaproteobacteria and *Negativicutes* on MWCNTs blended with biogenic Au	CF/ Sludge	178	[152]
Saccharomyces cerevisiae on PEI and CNTs	CNTs/ Glucose	344	[156]
Escherichia coli	Platinized titanium/ Glucose	502	[202]
Candida melibiosica	CF/ Methylene blue	640	[203]
Pseudomonas aeruginosa	Chitosan, vacuum-stripped graphene/ Glucose	1530	[204]
Saccharomyces cerevisiae on PEI and AuNPs	CF/ Glucose	2771	[155]
Saccharomyces cerevisiae on alginate	CF/Glucose	3900	[205]
Saccharomyces cerevisiae on PEI, with SDBS and FeMnNPs	CF/ Glucose	5838	[154]

* – power densities for MFCs based on phenylethanol, ryptophol and tyrosol, respectively

APAP – acetaminophen	OsRP – osmium redox polymer
APTES – γ-aminopropyltriethoxysilane	PD – power density
DSMZ – Deutsche Sammlung von Mikroorganismen und Zellkulturen (bacteria growth medium)	PEI – polyethylenimine
MB – methylene blue	PU – polyurethane
MWCNTs – multi-walled carbon nanotubes	PQ – 9,10-phenanthrenequinone
NPs – nanoparticles	QS – quorum sensing

3. MATERIALS & METHODS

3.1 Materials

For the SECM investigation methodology, the following materials were used. Phosphate buffer (pH 6.5) containing 0.05 M Na_2HPO_4, 0.05 M NaH_2PO_4, and 0.1 M KCl was prepared in distilled water. The redox mediator ferrocene monocarboxylic acid (FcCOOH) was dissolved in phosphate acetate buffer or 96% ethanol from UAB Vilniaus Degtine (Vilnius, Lithuania). All chemicals used in the study were purchased from Sigma-Aldrich (St. Louis, USA). The following cell culture components were used: Iscove's Modified Dulbecco's Medium (IMDM) and fetal bovine serum (FBS) (Gibco, Langley, USA), 100× penicillin and streptomycin solution, fibronectin from Merck (Carrigtohill, Ireland), and gelatin from Calbiochem (San Diego, USA).

For cell surface marker analysis, atrial hmMSCs were harvested using 0.25% trypsin/EDTA, centrifuged at 500×g for 5 minutes, and resuspended in PBS containing 2% BSA (Sigma Aldrich, St. Louis, MO, USA). Cells were incubated on ice for 30 minutes, then washed once with PBS and incubated with antibodies against standard MSC surface markers: CD29-IgG1-APC (1A-219-T100, Exbio, Praha, Czech Republic); CD44-IgG2b-FITC (555478, BD Biosciences, San Jose, CA, USA); CD90-IgG1-FITC (328108, BioLegend, San Diego, CA, USA); CD105-IgG1-APC (MHCD10505, Thermo Fisher Scientific, Waltham, MA, USA); CD45-IgG2a-FITC (sc-70686, Santa Cruz Biotechnology, Dallas, TX, USA); CD34-IgG1-FITC (1F-297-T100, Exbio, Praha, Czech Republic); CD73-IgG1-FITC (561254, BD Biosciences, San Jose, CA, USA); CD40-IgG1-APC (555591, BD Biosciences, San Jose, CA, USA); and CD14-IgG2a-APC (301808, BioLegend, San Diego, CA, USA). After incubation, cells were washed, centrifuged, resuspended in PBS with 2% BSA, and analyzed using a BD FACSAria™ II flow cytometer.

Cells were grown in complete medium (IMDM with 10% FBS), cardiac differentiation medium (DMEM/F12 with 2% FBS), and differentiation medium supplemented with 1 or 2 μM SAHA for 3 days. On the day of measurement, cells were detached using trypsin/EDTA, centrifuged at 500×g for 5 minutes, washed with PBS, and fixed with 4% paraformaldehyde for 15 minutes at room temperature (RT). After fixation, cells were washed and permeabilized with PBS containing 0.1% Triton X-100 for 15 minutes at RT. Cells were then incubated with anti-acetyl lysine primary antibody (ab21623, Abcam, CA, USA) for 60 minutes at 37°C. Following washing with PBS containing 1% BSA, cells were incubated with a secondary antibody (A-

11008, Thermo Fisher Scientific, MA, USA) for 30 minutes at 37°C. After a final wash, cells were analyzed by flow cytometry (BD FACSAria™ II) and data analyzed with FACSDIVA software.

For the investigation of MFCs electrochemically and biologically, these materials were used. Carl Roth supplied potassium ferrocyanide (>99%) and potassium ferricyanide. Cyclopore Track Etched Whatman®, YPD broth, D-(+)-glucose (99%), citrate-buffered 10 nm gold sphere nanoparticles (OD=1), phosphate-buffered saline (PBS) tablets, pyrrole (98%), and 9,10-Phenanthrenequinone were purchased from Merck. The yeast cell strain *S. cerevisiae* Y00000 (BY4741 Matαhis 3Δ1 leu 2Δ0 met 15Δ0 ura 3Δ0) was sourced from EUROSCARF in Frankfurt, Germany. Thermo Fisher supplied the graphite rod electrodes (99.9995%). Spiritus Vilnensis supplied ethanol (96%).

3.2 Isolation and characterization of human atrial hmMSCs

3.2.1 Human atrial tissue procurement and hmMSC isolation

Human healthy heart biopsies were obtained from the right atrial myocardium of patients without mitral valve disease and with a non-dilated left ventricle. Dilated right atrial samples were collected during mitral valve surgery from patients with clinically diagnosed dilated hearts. Biopsies were collected after obtaining informed consent at Santariškių Clinic (Bioethics approval No. 158200-14-741-257).

Biopsies from the human right atrium were kept on ice and transported to the laboratory for hmMSC isolation. Cells were isolated following previously published protocols with slight modifications (Davis et al., 2009; Miksiunas et al., 2020). Briefly, biopsy specimens were minced into fragments smaller than 2 mm^3, washed once with PBS containing 2% antibiotics, and digested with trypsin for 15 minutes. After digestion, tissue explants were cultured on fibronectin (2 mg/ml)-coated 6-well plates in IMDM supplemented with 10% FBS and 1× PEST (100 U/ml penicillin G and 100 U/ml streptomycin). Within 2–3 weeks, a layer of stromal-like cells appeared. When cultures reached confluence, cells were detached using trypsin and seeded into gelatin-coated flasks for further growth. Isolated stromal-like cells were characterized by expression of mesenchymal stem cell markers (Lv et al., 2014). Under standard culture conditions, hmMSCs were maintained in complete IMDM (IMDM with 10% FBS and antibiotics). For electrochemical measurements, cells were incubated in cardiomyogenic differentiation medium DMEM/F12

with 2% FBS (referred to as Diff. medium) or DMEM/F12 with 2% FBS supplemented with 1–2 μM HDAC inhibitor SAHA for 3 days.

3.2.2 Morphometric analysis of hmMSC cell size

Healthy and pathological atrial hmMSCs were seeded and grown until reaching 60–80% confluence. Cell attachment area was measured using the ImageJ software. Micrographs were calibrated to estimate cell surface area in square micrometers. Individual cells were outlined to determine their attachment area. Size distribution was calculated from 150 cells (n=150) derived from three separate micrographs per group (healthy or pathological). Data analysis was performed using GraphPad Prism 6.0 and Microsoft Excel.

3.2.3 Evaluation of mitochondrial membrane potential

Mitochondrial membrane potential (MMP) was assessed using the JC-1 dye and flow cytometry. JC-1 accumulates in mitochondria in a potential-dependent manner, forming red fluorescent J-aggregates at high membrane potential (excitation 488 nm, emission 595 nm; PE channel). At low membrane potential, JC-1 remains monomeric and fluoresces green (excitation 488 nm, emission 530 nm; FITC channel). The ratio of red to green fluorescence reflects mitochondrial activity, with healthier mitochondria exhibiting a higher PE/FITC ratio.

Cells were cultured in complete medium, differentiation medium, or differentiation medium with 1 or 2 μM SAHA for 3 days. After treatment, cells were incubated with 5 μM JC-1 dye at 37°C for 30 minutes, washed with PBS containing 1% BSA, and analyzed by flow cytometry. MMP was expressed as the PE/FITC fluorescence ratio.

3.2.4 Determination of total intracellular NAD^+ levels

Total intracellular NAD^+ levels were measured using Cayman's NAD/NADH Cell-Based Assay Kit (Cayman Chemicals, 600480), a colorimetric assay detecting intracellular NAD^+ and NADH in cultured cells. NAD^+ is reduced to NADH by alcohol dehydrogenase during ethanol oxidation to acetaldehyde. The resulting NADH oxidizes a tetrazolium salt substrate (WST-1) to a colored formazan, measurable at 450 nm. Formazan production is proportional to total NAD in cell lysates.

Cells were seeded in 96-well plates and grown in complete medium, differentiation medium, or differentiation medium supplemented with 1 or 2 μM SAHA for 3 days. Cells were lysed and processed according to the

manufacturer's instructions. NAD^+ concentration was calculated from a standard curve and expressed as nM/mg protein.

3.2.5 Preparation of hmMSCs for SECM measurements

For electrochemical experiments, 5×10^3 healthy and pathological right atrium-derived hmMSCs were seeded on 12 mm diameter coverslips coated with 0.2% gelatin, placed in 3 cm Petri dishes, and incubated for 24 hours. Cells were then cultured in IMDM with 10% FBS and antibiotics, cardiomyogenic differentiation medium (DMEM/F12 with 2% FBS), or differentiation medium supplemented with 1–2 μM HDAC inhibitor SAHA for 3 days. Prior to measurements, media were replaced with IMDM without FBS, supplemented with 25 mM HEPES. Samples were transferred to the electrochemical SECM cell for measurements. Each sample was measured for no longer than 30 minutes, which caused negligible (<5%) changes in cell metabolic activity as assessed by CCK-8 reagent (data not shown).

3.2.6 Ethical Statement and Statistical analysis

This study was conducted in accordance with the principles of the Declaration of Helsinki. The protocol was approved by the local Ethics Committee (license No. 158200-14-741-257). All patients provided written informed consent for each investigational procedure.

Statistical analysis was performed using data from experiments with 2–3 cells of each type per experiment. Analyses were conducted using GraphPad Prism and Microsoft Office Excel software. Data are presented as mean ± SD. Statistical significance was considered at $*p \leq 0.05$, $**p \leq 0.01$, and $***p \leq 0.001$ when comparing cell types and the effects of SAHA on the cell samples.

3.3 SECM measurements evaluations

3.3.1 Electrochemical assessments, Hill's function

Particularly in cyclic voltammetry analysis, the application of sigmoidal fitting functions is a useful tool for interpreting current-potential relationships, especially when dealing with complex, biologically mediated electron transfer, in the electrochemical characterization of MFCs.

It is used to simulate the form of the current response connected with redox-active activities at the electrode interface. Originally designed for biochemistry to explain ligand-binding cooperativity, this mathematical model has proved useful in electrochemical systems including biofilm-based

or microbial electron transfer because it can account for cooperative or multi-site reaction mechanisms that often arise in biological environments. In MFCs using modified microorganisms like yeast, the electron transport to the electrode may follow many, perhaps interacting paths, hence classic linear or solely Nernstian models are not adequate to completely characterize the behavior of the system. The peaks of the CV were evaluated using a modified Hill function with an offset:

$$j = \frac{C^n}{k^n + C^n} \tag{2}$$

where j is the current density, C is the glucose concentration, k is a constant that determines glucose concentration at half of the maximum current density registered, and n is Hill's coefficient.

By including an offset potential into the Hill function, the peak position of the modeled current may be matched with the formal or midway potential of the redox-active mediators or biological electron carriers in the system. In MFC investigations, where the addition of CPs or nanoparticles alters the electron transfer channel and changes the apparent redox potential, this is extremely helpful. Deconvolution of capacitive contributions and separation of the faradaic component related with direct microbial electron transport is made feasible by fitting CV data to this form. Furthermore, revealing the cooperative character or kinetic sharpness of the redox process is the Hill coefficient (n).

Thus, in microbial fuel cell research, the use of the Hill function appropriate offers a strong, interpretable, and comparable approach for evaluating and optimizing electron transport properties.

3.3.2 Evaluation of hmMSCs redox activity by SECM

SECM and a disk-shaped Au-based ∅50 µm UME with R_g value of 10, which represents a ratio between the radius of the insulating and the radius of the conducting part of the UME, both were purchased from Sensolytics (Bochum, Germany) and were used for SECM-based experiments. Measurements were performed using a potentiostat Autolab 128N from Metrohm AG (Herisau, Switzerland). Before the experiment, the UME was cleaned with ethanol, then it was polished with 0.3 µM grain-size polishing paper, and cyclic voltammetry was performed in 0.5 M H_2SO_4 solution in a range from 0 to 1.7 V with a step of 50 mV until no redox peaks were observed. Measurements were performed in a three-electrode electrochemical

cell, where the UME was connected as a working electrode, Pt wire was used as an auxiliary/counter electrode and Ag/AgCl in 3M KCl served as a reference electrode. The electrochemical measurements of the cells were performed in regular IMDM growth medium and differentiation medium with and without 1 or 2 μM of HDAC inhibitor SAHA. The FcCOOH is a cell impermeable redox mediator, and the working concentration was 6 μM.

3.3.3 Parameters of SECM measurements

The approaching curves were registered by moving the UME in a vertical (z) direction at 0.5 μm/s speed, 0.5 μm step, with a hold time of 10 ms. The reduction of $[FcCOOH]^+$ near the cell membrane generated an electrical current measured at +400 mV vs Ag/AgCl 3M KCl. Approach curves were registered at different points, 20 curves for each experiment.

3.3.4 Mathematics of electrochemical measurements

Approach curves were fitted to the mathematical model following Cornut and Lefrou's approximations, [206] which were based on Bard–Mirkin's formalism, [26] where probe parameters (r_T – the conductive electrode radius and R_g– r_{glass}/r_T, r_{glass} – insulating shroud of the electrode) are obtained separately from the approach experiments. SECM approach curves are represented with normalized tip current versus normalized distance according to the outline in Eqs. 3 and 4:

$$I_T = \frac{i_T}{i_{T,\infty}} \tag{3}$$

$$L = \frac{d}{r_T} \tag{4}$$

where i_T – is experimentally measured tip current, r_T – UME tip radius, $i_{T,\infty}$ – steady-state current, d – the distance between the tip and the sample.

The steady-state current is dependent on diffusion of the redox active species when UME is far from the sample surface and can be described by [14]:

$$i_{T,\infty} = 4\, n_e\text{-}FDCr_T \tag{5}$$

where n_e- is the number of electrons involved in the reaction on the UME, F – Faraday's constant, D – diffusion coefficient of redox species, C – concentration of the FcCOOH, and r_T – radius of the UME.

Even though redox species form on the tip and are recovered by the sample *via* redox reaction at a constant rate λ. Living cells are not total electric current insulators nor conductors but rather something in between; therefore, the tip current, according to Cornut and Lefrou must be governed by a mathematical model which covers both surface types [206]:

$$I_T(L,\lambda,R_g) = I_T^{cond}(L,R_g) + \frac{I_T^{ins}(L,R_g)-1}{(1+2.47{R_g}^{0.31}L\lambda)(1+L^{0.006R_g+0.113}\lambda^{-0.236R_g+0.91})} \quad (6)$$

where, $I_T^{cond}(L,R_g)$ – is model for conductive surface, $I_T^{ins}(L,R_g)$ – is model for insulating surface, λ – is kinetic constant, R_g– ratio between radius of insulating shroud and radius of conductive surface, L – normalized distance.

$$I_T^{cond}(L,R_g) = \alpha(R_g) + \frac{\pi}{4\beta(R_g)ArcTan(L)} + \left(1-\alpha(R_g)-\frac{1}{2\beta(R_g)}\right)\frac{2}{\pi}\,ArcTan(L) \quad (7)$$

$$\alpha(R_g) = ln2 + ln2\left(1-\frac{2}{\pi}\,ArcTan\left(\frac{1}{R_g}\right)\right) - ln2\left(1-\left(\frac{2}{\pi}\,ArcCos\left(\frac{1}{R_g}\right)\right)^2\right) \quad (8)$$

$$\beta(R_g) = 1 + o.639\left(1-\frac{2}{\pi}\,ArcCos\left(\frac{1}{R_g}\right)\right) - 0.186\left(1-\left(\frac{2}{\pi}\,ArcCos\left(\frac{1}{R_g}\right)\right)^2\right) \quad (9)$$

$$I_T^{ins}(L,R_g) = \frac{\frac{2.08}{{R_g}^{0.358}}\left(L-\frac{0.145}{R_g}\right)+1.585}{\frac{2.08}{{R_g}^{0.358}}(L+0.0023R_g)+1.57+\frac{lnR_g}{L}+\frac{2}{\pi R_g}\ln\left(1+\frac{\pi R_g}{2L}\right)} \quad (10)$$

From the fitted approach curve, the kinetic constant λ can be calculated. All approach curves were fitted using this method, and statistics were calculated with a 95 % confidence level for the experimental parameters, and λ is presented as a mean ± standard error.

3.4. MFC preparation and evaluation

3.4.1 Yeast solution preparation

Using a laminar flow cabinet and a thermo-regulated shaker, Batch Y00001 developed a *S. cerevisiae* culture. Using YPD broth - yeast extract peptone dextrose solution - yeast proliferation was increased in a +30°C incubator under agitation at 200 revolutions per minute. Made from a peptone solution in deionized water, this broth has glucose and yeast extract added. Every single inoculation of the YPD broth made use of a 100-microliter cultured *S. cerevisiae* solution derived from a frozen, extremely deep-level library sample. Every batch was generated within a 24-hour growth cycle. Not one of the batches kept for more than forty-eight hours after the end of the development phase. Every time the growing process stopped, the PBS yeast solution was rinsed. The process consisted of centrifugation for two minutes at 3000 rpm at room temperature after the yeast solution was transferred to Eppendorf tubes. Every tube had its supernatant collected; PBS was then added back to the precipitate; the solution was mixed using an automated micropipette; and centrifugation was once again conducted. The contents of the tube were diluted to a 1:1 mass ratio with PBS using a PBS density of 1 g/L, therefore guaranteeing a standardized yeast solution of 1 g/mL after centrifugation and subsequent supernatant removal. The experiment applied the modifications in addition to this solution.

3.4.2 Electrode preparation

Graphite rod electrodes, 3.05 mm diameter x 30 mm long, were polished using various sanding papers with grit sizes ranging from 300 to 10000, cleaned with 96% methanol and deionized water, and dried. All of it is done to sustain the traceability of the experiments conducted and to ensure that the environment does not contaminate the electrode in any way. The graphite electrode was placed in a silicone tube to cover and insulate ¾ of the electrode side – the rest is left for the adaptors of the wiring and the experiment itself. The working surface area is 7.302 mm^2.

9,10-phenanthrenequinone (PQ) was used as the lipophilic mediator; when dry, it was dissolved in 96% ethanol, and a 2 µL 3 mM drop was deposited onto the graphite electrodes. The concentration and the amount are chosen due to expertise of our laboratory. Furthermore, every electrode was modified by drop-casting 2 µL of 1 g/L of yeast solutions, which were either non-modified or modified by gold nanoparticles and/or polypyrrole.

Also, in the later research period, a 3mM solution of 9,10-phenantrenequinone was prepared in 96% ethanol; 4 µL of the mediator solution was drop-casted onto the polished end of the graphite electrode. After the solvent had evaporated, 2 µL of the yeast cell solution was applied to the mediator modified surface. Lastly, the electrode surface was covered with a membrane and held in place with laboratory tape. The prepared electrode was submerged in PBS. The prepared system scheme and theoretical working mechanism can be observed in Figure 7 diagram.

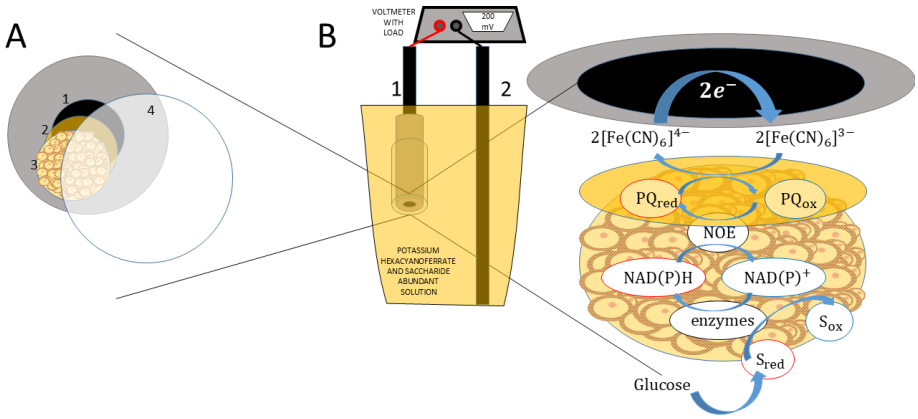

Figure 7. Our MFC structure working mechanism. Yeast metabolizes saccharides and the double-mediator system ensures electron transfer through the electrodes. Polymeric and nanoparticle modifications can enhance the conductivity of the yeast cells not to jam the current or the electrode. All-holding PCTE membrane with 3 µm pores ensure the yeast colony presence on the anode.

The finalized electrode construct was immersed in PBS due to its isotonic properties and ability to buffer pH levels. This choice was made to ensure that cellular integrity is preserved during the various measurement phases. PBS effectively reduces electrochemical interference because its ionic components, including Na^+, K^+, Cl^-, and PO_4^{3-}, do not react with the redox couples used in this system. The prepared configuration represents a thoughtful balance that considers biological viability, the efficiency of mediator-electrode interactions, and the physicochemical stability necessary for consistent electrochemical measurements. Figure 7 offers a schematic representation of the system configuration and the proposed theoretical mechanism. This visual framework aids in understanding the electron transfer pathways, enhancing

the interpretation, and supporting further data analysis within the realm of microbial fuel cell development.

3.4.3 Modifications by polypyrrole and nanoparticles

The polypyrrole modification was performed according to a patent [207] recipe with some changes. The main ingredient, pyrrole, was introduced in the solution, consisting of potassium ferrocyanide (II), glucose, and yeast solution, all in PBS at a volumetric ratio represented in Table 1.

Table 1. Preparation of polypyrrole modified yeast, the recipe.

Component	Initial concentration	Mixture concentration
Yeast	1 g/mL	0.2 g/mL (20 %)
Glucose	1 M	400 mM (40 %)
Potassium ferrocyanide (II)	0.4 M	80 mM (20 %)
PBS [1]	0.1 M	0.1 M
Pyrrole	98 %	8 mM / 0.112 % to 200 mM / 2.8 %

Main solvent, consisting of pH 7.4 standard PBS solution in water.

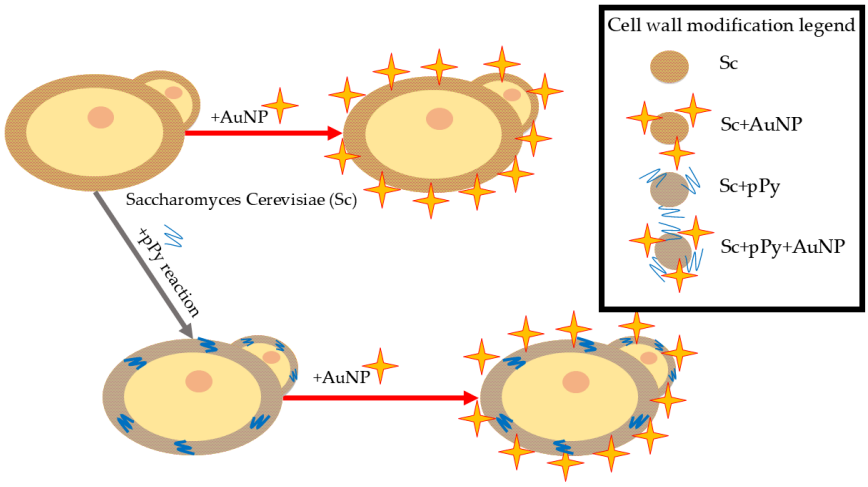

Figure 8. *S. cerevisiae* (Sc) modification scheme. pPy – polypyrrole within yeast cell wall. AuNP – gold nanoparticles, 10 nm spheres.

10 nm gold sphere nanoparticles were used for additional modifications. The ratio for modification was two-parts yeast solution per one part of nanoparticle solution as the previous, non-published, experimentation suggested. Table 1 specifies the appropriate volumetric ratios for the operation, carefully prepared to enhance polymer coverage and guarantee that

cytotoxicity or metabolic inhibition impacting the yeast population is not present.

3.4.4 Viability investigation

A 100 µl yeast suspension is diluted with PBS buffer solution to achieve a concentration of 10^5–10^6 cells per solution. 100 µl of the diluted yeast suspension is plated onto agar-solidified YPD medium. Petri dishes are incubated in a thermostat for 48 hours at 30°C temperature. Colonies are counted, and the number of colony-forming units (CFU) per milliliter is determined using the following formula:

$$CFU = A \cdot 10^n \cdot 10 \quad (1)$$

Where:

CFU – number of viable yeast per 1 ml;
A – number of colonies on the plate;
10^n – dilution factor;
10 – correction factor accounting for 0.1 ml of suspension plated onto the dish.

The vitality of *S. cerevisiae* living cells was studied as they are the only ones able to perform metabolic activities producing electrons. When yeast cells lose their vitality they cannot function in the generation of electrical current, which finally reduces the running efficiency of the fuel cell. This is because the yeast cells cannot generate electrical current on their own and are basically killed by the environment and mediators used. To ensure that the system is running as it ought to and that the microorganisms are behaving as they should, viability testing is done.

3.4.5 CV and DPV measurement parameters

A three-electrode setup consisted of a PQ and yeast-modified graphite MFC as a working electrode, an Ag/AgCl reference electrode and a platinum counter electrode (Metrohm AG, Switzerland). The electrochemical cell is filled with PBS containing 20 mM of potassium ferricyanide ($K_3[Fe(CN)_6]$) and 20 mM of glucose. Experiments started after 20 minutes. All electrochemical measurements were conducted using a potentiostat Autolab PGSTAT302N (Metrohm AG, Switzerland). Measurements were conducted mainly by sweeping the potential from -0.6 V to +0.6 V, at 50 mV/s rate.

This work used a conventional three-electrode configuration, which is a standard established out in the area of electrochemical research, to properly control and measure the potential of a working electrode with respect to a stable reference electrode.[208] Examining the paths of electron transport at the electrode interface and evaluating the electrochemical performance of the modified microbial fuel cell (MFC) electrode system mostly drives this arrangement.

The reference electrode for the prospective control was Ag/AgCl electrode. Ag/AgCl is sometimes used as a reference electrode in aquatic systems because of its stable and well-defined potential. Thus, in the realm of electrochemical study, it is a useful substance for doing comparative tests. The counter electrode was a platinum wire chosen for its exceptional conductivity and durability in electrochemical procedures. This decision guaranteed suitable balancing of any current passing through the system, therefore maintaining the consistency of the experimental findings.

Phosphate-buffer saline (PBS), which created a steady ionic environment, filled the electrochemical cell itself. The cell's pH and ionic strength stayed the same thus it fit for both biological and electrochemical processes. A potassium ferricyanide ($K_3Fe(CN)_6$) (20 mM) solution was introduced to the PBS solution to enable electron transfer activities and simulate electron acceptor conditions.

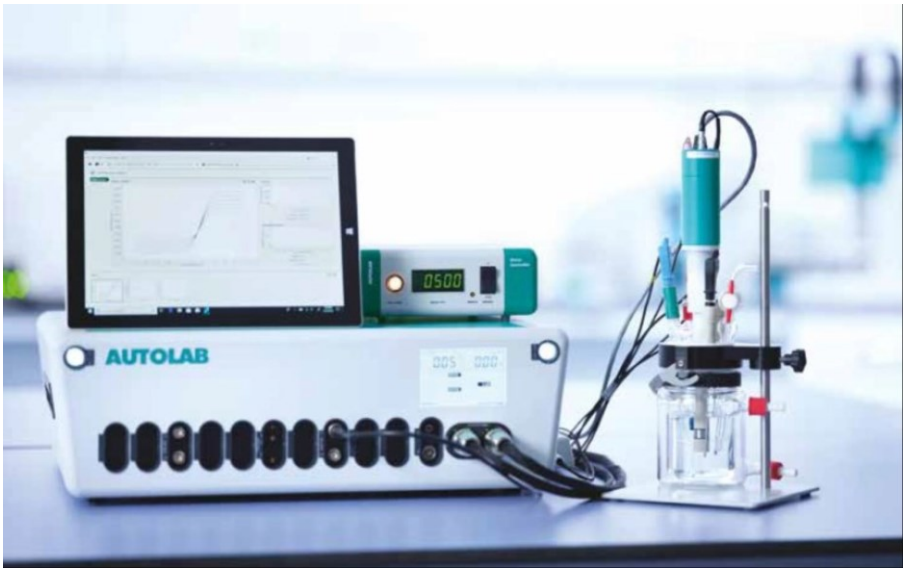

Figure 9. Representation of the potentiostat of Methrom, Autolab PGSTAT302N, used in our research. Image taken from Labx.com[209]

All the electrochemical tests were conducted using a high precision potentiostat (Autolab PGSTAT302N, Metrohm AG, Switzerland, Figure 9). This strong potential allowed exact control of the applied potential as well as thorough study of the current responses. Using cyclic voltammetry (CV), which involved sweeping the voltage of the working electrode from -0.6 V to +0.6 V at a scan rate of 50 mV/s, an amount of the tests was conducted. This approach sounded interesting since it allowed one to disclose such information on redox processes, electrode kinetics, and the electrochemical activity of the modified electrode system.

This configuration was meant to examine the interaction among the conductive polymer, yeast cells, and electron mediators to increase the ratio of bioelectrochemical energy conversion and thereby enhance the efficiency of microbial fuel cells.

3.4.6 Power density measurements

The experiments in the first period were conducted with graphite rod electrodes: one, modified with the yeast and/or corresponding chemicals under the membrane, as anode; the other – unmodified graphite rod, cleaned with 96% methanol and dried, as a cathode. The media prepared in PBS solution with 20 mM $K_3[Fe(CN)_6]$ and 20 mM glucose. Before every experiment, the working electrode was incubated in the solution for 20 minutes. The environment for the experiment was aerobic. All experiments were conducted at least four times, with each trial using a newly made electrode. After an incubation period of 20 minutes, potential measurements were done at least four times for each load. Resistance was lowered in a logarithmic scale gradually, from 1000 kΩ to 1 Ω.

For the power density measurements of the subsequent period, a single chamber MFC was constructed, which consisted of a yeast and mediator modified graphite anode, a graphite cathode (the surface of the cathode exceeded the surface of the anode by order of at least 10 times), submerged in a solution containing beaker. The experiments were conducted in either a laboratory media, consisting of 20 mM $K_3[Fe(CN)_6]$ and 50 mM glucose in PBS, or municipal wastewater samples, provided by UAB “Vilniaus Vandenys”, a wastewater treatment facility. Before measurements, the working electrode was left in the solution for 20 minutes for incubation.

The power density of the constructed MFC was evaluated by using an external load, with resistances ranging from 1000 kOhm to 100 Ohm (for wastewater samples) or from 1000 kOhm to 1 Ohm (for laboratory samples). Voltage was measured during the connection of the external load and each minute after, for 3 minutes in total.

4. RESULTS AND DISCUSSION

4.1 The SECM and hmMSCs work

4.1.1 Characterization of healthy and pathological atrial hmMSCs

Human atrium-derived hmMSCs were isolated from both healthy and dilated atrial myocardium using the explant outgrowth method and cultured in complete IMDM growth medium. Both healthy and pathological hmMSCs exhibited a spindle-like morphology. However, hmMSCs isolated from dilated myocardium (Figure 10B) appeared larger in size compared to those from healthy tissue (Figure 10A). Quantitative analysis of the cell attachment area using ImageJ software confirmed that pathological hmMSCs displayed a significantly larger attachment area (4000–5000 μm²) compared to healthy hmMSCs (1000–2000 μm²) (Figure 10C).

Both healthy and pathological hmMSCs expressed typical mesenchymal stem cell surface markers (CD29, CD44, CD90, CD73, and CD105), while lacking expression of hematopoietic and immune markers (CD34, CD45, CD14, and CD40), confirming their mesenchymal origin (Figure 10E). These findings demonstrate that hmMSCs derived from dilated atrial myocardium exhibit an enlarged morphology relative to those from non-dilated myocardium, while maintaining the characteristic MSC surface marker profile. However, despite MSCs having the potential to be used in tissue engineering, gene therapy, transplants, and tissue injuries, their identification in different tissues is still a challenge [210].

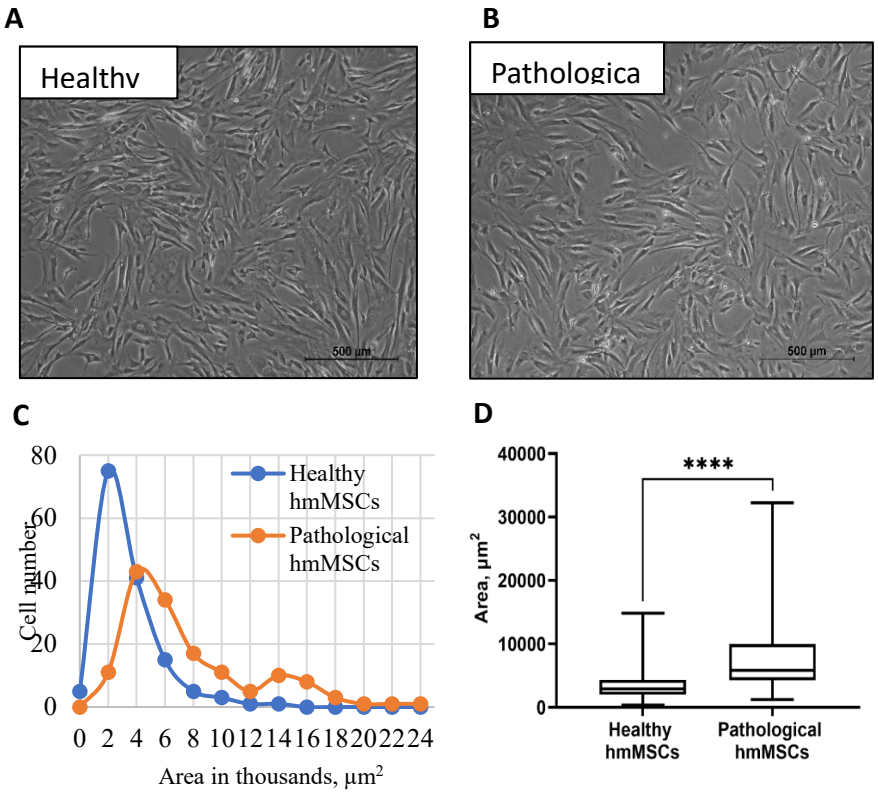

E

	CD29	CD44	CD90	CD73	CD105	CD34	CD45	CD14	CD40
Healthy hmMSCs	96.4±0.6	91.6±2.6	79±11	86±5.6	90.5±5.6	2.3±0.4	1.3±0.3	1.5±0.2	4.7±1.2
Pathological hmMSCs	96.1±2.2	75.7±7.3	73±5.8	82±2.4	70.4±4.7	0.5±0.2	0.7±0.1	1.1±0.7	1.6±0.5

Figure 10. Phenotypic comparison of hmMSCs isolated from healthy and dilated/pathological atrial myocardium. (A) Morphology of hmMSCs derived from healthy, non-dilated atrial tissue. (B) Morphology of hmMSCs derived from pathological, dilated atrial tissue. Scale bar = 500 µm. (C) Distribution of cell attachment area in healthy and pathological hmMSCs; n = 150 cells from three micrographs. (D) Quantitative comparison of attachment area between healthy and pathological hmMSCs; n = 150 cells from three micrographs. (E) Surface protein level profiles of healthy and pathological hmMSCs. Data are presented as mean ± SD. Differences were considered significant at $p \leq 0.05$.

4.1.2 Total acetylation measurement in healthy and pathological hmMSCs

Since SAHA is a histone deacetylase inhibitor, its effect on the total level of acetylated proteins in both healthy and pathological hmMSCs was evaluated (Figure 2A). Healthy (non-dilated) and pathological (dilated) atrial myocardium-derived hmMSCs were cultured for 3 days in complete growth

medium (IMDM with 10% FBS) or in cardiomyogenic differentiation medium (DMEM/F12 with 2% FBS), with or without 1 or 2 µM SAHA. At baseline, pathological atrial hmMSCs exhibited a lower level of protein acetylation compared to healthy cells. Both SAHA concentrations promoted protein acetylation, with a more pronounced effect in pathological hmMSCs (up to 2-fold increase), whereas the effect in healthy cells was milder (up to 1.5-fold) relative to untreated controls (Figure 11).

Similar results were reported in our previous study comparing hmMSCs derived from human healthy and dilated ventricular myocardium and assessing SAHA's effect on their cardiomyogenic differentiation potential.[211] Other studies have also demonstrated that regulation of histone acetylation/deacetylation plays an important role in the cardiomyogenic differentiation of murine MSC lines such as C3H10T1/2 [212] and P19CL6 cells, via upregulation of Isl1. [213] However, the number of published research studies investigating the regenerative potential of human myocardium-derived hmMSCs through epigenetic modulation remains.

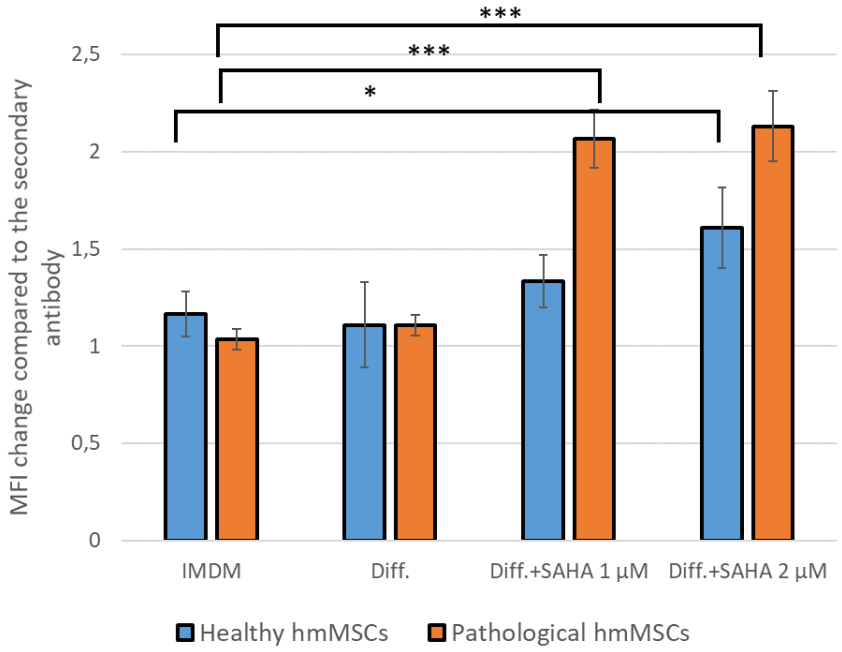

Figure 11. Total protein acetylation levels in healthy and pathological hmMSCs. Cells were cultured for 3 days in complete growth medium (IMDM with 10% FBS), cardiac differentiation medium (Diff) (DMEM/F12 with 2% FBS), or cardiac differentiation medium supplemented with 1 or 2 µM SAHA. Protein acetylation levels were assessed by flow cytometry as described in the Methods section. Data are presented as mean ± SD. Statistical significance was defined as *$p \leq 0.05$ and ***$p \leq 0.01$.

4.1.3 The evaluation of mitochondrial activity of healthy and dilated hmMSCs

In addition, mitochondrial membrane potential (MMP) was assessed by flow cytometry using JC-1 dye (Figure 12). At baseline, pathological hmMSCs showed significantly lower MMP compared to healthy cells. SAHA treatment enhanced MMP in both cell types, mirroring the acetylation data. Specifically, MMP increased approximately 2-fold in pathological cells and 1.4-fold in healthy cells relative to controls cultured in standard IMDM medium (Figure 11). Our earlier work [44] also demonstrated that SAHA improves mitochondrial function in both healthy and dilated human ventricular myocardium-derived hmMSCs. Additional studies have shown that SAHA protects neonatal rat ventricular myocytes and human embryonic stem cell-derived cardiomyocytes from ischemia/reperfusion injury by preserving mitochondrial homeostasis. [214] Similarly, the HDAC6 inhibitor tubastatin A has been shown to protect mouse hearts from TNF-α-induced mitochondrial injury. [215]

These findings support the relevance of HDAC inhibitors in regulating mitochondrial function and viability in hmMSCs derived from both healthy and diseased human atrial myocardium.

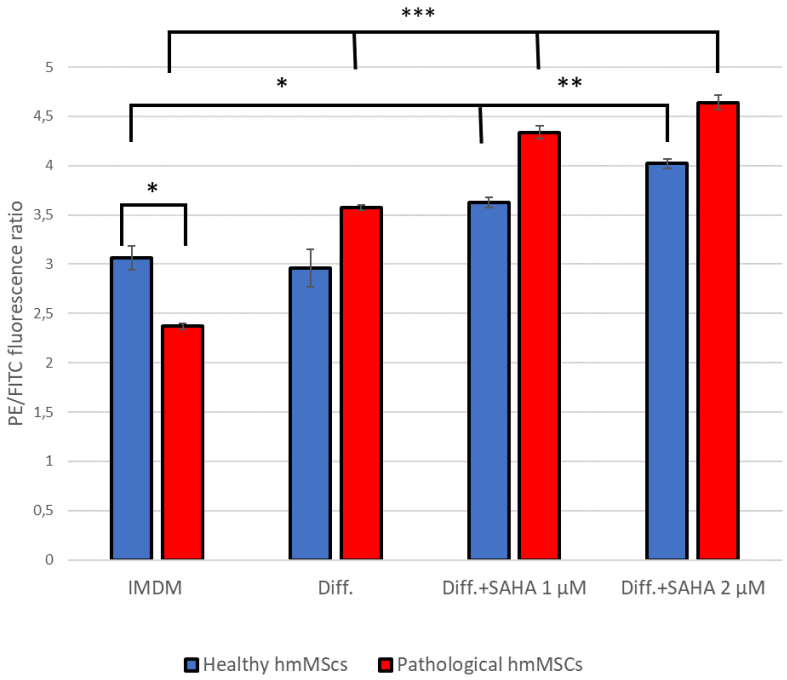

Figure 12. Mitochondrial membrane (MMP) potential in healthy and pathological hmMSCs. Cells were cultured for 3 days in complete growth medium (IMDM with 10% FBS), cardiac differentiation medium (Diff.) (DMEM/F12 with 2% FBS), or cardiac differentiation medium supplemented with 1 or 2 µM SAHA. MMP was measured by flow cytometry using JC-1 staining, as described in the Methods section. Data are presented as mean ± SD. Statistical significance was determined at $*p \leq 0.05$. Measurements were performed on samples from at least three independent patient-derived cell lines of each type.

4.1.4 The evaluation of the total NAD+ level of healthy and pathological hmMSCs

Total intracellular NAD^+ levels were also quantified (Figure 13). Pathological hmMSCs exhibited significantly lower NAD^+ levels - nearly two-fold less - compared to healthy cells under control conditions. Interestingly, SAHA had a greater effect on NAD^+ levels in healthy cells than in pathological ones. This suggests that the NAD^+ salvage and synthesis pathways in healthy atrial hmMSCs are less impaired and more responsive to HDAC inhibition compared to pathological cells.

It is known that NAD^+ plays a central role in cellular metabolism, signaling, and gene regulation, and is crucial for cell survival, stress response, and immune function. [216] It acts as a coenzyme in hundreds of redox reactions

and as a cosubstrate for multiple enzyme systems, also influencing transcription initiation. [217] Notably, NAD^+ is essential for the activity of sirtuin 1, a NAD^+-dependent histone/protein deacetylase that promotes cardiomyocyte survival under oxidative stress when localized in the nucleus. [218] Furthermore, de novo NAD^+ biosynthesis enhances mitochondrial function, which is vital for proper cardiac physiology. [219]

Taken together, these results indicate that SAHA more effectively enhances acetylation and mitochondrial activity in pathological atrial hmMSCs compared to healthy ones. However, the NAD^+ biosynthetic system in pathological cells appears to be more compromised and less responsive to SAHA, highlighting the complexity of NAD^+ regulation in diseased cells. Further investigation is required to better understand these differences and to optimize HDAC-targeted therapies for DCM.

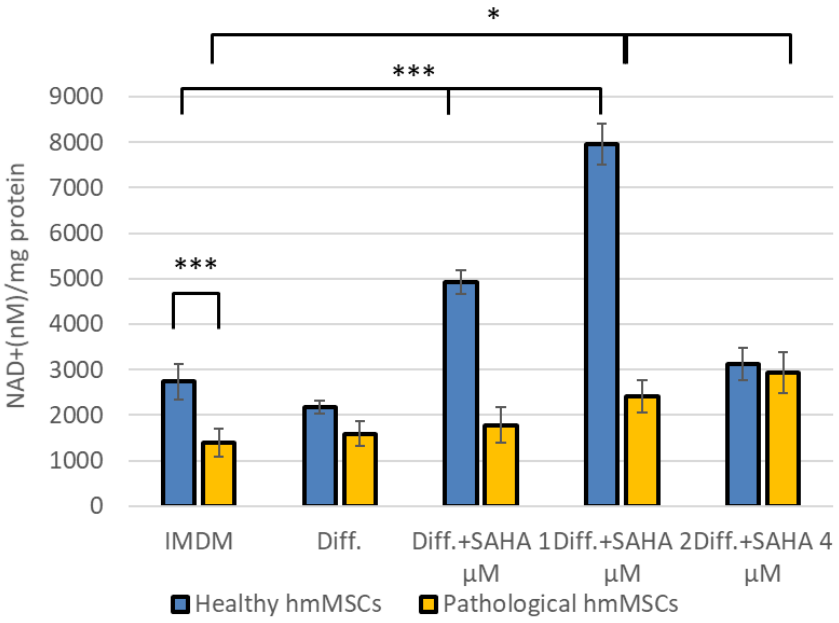

Figure 13. Total NAD^+ levels in healthy and pathological hmMSCs. Cells were cultured for 3 days in complete growth medium (IMDM with 10% FBS), cardiac differentiation medium (Diff) (DMEM/F12 with 2% FBS), or cardiac differentiation medium supplemented with 1 or 2 µM SAHA. Total NAD^+ levels were measured spectrophotometrically as described in the Methods section. Data are presented as mean ± SD. Statistical significance was determined at $p \leq 0.05$. Measurements were performed using at least three independent patient-derived cell lines of each type.

As a next step, we assessed intracellular redox status in healthy and pathological atrial hmMSCs before and after SAHA treatment using scanning

electrochemical microscopy (SECM) with cell-impermeable redox mediator ferrocenecarboxylic acid (FcCOOH). The goal was to compare redox responses between cell types by measuring NAD^+ levels both biochemically (in lysates) and electrochemically (bio-harmlessly). These findings may broaden the application of SECM in evaluating intracellular redox dynamics in human atrial-derived hmMSCs.

4.1.5 Application of SECM for measuring released or intracellular redox compounds using the cell-impermeable mediator FcCOOH

In SECM experiments, current is recorded by an UME positioned at varying distances from immobilized cells. The current–distance dependencies are measured in feedback mode by vertically (z-direction) approaching the cell surface. For SECM measurements, the cell-impermeable redox mediator FcCOOH was chosen. The scheme in Figure 14 illustrates that in a single-mediator system, FcCOOH can report on two types of redox activity: (A) the release of intracellular reducing compounds (e.g., GSH, NADH, NADPH, etc.) from damaged or dying cells following toxic exposures that compromise membrane integrity; and (B) membrane-associated electron transfer from viable cells via plasma membrane-bound or transmembrane NAD(H)/NAD(P)H oxidoreductases.

In line with the model shown in Figure 14A, it has been demonstrated that Ras transformation, used as an in vitro cancer model, damages human non-tumorigenic breast epithelial cells (MCF10A), resulting in the release of reduced glutathione (GSH), which in turn reduces extracellular FcCOOH, as detected by SECM. [220,221] Early reports suggested that NAD(H) is released only from dying cells. [222] However, later studies revealed that living cells may actively export NAD(H) through vesicular trafficking mechanisms (e.g., exocytosis/endocytosis) or via transient pore openings mediated by gap-junction proteins such as connexin 43 or pannexin 1. [223,224] SECM, particularly when combined with electrochemical impedance spectroscopy, has also been applied to detect irreversible electroporation-induced cell death in yeast. [225] as well as to monitor the extracellular release of reactive oxygen and nitrogen species (ROS, RNS) in transformed, metastatic, or non-metastatic cancer cells. [226,227]

The scheme in Figure 14B represents an alternative mechanism in which FcCOOH is reduced at the cell surface by viable cells via plasma membrane electron transport (PMET). This involves membrane-bound or transmembrane oxidoreductases that utilize intracellular reducing equivalents (mainly NADH, less so NADPH), without requiring their release into the extracellular space.

In this context, FcCOOH serves as a benign redox probe for measuring intracellular redox activity indirectly through the plasma membrane.

Our previous studies in human heart ventricle-derived hmMSCs demonstrated that sub-toxic concentrations of SAHA (1–2 µM for 3 days) enhanced mitochondrial function and improved the energy status of both healthy and dilated cells, facilitating cardiomyogenic differentiation. [211,228,229] These findings motivated us to further investigate intracellular redox status using two complementary approaches: electrochemical measurements in intact, non-lysed cells using SECM, and biochemical assays in lysed cells.

Therefore, in this study, we compared the effects of non-cytotoxic SAHA treatment on the intracellular redox potential of healthy and pathological atrium-derived hmMSCs, focusing on its detection via the plasma membrane electron transport (PMET) system using the cell-impermeable mediator FcCOOH.

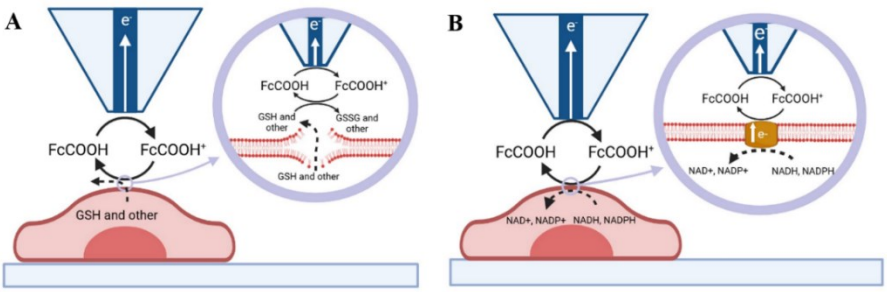

Figure 14. The SECM measurements of released and intracellular redox compounds using cell impermeable mediator FcCOOH. A. The reduction of FcCOOH by released intracellular redox compounds during cell damage. B. The reduction of FcCOOH is achieved by applying membrane-bound and/or transmembrane NAD(H)/NAD(P)H enzyme systems when the cells are not damaged and reducing compounds are not extracellularly released.

4.1.6 Functional plasma membrane electron transport (PMET) system in human atrial hmMSCs for electrochemical measurements of intracellular redox activity with FcCOOH

The NAD^+/NADH and $NADP^+$/NADPH redox couples play essential roles in maintaining the intracellular redox state, supporting cellular energy metabolism, mitochondrial function, gene expression, signaling pathways, and other physiological processes. [35,230] Among these, the NAD^+/NADH couple is particularly critical in cardiac tissue, where oxidative phosphorylation is the primary ATP-generating pathway. [231]

The plasma membrane electron transport (PMET) system was first identified upon observing that membrane-impermeable oxidants can be reduced by intact cells. [232] Since then, PMET has been recognized as a key regulator of redox homeostasis, cell proliferation, and survival. [223,233,234] In the context of electrochemical measurement using the cell-impermeant redox mediator FcCOOH, the PMET system in human atrial hmMSCs can be schematically represented as follows:

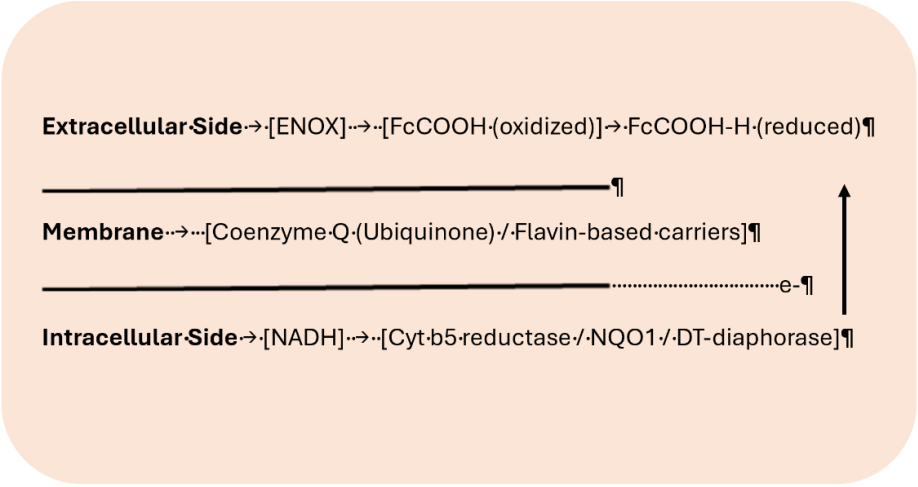

Figure 15. Scheme of PMET in human heart atrial cells for the electrochemical redox studies applying cell-impermeable FcCOOH. ENOX – exto-NOX or cell surface NADH oxidase.

Cytosolic NADH is primarily generated via glycolysis (particularly the GAPDH step), the malate–aspartate shuttle (MAS), lactate dehydrogenase (LDH), and alcohol dehydrogenase. This NADH pool can donate electrons to PMET via intermediate reductases such as: NADH-cytochrome b5 oxidoreductase (CYB5R3), also known as cytochrome b5 reductase, which exists in both cytosolic and membrane-bound forms, which also reduces coenzyme Q (CoQ) and ascorbate, supporting antioxidant defenses and protecting against lipid peroxidation. [235] and NAD(P)H:quinone oxidoreductase 1 (NQO1), primarily a cytosolic enzyme, which reduces quinones but may also interact with membrane-bound ubiquinone and transfer electrons to plasma membrane. [236,237] Both enzymes are the main cytosolic NADH transporters to the plasma membrane.

The plasma membrane PMET part includes CoQ (ubiquinone and favin containing NADH oxidases (Figure15). Though the canonical Q cycle is confined to mitochondria, CoQ/ubiquinone has been proposed to act as a

lateral electron shuttle within the lipid bilayer of the plasma membrane in specific contexts. [235] The NADH-CoQ oxidoreductase present at the plasma membrane appears to favor NADH as a substrate over NADPH and facilitates the transfer of electrons to external acceptors such as oxygen or redox-active compounds like FcCOOH, generating measurable electrochemical current corresponding to the cell's redox state. [234,235] Plasma membrane NADH oxidase is another flavin-based, cyanide-resistant, and hormone-responsive oxidase intrinsic to the plasma membrane of both plant and animal cells that also participates in electron transfer from NADH to FcCOOH [238] oxidize NADH and transfers electrons to O_2 or artificial mediators like ferricyanide and FcCOOH, further supporting extracellular electron transport.

In summary, the PMET system in human atrial-derived hmMSCs is functionally capable of reducing cell-impermeant mediators such as FcCOOH, making it suitable for bio-harmless electrochemical monitoring using SECM (scanning electrochemical microscopy). This redox-responsive activity reflects intracellular NADH availability and can be modulated by metabolic interventions such as treatment with HDAC inhibitors like SAHA. Both healthy and pathological/dilated human heart-derived mesenchymal stem cells (hmMSCs) possess an active plasma membrane electron transport (PMET) system, which reflects the intracellular redox potential of heart cells—based on the NAD^+/NADH ratio—and can be evaluated electrochemically.

4.1.7 FcCOOH-based SECM evaluation of intracellular redox state of atrial hmMSCs

When the ultramicroelectrode (UME) probe is positioned far from the cell membrane, the current measured in the bulk solution originates from the reduction of $FcCOOH^+$ by redox-active products that have diffused or been released from the cells. In this case, the sample acts as a bipolar electrode, reducing $[FcCOOH]^+$ to FcCOOH or, more precisely, reducing ferrocenium ion ($[FcCOOH]^+$) to ferrocene (FcCOOH). This process increases the local concentration of FcCOOH near the electrode, resulting in a corresponding rise in the measured current. [3]

However, when intracellular reducing compounds are not released extracellularly, and the UME is positioned close to the cell membrane, FcCOOH interacts directly with transmembrane NAD^+/NADH oxidases and oxidoreductases that constitute the plasma membrane electron transport (PMET) system. These enzymes shuttle electrons from intracellular NADH to

extracellular $FcCOOH^+$, thereby reducing it and increasing the measured current. This current is proportional to the intracellular redox state.

In this study, SECM approach curves using the cell-impermeable redox mediator FcCOOH revealed a pronounced difference in the positive feedback signal between healthy and pathological human atrial hmMSCs cultured in standard IMDM medium (Figure 16 and Figure 17). Specifically, the current signal from healthy hmMSCs was approximately 20 times higher than that from pathological hmMSCs (46.6 vs. 2.14, respectively). This suggests that healthy hmMSCs possess significantly greater intracellular reducing and PMET capacity, which may correlate with superior regenerative potential. In contrast, the low redox activity and PMET in pathological cells indicate a greater vulnerability to oxidative stress and/or other cytotoxic effects. [239]

When cells were cultured in cardiomyogenic differentiation medium (Diff.), treatment with the HDAC inhibitor SAHA substantially increased the intracellular redox capacity. In healthy hmMSCs, the SECM signal increased more than fourfold (from 27.3 to 110), while in pathological hmMSCs, the increase was approximately 1.5-fold (from 2.85 to 4.15). Importantly, even though the effect was less pronounced in pathological cells, they still responded positively to SAHA, indicating a partial restoration of redox activity and PMET.

These findings suggest that SAHA enhances not only mitochondrial activity and membrane potential, as previously shown, but also the overall intracellular redox capacity in both healthy and diseased atrial myocardium-derived hmMSCs. Furthermore, SECM measurements with the cell-impermeable mediator FcCOOH offer a valuable, bio-friendly electrochemical tool for probing intracellular redox and PMET activity under various physiological and pathological conditions. Future studies are needed to further elucidate the molecular mechanisms underlying SAHA's effects on atrial cell function, redox, and PMET regulation.

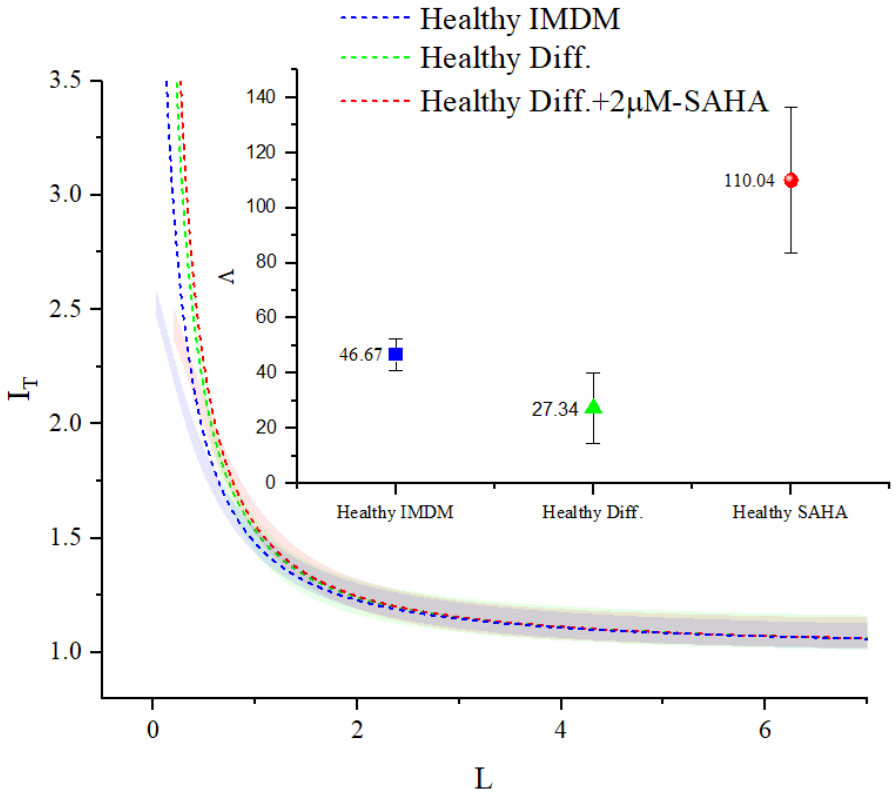

Figure 16. SECM UME approach curves of healthy (non-dilated) hmMSCs. Blue – healthy hmMSCs in complete IMDM growth medium; Green – healthy hmMSCs in cardiomyogenic differentiation medium (Diff.); Red – healthy hmMSCs in Diff. medium supplemented with 2 μM SAHA for 3 days. Measurements were performed at a potential bias of +400 mV vs. Ag/AgCl using 6 μM FcCOOH as the redox mediator. Experimental data were fitted using a mathematical model based on Cornut and Lefrou's approximations to determine the reaction rate kinetics by evaluating the kinetic parameter λ (lambda). Data are presented as mean ± SD from at least three independent measurements using cells from three different donors. Transparent curves represent experimental data with a 95% confidence interval. Dotted lines indicate the theoretical fit based on the applied model.

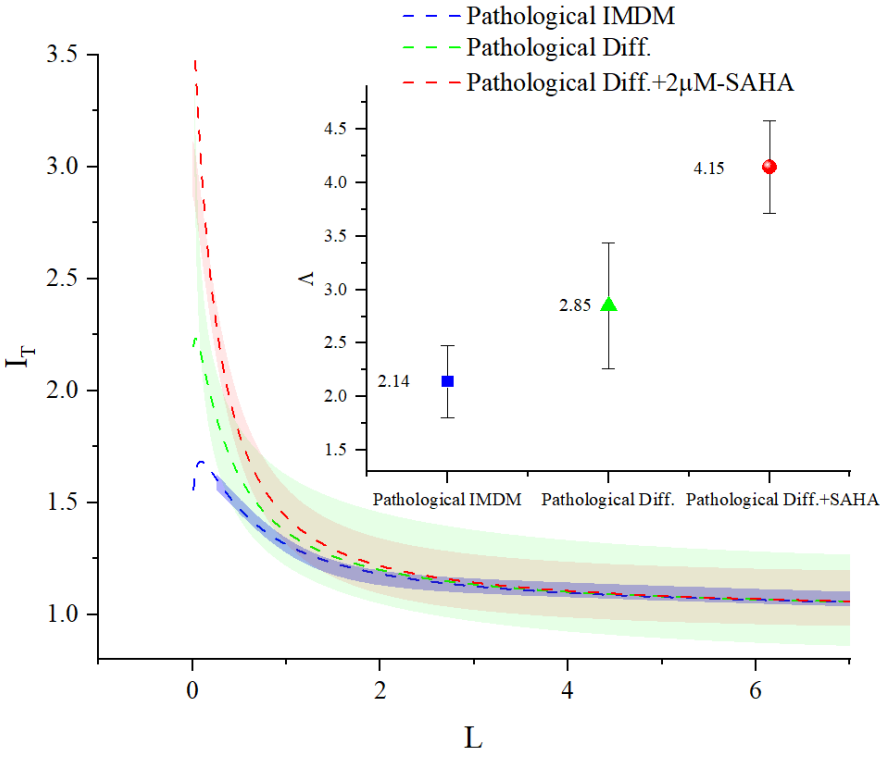

Figure 17. SECM UME approach curves of pathological (dilated) atrial hmMSCs. Blue – pathological hmMSCs in IMDM medium; Green – pathological hmMSCs in cardiomyogenic differentiation medium (Diff.); Red – pathological hmMSCs in Diff. medium supplemented with 2 μM SAHA for 3 days. Measurements were performed at a potential bias of +400 mV vs. Ag/AgCl using 6 μM FcCOOH as the redox mediator. Experimental data were fitted using a mathematical model based on Cornut and Lefrou's approximations to determine reaction rate kinetics by evaluating the kinetic parameter λ. Data are presented as mean ± SD from at least three cells obtained from three different patients. Transparent curves represent experimental data with a 95% confidence interval. Dotted lines correspond to the theoretical fit derived from the mathematical model.

Thus, our findings demonstrate that healthy human heart hmMSCs have more active PMET than pathological and treatment with SAHA enhanced the redox and PMET activities of both healthy and dilated atrium-derived hmMSCs, as assessed by extracellular FcCOOH reduction. This suggests an improvement in intracellular redox status, likely mediated by elevated NADH availability and/or activation of membrane-associated NADH oxidoreductases such as cyt b5 reductase or NQO1. These results align with SAHA's known role in modulating mitochondrial function and NAD^+

metabolism, and highlight PMET as a functional readout of cellular redox capacity in human myocardial-derived stem/stromal cells.

4.2 The MFCs work

4.2.1 Initial electrochemical measurements of the MFC

Consistent, dependable, and successful experimental outcomes rely critically on our preparation and treatment of the surfaces of electrodes. In the field of MFC, where the interesting worlds of biology and electrochemistry converge, it is essential to control the properties of the electrode surface. Effective electron transport between the microbial catalyst and the electrode substrate depends on this regulation, thereby enabling major developments in the sector.[240] We were lured to graphite rod electrodes for our work by their well-known chemical stability, remarkable mechanical strength, and great conductivity. For investigating both abiotic and bioelectrochemical processes, these features make graphite rods particularly useful. Furthermore, graphite is a substance that repels water, which presents unique problems at the interface in terms of interactions with biological systems found on water. Starting from 300 and working all the way up to 10,000, the polishing process uses sanding papers with ever finer grit levels. In this context, this technique has two main purposes. This procedure improves surface topography's homogeneity by fixing micro-defects and surface imperfections. It also reduces the possibility of nonspecific microbe adherence, hence producing a more consistent and successful result. We expose new, reactive layers of graphite by means of electrochemical fine polishing. This exposure greatly increases the kinetics of electron exchange and helps to provide a more constant baseline in electrochemical activity. This approach is particularly important considering physiological changes over many electrodes. It lessens the variation brought about by variations in surface form.

Crucially, the cleaning process after polishing consists of using 96% methanol followed by washing with deionized water. This mechanism is meant to remove any organic pollutants that could interfere with the subsequent electrode changes in addition to the small particles left over following polishing. Dissolving organic waste depends much on methanol, with its special polarity and volatility. Unchecked, these residues could produce insulating layers on the graphite surface, therefore impeding the crucial electron transport processes. In the sterilizing process, methanol is rather important as it helps to reduce the possibility of contamination by undesired bacteria. [241] This is crucial as such contamination may interfere with

the exact interactions between the electrode under study and the yeast. Rinsing with deionized water ensures that any residual methanol or soluble contaminants are eliminated. Maintaining the ionic conductivity of the electrolyte and guaranteeing the unchanged binding between the mediator and the electrode depend on this stage. Aiming at limiting the electrochemically active region, the cautious engineering choice of three-quarters of each electrode is to insulate them with silicone tubing. This layout guarantees that the flow of current is only connected to the deliberately left exposed surface area. Expressed in μA/cm2 or μA/mm2, this design helps the current output to be reliably normalized with respect to the electrode area. This feature is crucial for a good comparison of electrochemical responses in studies including many yeast mutations or alternative mediator setups.

The choice of 9,10-phenanthrenequinone as the mediator results from its known redox activity and beneficial interaction with microbial systems, particularly in fostering the processes of EET. Part of a broader family of quinone derivatives, PQ finds usage in bioelectrochemical systems. This is mostly due to its well-known reversible redox chemistry and fit for biological surroundings. This compound's lipophilic character helps it to interact well with the hydrophobic regions of microbial cell envelops. This contact greatly increases the proximity of redox centers to the electrode surface, therefore enabling improved performance. Making PQ solution started by dissolving it in 96% ethanol. This specific solvent was chosen because, at ambient temperature, it evaporates cleanly and rapidly dissolves lipophilic organic molecules. It thereby leaves on the graphite surface a smooth, uniform coating of mediator. Based on our many years of laboratory expertise, the initial use of 2 μL of a 3 mM PQ solution is a deliberate optimization.[242] This approach strikes a careful balance, ensuring there is enough surface coverage to facilitate effective electron transfer, while also preventing any excess deposition that might obstruct ion diffusion or lead to aggregation.

The next step involves modifying the electrode with 2 μL of yeast suspension, which can either be unmodified or pre-treated with AuNPs and/or polypyrrole PPy. This technique is necessary for bioelectrochemical interaction. Under normal circumstances, yeast cells inherently have little capacity to move electrons outside of themselves. The modifications done in this study were meant to improve the conductivity characteristics of the cell outer layers. Gold nanoparticles, celebrated for their impressive electrical conductivity and compatibility with biological systems, are believed to create conductive connections between the intracellular electron transfer chains of *S. cerevisiae* and the surface of the electrode. At the same time, polypyrrole,

which is a conductive polymer, adds another dimension of electron delocalization pathways. This addition significantly increases the chances of effective electron movement from the biological phase into the non-biological conductor. When we drop-cast these specially modified yeast suspensions onto PQ-coated graphite, we create a unique interface that works in harmony.[243] Here, the mediator plays a crucial role in enabling charge transfer between the biological components and the non-biological materials. Meanwhile, the enhancements made with nanomaterials or polymers help to lower the barriers for electron tunneling at the interface between the cells and the electrode.

Subsequent improvements to the experimental design led to an increase in the PQ drop-cast volume to 4 μL. This change was inspired by initial observations that indicated a greater loading of the mediator could enhance the consistency of redox cycling throughout longer experimental periods. This change in procedure highlights the ongoing process of refining experiments in the field of electrochemical research. This is especially true when working with biofunctionalized surfaces, where factors such as mediator leaching, microbial metabolism, and interactions with electrolytes can all play a significant role in maintaining signal stability over time. After the deposition of the mediator and the evaporation of the solvent, we used the same yeast suspension protocol to maintain a consistent biological loading throughout the process. To enhance the stability of the yeast layer, a membrane was carefully placed over the prepared electrode and secured with laboratory tape. This thoughtful approach aimed to prevent drying out during extended immersion and to reduce any mechanical disturbances that might occur during handling and measurement.[244]

Well known as a prominent redox mediator with reversible electrochemical activity, potassium ferricyanide helps the efficient electron transfer between the electrode and yeast, a biological system.[245] Furthermore included as a substrate to increase the metabolic activity of the yeast cells was 20 mM glucose. Because of the oxidation of glucose, this produced more bioelectrochemical interactions as well as electron release.

Before any measurements were made, a twenty-minute stabilization interval was allowed for the system to ensure that the electrode surface, electrolyte solution, and biological components were all in balance. Apart from lowering the noise level in the electrochemical signal, this stabilization period guarantees consistent results.[246]

One well-known technique in bioelectrochemistry for surface modification of bacteria is pyrrole polymerization process. [207] Using potassium ferrocyanide (II) as an oxidizing agent in chemical reactions that would

compromise cellular life by allowing mild oxidative polymerization of pyrrole in water, researchers investigating CPs and their capacity to enhance electron flow between conductive surfaces and biological systems found a planned and cautious use of this agent. Two crucial roles of glucose in the reaction environment ensure full completion of the process. First, it is vital to maintain *S. cerevisiae's* metabolic activity all during the polymerization process, thus assuring the survival in the polymerization environment of the cells. Furthermore, acting as a competitive reductant, glucose generates a balanced reducing environment that can aid to slow down oxidative polymerization. Achieving this equilibrium is especially important when polymerizing directly on biological surfaces. It ensures that the expansion of the polymer primarily points towards the interface of the cellular membrane, therefore avoiding any undesired clumping in the surrounding bulk solution.

We selected further modifications utilizing 10 nm spherical gold nanoparticles because to their well-known potential to conduct electricity, their compatibility with living systems, and their documented usefulness in increasing electron transfer channels across many biological settings.[247,248] As in our case the nanoparticles used were considered standard batch, the system was described in the specifications sheet. The remarkable surface area-to-ratio of gold nanoparticles greatly enhances their interaction capacity with any conductive polymer layer that could also be present as well as biological membranes. First laboratory optimization studies intended to improve the process led to the decision to utilize a two-to-one volumetric ratio of yeast solution to gold nanoparticle suspension. These internal, unpublished investigations revealed that this ratio reduced the agglomeration of nanoparticles, thus elegantly decorating the surface of the yeast cells. The phenomenon of agglomeration is significant as it might confound our understanding of the interactions between nanoparticles and biological systems. Maintaining electrochemical performance primarily relies on this control of the concentration of nanoparticles, hence it is essential. This careful monitoring ensures the integrity of the membrane and helps to reduce osmotic stress.

Starting with careful application of conductive polypyrrole, the dual-modification process is enhanced by the addition of gold nanoparticles.[249] It will promote many other developments, improving the electron transfer capacity in a synergistic fashion would greatly help the future uses of microbial fuel cells. Great portion of the flow of electrons from within cells to the outside environment is made possible by the ideal routes created by CPs like polypyrrole. Acting as tiny electron relay stations, gold nanoparticles aid

to shorten the distance charges must travel during transfer events. Particularly the modified yeast cells, these changes aid to reduce the interfacial resistance between the electrode surface and the microbial catalyst. The modifications collaborate to create an intentionally produced interaction between electrodes and yeast. This approach aims to enhance bioelectrochemical performance by means of a meticulous and comprehensive building plan combining aspects of materials science, chemistry, and biology.

To determine the effect of pPy on yeast, cyclic voltammetry experiments (Figure 18) were performed without yeast (A), with unmodified yeast (B), and with yeast, in which the cell wall was modified (C) with 200 mM pyrrole. Measurements were performed before and after yeast incubation for 20 min. in the working solution. PQ peaks stayed almost the same, while potassium ferrocyanide peaks increased within the given time suggesting glucose metabolism in yeast effects only the start of redox in ferrocyanide. From the registered CVs (Figure 18), the current density increased using pPy-modified yeast compared to non-modified or control (without yeast). Comparing redox peaks (Figure 18D) of ferro/ferri in the working solution between the empty electrode and regular yeast MFC, the acquired current density on the oxidative peak was increased twice with yeast, from 1.806 mA/cm^2 to 3.759 mA/cm^2, and on the reductive peak, from 1.680 mA/cm^2 to 3.258 mA/cm^2. After comparing bare yeast and polypyrrole-modified yeast MFCs, modified electrode oxidative peaks showed a 33% increase in current density, in total reaching 5.008 mA/cm^2 (Figure 18C). Reductive peaks reached 3.606 mA/cm^2, an increase, all in comparison with blank electrode (Figure 18A) and non-modified yeast electrode (Figure 18B) CV peaks.

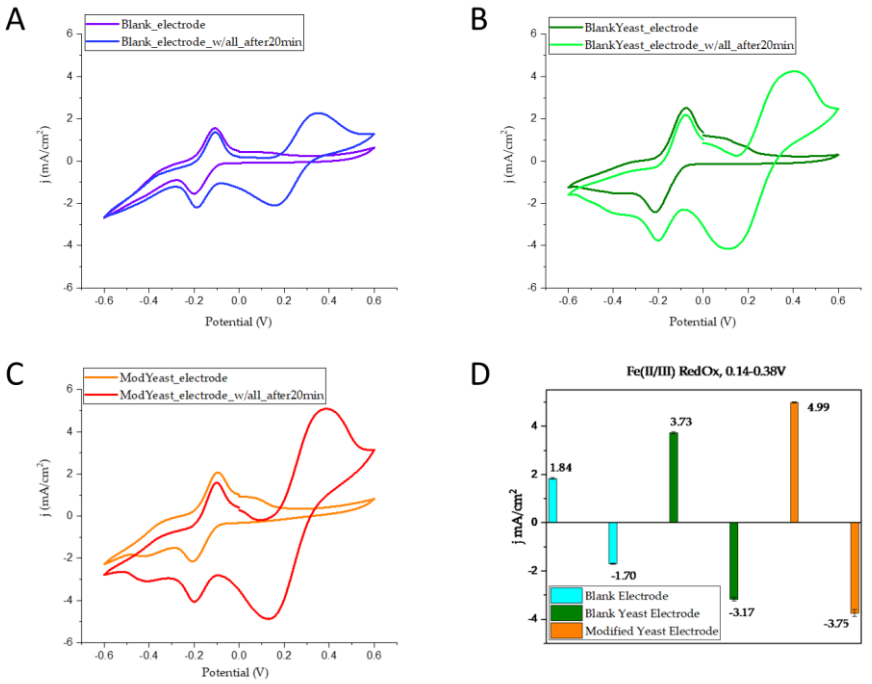

Figure 18. Cyclic voltammetry of three types of PQ-covered graphite electrodes: A. Blank, without other additives; B. Blank-Yeast, only with bare *S. cerevisiae* and PCTE membrane with 3 µm pores; and C. Mod-Yeast, 200 mM polypyrrole modified *S. cerevisiae* with the same PCTE membrane. D. the diagram represents CV peaks or ferrocyanide reduction and oxidation. Measurements were conducted by sweeping the potential from -0.6 V to +0.6 V, at 50 mV/s rate, using an Ag/AgCl reference electrode in KCl 3M and Pt counter electrode. Working solution: 20 mM glucose and 20 mM ferrocyanide in PBS.

In comparison to other studies, these Fe^{2+}/Fe^{3+} redox peaks and the representative current density, in these solution conditions, are not thoroughly discussed. That is how we could determine this investigation as a novel approach to a MFC comparison. The conditions in the given approach states the control for the experiment and a clean yeast with or without modification on this microbial technology device can be qualitatively evaluated the advancement in accessing the full potential of the MFC.

The obtained CV data was fitted using the modified Hill function (Equation 1) to plot and predict the current density response of MFC to the changes in glucose concentration (Figure 19). The resulting Hill's coefficient values *n* for both systems (utilizing either modified or non-modified yeast cells) was greater than 1 (Figure 19); this indicates positive cooperativity between

substrate (ferrocyanide) and enzyme (in yeast) molecules, meaning the addition of glucose enhances the reaction of substrate molecules. Additionally, the *k* value, which represents the concentration of glucose in the system where half of the current is produced, is lower in the non-modified yeast system (*k* = 12.9 mmol/L) – this indicates that unmodified yeast possesses a greater affinity for the substrate, unlike the modified yeast (*k* = 46.9 mmol/L). Even though pPy-modified yeast may possess inferior substrate affinity, the current density curve of the system demonstrates improved performance, indicating that the system has a greater capacity for power generation. Therefore, more electrical energy can be generated using modified yeast.

Polypyrrole seems to solve the problems related with traditional cellular electron transfer systems by improving the efficiency of charge transport from within yeast cells to the electrode surface. Moreover, the positive cooperativity shown by Hill's coefficient values in both systems implies that a change in glucose concentration improves the bioelectrocatalytic activity, hence motivating additional substrate consumption. The improved cooperative behavior of the changed system might result from changes in structure or metabolism brought about during the modification process. This may therefore cause a change in the interaction dynamics between the electron mediator and intracellular enzymes.

The results taken together show that changing the yeast surface chemistry has the potential to greatly improve the bioelectrochemical efficiency of microbial fuel cells even with a sacrifice in substrate affinity. This draws attention to the great possibility of conductive polymer-modified biocatalysts as substitutes to improve the efficiency of microbial fuel cells, especially in situations requiring more power outputs. Future research should strive to improve the modification process thus guaranteeing a harmonic balance between conductivity and affinity to attain the greatest possible performance.

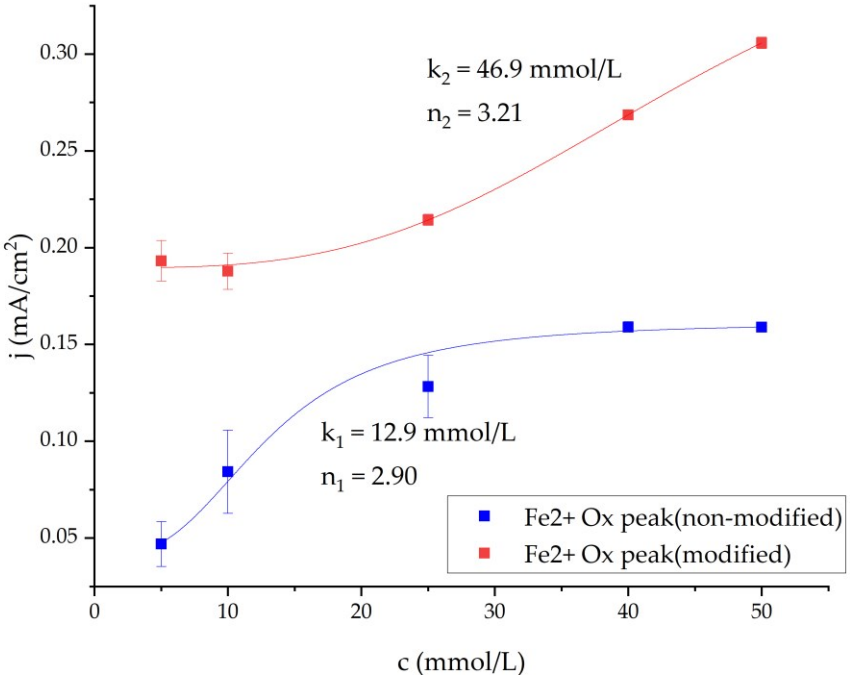

Figure 19. Current density dependencies on glucose concentration extracted from $[Fe(CN)_6]^{4-}$ peaks in CV. 200 mM pyrrole-modified and non-modified yeast used in the experiments, fitted using Hill's equation (Equation 2).

Additionally, yeast was altered using 50 mM pyrrole and 10 nm gold nanoparticles, combined in a two-to-one ratio of yeast to nanoparticle solution, since this concentration ratio was examined but not documented in any publications. The same approach of CV was used for the determination of the best performance. Then the power density measurements took place. In the Figure 20A potential dependance on resistance is represented

Maximum power densities were obtained using 10 kΩ load at 0 min as seen in Figure 20B. Bare yeast has shown the lowest power density in this experiment – on the load of 10 kΩ the MFC reached 73.7 mW/m^2 (Figure 20B, yellow Sc part). In comparison, power density of 86.5 mW/m^2 peaked at the same load for 50 mM pyrrole polymerized *S. cerevisiae* cell wall MFC (same graph, orange, Sc + pPy part) during the same moment measurement. The addition of 10 nm gold nanoparticles to MFC, in composition, has shown a rise in potential and the calculations determined that the power density of MFC of bare yeast with such add-on reaches 122.8 mW/m^2, which is 66.6% higher than without the addition of nanoparticles (gray, Sc + AuNP). Then polypyrrole-modified yeast cell wall with the same nanoparticles MFC was

studied in the same manner, power density reached 147.8 mW/m^2, twice the peak power density of bare yeast anode.

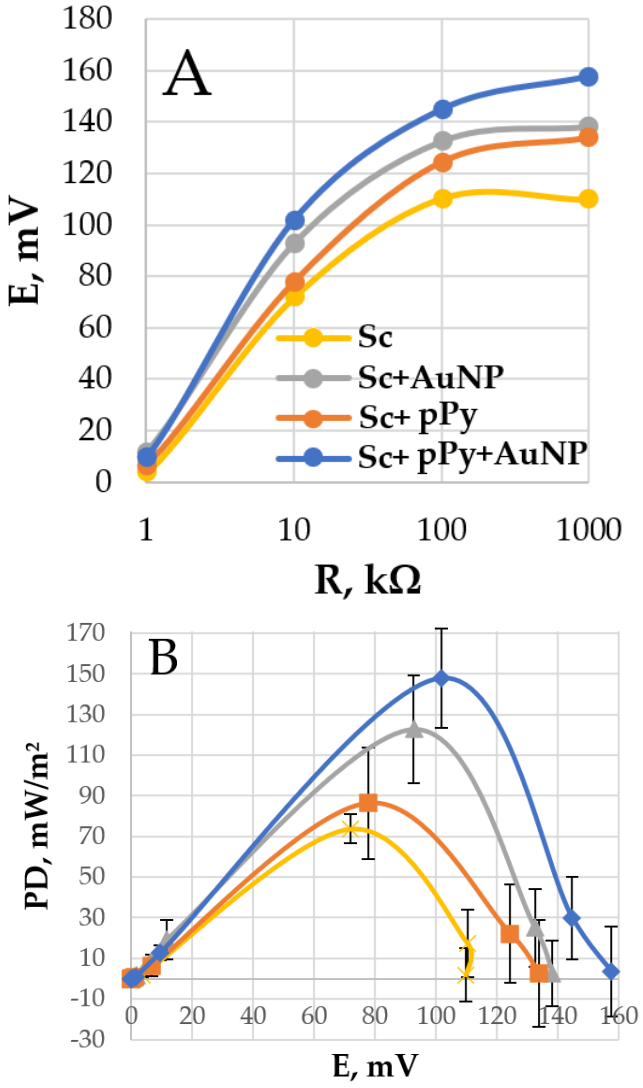

Figure 20. A. Potential dependencies on load. B. Power Density (PD) dependencies on potential. Measurements were performed in the PBS solution with glucose (20 mM) and $K_3[Fe(CN)_6]$ (20 mM). Electrodes used were covered with PQ and *S. cerevisiae* with various modifications shown in Figure 8.

MFC power density dependencies on different loads were measured every minute for a 3-minute period (Figure 21). It was found that power density dropped with every minute. However, it can be seen, that highest power density was observed when yeast was modified with pPy and gold

nanoparticles. This tendency should be interpreted as the best modification determined by this dissertation.

In comparison to previous studies shown in Table 3 of the Conclusions section, our MFC, with a fully modified graphite rod anode structure, achieves the best instantaneous power density within this category. This might suggest for future applications use different anode materials, such as the highest power density reaching carbon felt and carbon brushes, as well as investigating other inertial substances or alloys used for the electrodes of MFCs.

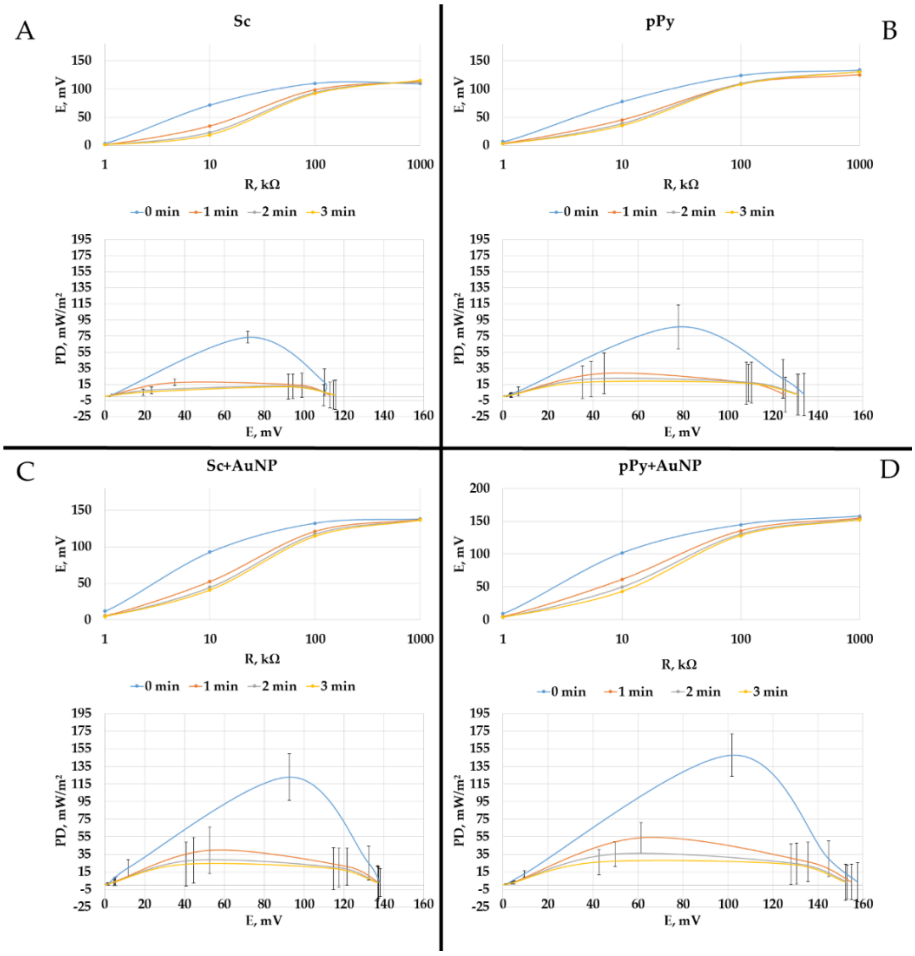

Figure 21. Potential vs. load and power density (PD) vs. potential dependencies, measured in time with glucose (20 mM) and potassium ferricyanide (20 mM) in PBS. A. Bare yeast MFC. B. Polymerized yeast cell wall MFC. C. Yeast modified with nanoparticles. D. Yeast modified with pPy and nanoparticles.

The best performing MFC configuration was determined to be with a 50 mM pyrrole polymerized yeast cell wall with an add-on of 10 nm Au nanosphere particles on a polished graphite rod covered with PQ and an all-topping 3 µm pore PCTE membrane. This configuration was used to conduct measurements in actual wastewater under a load of 10 kΩ. After a 3-minute evaluation, the power density reached an astonishing value of 179.2 mW/m^2 (Figure 22, the red dot). In comparison, the power density outcomes of the previous experiments after 3 minutes and with 10 kΩ load were 9.2 mW/m^2 for bare yeast MFC, 20.6 mW/m^2 for polypyrrole yeast MFC, 24.6 mW/m^2 for bare yeast with nanoparticles, and 61.1 mW/m^2 with MFC in PBS with glucose and potassium ferricyanide solution, after the same period of time.

These experiments indicate that comprehensive manipulation of the yeast's extracellular and intracellular environments is optimal for microbial fuel cells, since future projections show that such modifications using gold nanoparticles may eventually be economically viable. The main alteration here might be the change of the main anode material and upscaling the device for proper use.

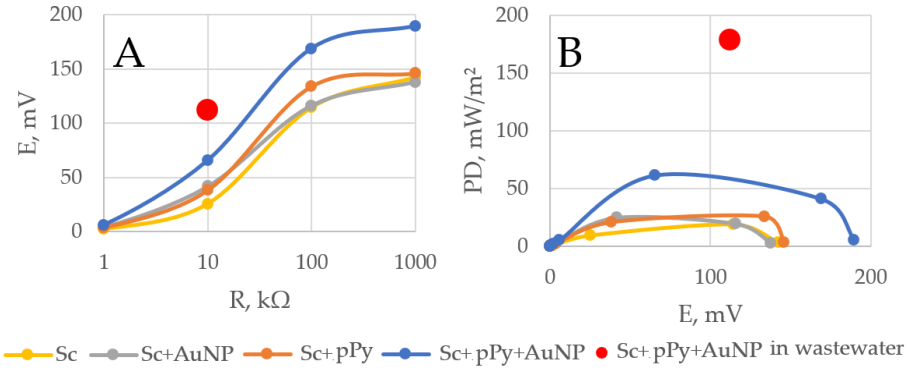

Figure 22. A. Potential dependencies on load. B. Power Density (PD) dependencies on potential. Measurements were performed in the glucose (20 mM) and $K_3[Fe(CN)_6]$ (20 mM) solution. The red dot represents a sample of UAB's "Vilniaus Vandenys" wastewater facility.

4.2.2 Evaluation of yeast cells' viability

In this experiment, we decided to grow *S. cerevisiae* mostly using YPD broth, a broth made from yeast extract peptone dextrose. This choice was selected considering the data demonstrating the broth's capacity to provide the essential nutrients needed for robust yeast growth and metabolism.[250,251] YPD, a quite advanced medium, consists of three components: yeast extract, peptone, and glucose. Each one of these components has a special and

significant function in enabling the organisms to grow and prosper throughout their lifetime.[252,253]ts: yeast extract, peptone, and glucose. Each one of these components has a special and significant function in enabling the organisms to grow and prosper throughout their lifetime.[252,253] Yeast extract is one reliable source of vitamins; it mainly includes the B-complex group. Apart from this, it comprises of free amino acids, peptides, and nucleotides – all of which are vital for the process of raising metabolic activity and promoting cellular reproduction. Together with yeast extract, peptone – generated from broken down proteins – forms a complimentary connection with each other. It contains enough of both polypeptides and amino acids, which are needed for enzymatic reactions and protein synthesis. Important in the metabolic paths of yeast, the glucose component is the major source of carbon and energy both during fermentation and respiration. Apart from producing sufficient biomass, the concentration of glucose in the broth is a major factor in terms of preparing the yeast cells for prospective application in microbial fuel cell systems in the present and future.[254–256] By now their capacity to move electrons outside the cell and change metabolistically becomes really essential. Past studies guided the decision to utilize a small agitation speed of 200 cycles per minute and to fix the incubation temperature at 30 °C.[257] These studies show that the presence of such circumstances improves the availability of nutrients and oxygen, which in turn assures that the cells will continue to live and stay healthy and speeds the growth of yeast. Regular shaking of the culture helped us to maintain a homogenous consistency, which at last prevented the cells from sinking to the bottom of the container. Moreover, this approach helped to promote aerobic respiration, a basic component of the mechanism enabling the cells to become more resilient and stronger. There are several applications for which this kind of resilience is needed, especially in the domains of bioelectrochemistry and electrochemical modification.

Moreover, the careful method used in the creation of the inoculum, washing, and standardizing the yeast suspensions was specifically aimed at ensuring that the outcomes could be repeated consistently. Particularly in connection to the electrochemical applications seen in MFCs, this meticulousness guarantees that the subsequent testing phases are compatible and consistent with each other. Across all the many culture batches, a surprising degree of genetic and phenotypic stability was attained using inoculation produced from cryopreserved, deep-level library samples of *S. cerevisiae*.[258] This method greatly reduced the likelihood of adaptive mutations or changes in physical features, therefore enhancing the consistency and reliability of the experimental outcomes. The well-organized culture time of 20-24 hours paired with strict advice to utilize the cells within a maximum of 40-48 hours after cultivation was produced helps to limit the dangers

associated with cell aging, metabolic depletion, or autolysis. These problems are well known to compromise not only the structural integrity of the cell wall but also the biological efficiency of metabolic activities.[259] PBS was then used in the following washing cycle to completely remove any last traces of any components still in the developing media. This step is vital as it guarantees that measurements of conductivity will always be exact and constant and helps to eliminate any interference resulting from electrochemical processes. PBS is isotonic and safe for yeast cells to utilize, hence during the washing process yeast cells may keep their shape and membrane structure. By carefully running many centrifugation and washing cycles, we were able to drastically reduce any possible carryover of medium components. Our major goal was to lower the number of metabolic byproducts and residual glucose already exist. If one aimed for a concentration of 1 g/mL, the final dilution of the yeast pellet became a somewhat crucial step. Correct findings needed consistent cell loading, hence this step ensured that every experimental duplicate has this feature. This rigorously regulated approach allowed accurate and reproducible modification of the yeast cells by use of CPs or nanomaterials.[260] Maintaining homogeneity is essential to provide constant electrochemical performance in applications of microbial fuel cells. The essential need to strike a point of equilibrium between electrochemical compatibility and biological viability informed the decisions taken all through the study. This method was meant to enhance the interactions between biological systems and electrical components, therefore complementing the objectives stated in this dissertation.

To evaluate the impact of polypyrrole modification on the growth and proliferation of *S. cerevisiae* yeast, colony-forming unit (CFU) assays were performed using polypyrrole solutions at varying concentrations. Colony-forming unit (CFU) quantifications are presented in Table 2.

Table 2. Dependence of colony-forming unit (CFU) count on polypyrrole solution concentration

Sample	CFU/ml
Yeast cells treated with an 8 mM concentration of polypyrrole solution	$2.5 \cdot 10^7 \pm 5 \cdot 10^{-2}$
Yeast cells treated with a 25 mM concentration of polypyrrole solution	$1.6 \cdot 10^7 \pm 5 \cdot 10^{-2}$
Yeast cells treated with a 50 mM concentration of polypyrrole solution	$1.0 \cdot 10^7 \pm 5 \cdot 10^{-2}$
Yeast cells treated with a 100 mM concentration of polypyrrole solution	$0.6 \cdot 10^7 \pm 5 \cdot 10^{-2}$
Untreated yeast cells (control)	$5.0 \cdot 10^7 \pm 5 \cdot 10^{-2}$

The presented bar chart (Figure 23) on agarized YPD medium indicates how polypyrrole modification influences *S. cerevisiae* colony development. The 100 mM concentration of polypyrrole solution had the biggest influence

on yeast cells proliferation and growth using a CFU/ml of polypyrrole-treated yeast cells with a value of 0.6 x $10^{7}\pm 5{\cdot}10^{-2}$.

Figure 23 illustrates how polypyrrole solutions restrict the growth of yeast colonies. Unlike the control, all polypyrrole concentrations employed in the experiment clearly influenced yeast cell proliferation. Increased polypyrrole concentrations might have caused oxidative stress and pH imbalance in yeast, therefore compromising cell development and proliferation.

Their vitality was assessed as only living *S. cerevisiae* cells could perform metabolic activities generating electrons. These electrons are essential for producing energy in the MFC. Should the yeast cells be non-viable, the fuel cell's efficiency diminishes because they cannot contribute to creating electrical current. Testing viability ensures active microorganisms and that the system functions as it should.

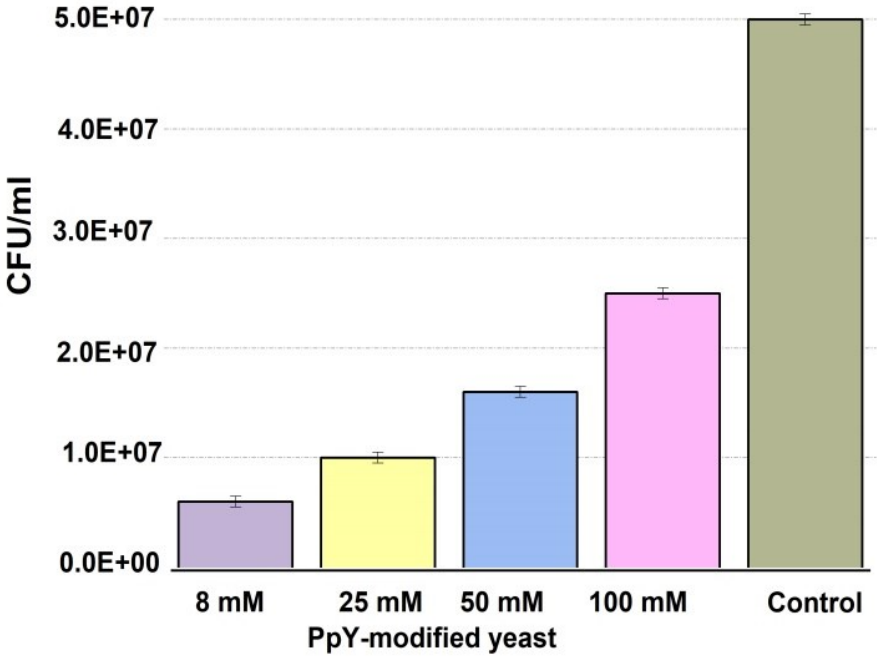

Figure 23. Effect of concentration of polypyrrole on viability of *Saccharomyces cerevisiae* yeast cells.

4.2.3 Voltammetric measurements of a more-cost-effective MFC

For the determination of the effect of pPy on modification of yeast cells which are used in the designing of yeast and PQ modified electrode, cyclic voltammetry measurements were performed (Figure 24A). The resulting peak

current density values of ferri/ferro redox couple were plotted against the concentration of pPy used in the modification of the yeast cells are shown in the Figure 24B. The maximum current density of 2.949 mA/cm^2 (for oxidative peak) and -2.504 mA/cm^2 (for reductive peak) were observed when using 100 mM of pyrrole for the modification of yeast cells. Moreover, using low concentrations of pyrrole (8 and 25 mM) when modifying yeast results in a lower current density against non-modified yeast cells used in the construction of the electrodes.

This result of low concentrations of the given CP might indicate an inhibitive effect of pPy on the catalytic activity of the fungus. My team and I recommend more inquiry into the impact of microplastics on yeast or other microorganisms used in MFCs for future research. This might lead to a new direction of using CPs in the upcoming decades – cells' metabolic inhibition is also a resourceful topic.

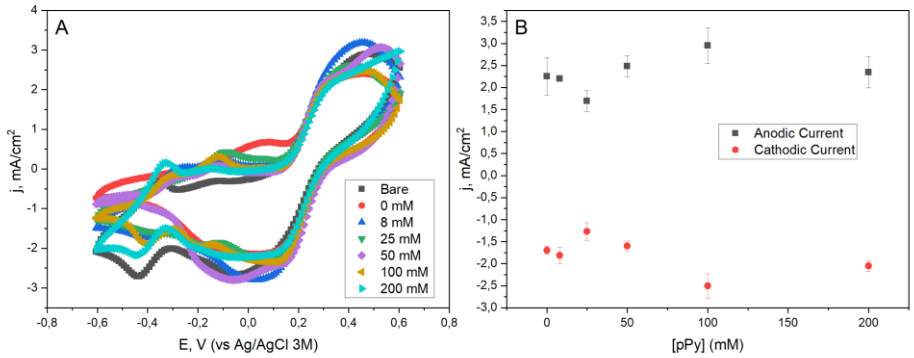

Figure 24. A - Cyclic voltametric curves of different PQ and modified yeast cell electrodes. Measurements were conducted by sweeping the potential from -0.6 V to +0.6 V, 50 mV/s, using an Ag/AgCl reference electrode in KCl 3M and a Pt counter electrode. Bare – PQ modified graphite electrode without yeast cells, 0 mM – PQ modified graphite electrode with unmodified yeast cells, 8 to 200 mM – concentration of pyrrole used in modifying yeast cells that are used in the construction of the electrode. B – current density registered for oxidative (0.32 V) and reductive (0.11 V) potentials of ferro/ferric redox couple for different concentrations of pyrrole used in the modification of yeast cells.

In addition to CV measurements, differential pulse voltammetry curves were also obtained for the same constructed electrodes with varying pyrrole concentrations during the modification of yeast cells (Figure 25).

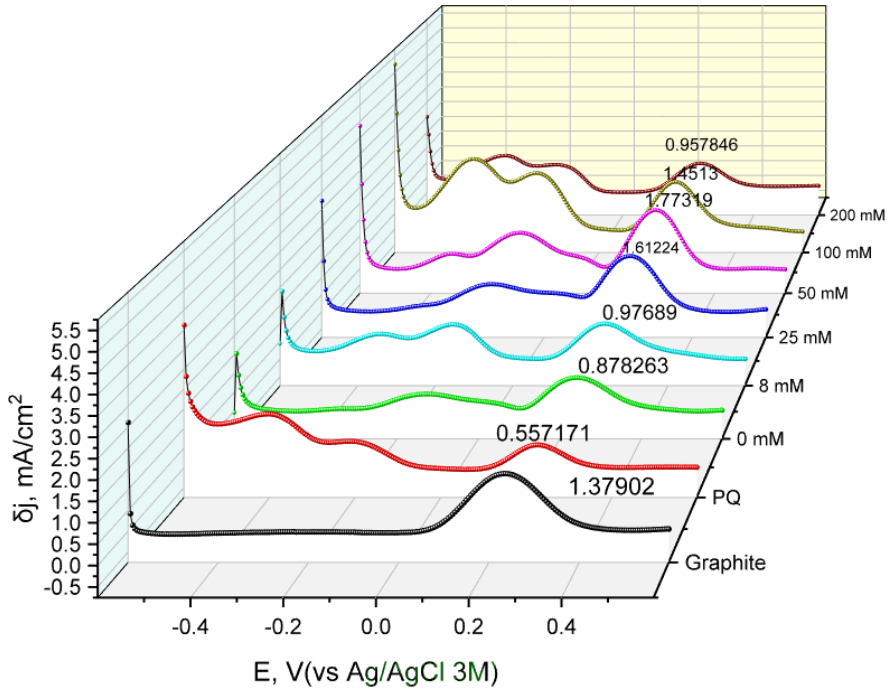

Figure 25. Differential current density curves for various modified working electrode samples used in the electrochemical system. Measurements were conducted by sweeping the potential from -0.6 V to +0.6 V, step potential of 5 mV, pulse amplitude of 50 mV for a duration of 20 ms, scan rate of 50 mV/s, using a Ag/AgCl reference electrode in KCl 3M and Pt as a counter electrode. Graphite – unmodified graphite electrode, PQ – PQ modified graphite electrode, 0 mM – non-modified yeast and PQ modified graphite electrode, 8 to 200 mM – PQ and pPy modified yeast on graphite working electrodes.

The resulting Fe^{2+} oxidative peak δj values were plotted against the concentration of pyrrole used in yeast modification (Figure 26). The change in the current density values indicate that using 50 mM of pyrrole results in the largest current density, which may be attributed to an increase in charge transfer due to conductive pPy properties.

This finding suggests the further investigation on the topic – the exact concentration determination would lead to a peak performance yeast MFC. The next power density measurements imply the same. This leads to the same conclusion – anode choice and modification technique optimization can lead to a breakthrough in yeast-based MFCs.

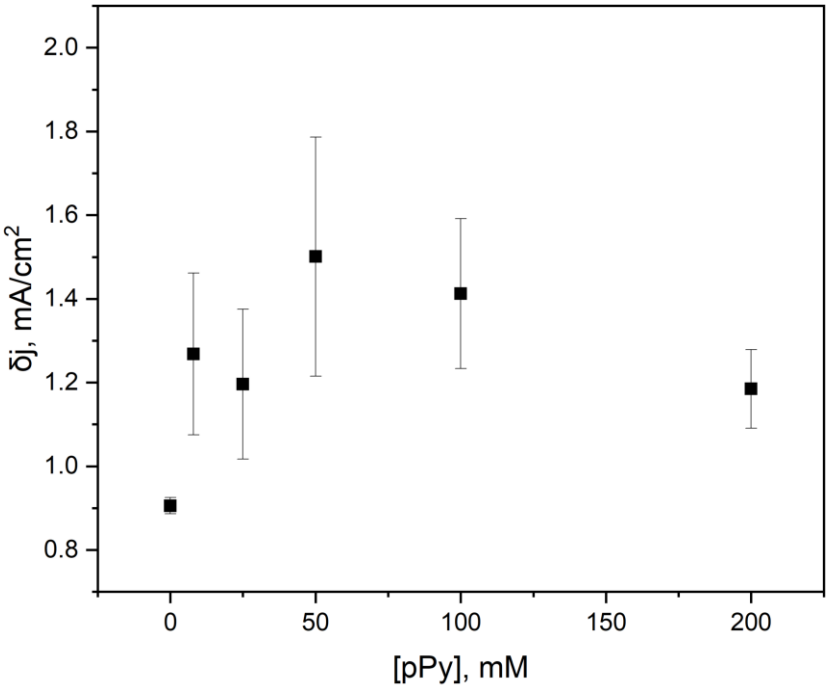

Figure 26. Differential current density dependency on the concentration of pPy used in the modification of yeast cells, utilized in the construction of the PQ-pPy yeast-graphite electrode. The values were taken as Fe^{2+} oxidative peak δj values.

4.2.4 MFC power density measurements with wastewater samples

In addition to voltametric methods, power density measurements were recorded to determine the power output of our modified yeast based MFC. A two-electrode, single-cell system was established using our yeast-modified graphite electrode as the anode and an entirely bigger surface area graphite rod cathode. Measurements were taken in either a glucose (50 mM) and $K_3[Fe(CN_6)]$ (20mM) solution in PBS (Figure 27A and C) or in municipal wastewater diluted and sterilized sludge samples (Figure 27B and D).

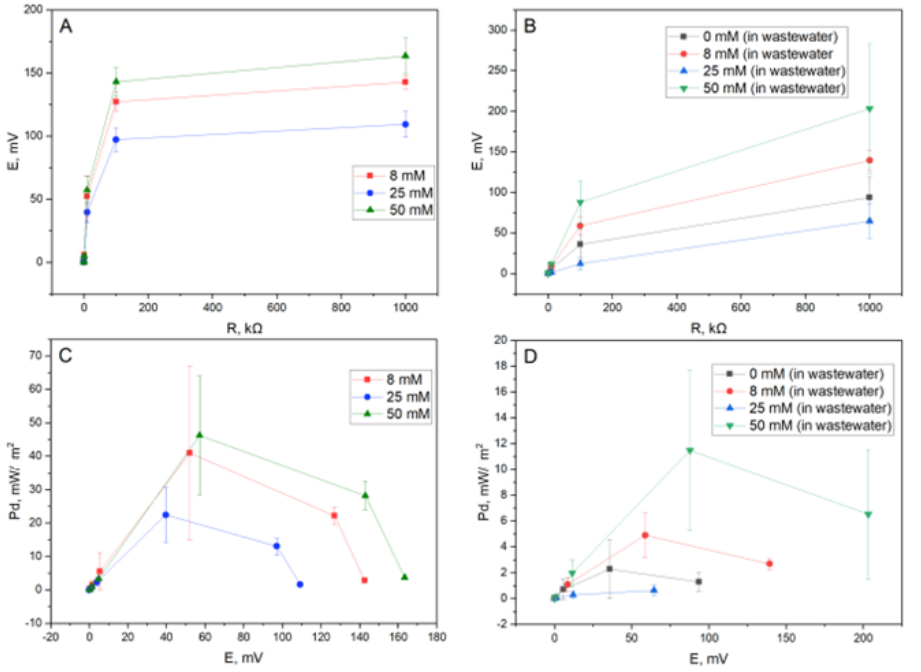

Figure 27. Power density measurements of the constructed yeast-based MFC's. A – Potential-load dependency of the MFC in 50 mM glucose and 20 mM $K_3[Fe(CN_6)]$ solution in PBS, while using yeast modified by different concentrations of pPy. B – potential-load dependency of the system in wastewater samples for different pPy concentrations used in the modification of the yeast. C – power density-potential dependency of the MFC in glucose/$K_3[Fe(CN_6)]$ samples. D – power density-potential dependency of the MFC in wastewater samples.

In the context of the highest potential/power output, it was discovered that the ideal dose of pPy, which was utilized for altering the yeast cell walls, was 50 mM for both medium samples. This finding is a complement to the study that was done before. Nevertheless, a clear drop in both potential and power density values is visible when using wastewater media instead of a glucose and $K_3[Fe(CN_6)]$ sample; this result may be attributed to a lack of a viable substrate for yeast metabolism or a lack of an optimal redox mediator in the wastewater sludge solution and it may warry drastically in concentrations, pH, temperature, and other factors.

The average concentrations of mediators in wastewater that has been sterilized might be determined using a more in-depth analysis and expanded study investigation. It is possible that this will result in the discovery of yeast MFCs under ideal circumstances. It is also recommended that the examination into the quantity of saccharide take place concurrently.

A cytotoxic or general inhibitory effect to this or lower concentration may lead to the decreased energy generation from the fungi. Additionally, a sharp decrease in power output is observed when using 25 mM of pPy when modifying the yeast cells, as was observed during the voltammetry measurements. Furthermore, this could indicate that the yeast cells are being modified in a manner that is causing them to produce less energy. Once again, the idea of doing research on microplastics is brought up.

4.2.5 Comparison to Previous Works

The observed performance enhancements in MFCs correspond with findings in the literature regarding advancements in nanomaterials and conductive polymers. [98] While some earlier yeast MFCs employing pyrrole or other mediators reported power densities in the range of tens of mW/m2, the incorporation of AuNPs in our system significantly elevated the power output. [261–263] This suggests a synergistic effect: polypyrrole by itself already improved charge transfer across cell wall/membrane (as evidenced by cyclic voltammetry); AuNPs improved this by providing more conductivity into the biosurface. Other studies have similarly raised electron transfer rates utilizing nanomaterials like gold nanoparticles or carbon nanotubes; our results support trend for yeast-based MFCs. Importantly, although our absolute power densities were lower than some specialized high-performance setups (for example, those using engineered carbon electrodes), the relative gain from the hybrid modification was significant (roughly two- to three-fold improvement). This confirms that the core strategy – combining polymer and nanoparticle modifications with appropriate mediators – is effective MFC.

Table 3. power density outputs in other works.

Microbe/anode material	Modification*	Substrate	Control PD (mW/m^2)	Max. PD (mW/m^2)	Ref.
Mixed culture/carbon veil	PEDOT:PSS	Urine	0.4305	0.5351	[264]
S. cerevisiae/graphite rod	pPy	Glucose	38.8	47.12	[98]
S. cerevisiae/graphite rod	pPy-AuNP's	Glucose Wastewater	9.2 -	61.1 (147.8 instant) 179.2	This work
Mixed culture/carbon felt	PEDOT:PSS-TEG	Glucose	0.8	68.7	[265]
Gluconobacter Oxydans/graphite rod	PEDOT:PSS-graphene-Nafion	Wastewater	-	82	[266]
Mixed culture/carbon cloth	BioAu-MWCNT	Glucose	114.24	178.34	[267]
Shewanella xiamenensis/BC-PANI	TiO_2	Glucose	137.4	179.4	[268]
Mixed culture/graphite plate	PANI	Potato powder oybean powder	91.5	256.4	[269]
S. cerevisiae C/glassy carbon	CNT's	Glucose	138	344	[270]
Mixed culture/nickel foam	$MgCoO_2$- PEDOT:PSS	Wastewater	2.5x lower	494	[271]
Mixed culture/carbon cloth	PANI-graphene	Acetate	454	884	[272]
Mixed culture/ stainless steel	pPy	Wastewater	40.59	1190.94	[273]
Mixed culture/graphite	FeNP's	Acetate	997	1856	[262]
S. cerevisiae /carbon felt	AuNP-PEI	Glucose	381	2771	[261]
Mixed culture/carbon brush	pPy-CMC-CNT	Acetate	683	2970	[274]
S. cerevisiae/carbon felt	PEI-FeMnNP	Glucose	380	5800	[263]

*FeNP- iron carbide nanoparticles,
PANI -polyaniline;
BioAu- biogenic gold nanoparticles;
CNT – carbon nanotubes;
MWCNT – multiwall carbon nanotubes;
BC – biocellulose,
PEI – polyethiylenimine;
FeMnNP – iron-manganese nanoflowers;
pPy – polypyrrole;
CMC – carbomethyl cellulose;
PANI – polyaniline;
PEDOT:PSS – poly(3,4-ethylene dioxythiophene):poly(4-styrene sulfonate);
TEG – thermally expanded graphite.

4.3 Future Directions

Building on these results, several avenues should be pursued to move toward real-world implementation:

4.3.1 Future Research Directions in SECM Applications

The further exploration of SECM's capabilities in monitoring cellular responses to various therapeutic interventions beyond HDAC inhibitors should be tested. Investigating the electrochemical dynamics of different cardiac cell types and their interactions with various treatments could provide deeper insights into cardiac regeneration strategies. Additionally, expanding the application of SECM to other pathological conditions and cell types may enhance its utility in regenerative medicine. Future studies could also focus on optimizing SECM techniques for real-time monitoring in clinical settings, potentially leading to personalized treatment approaches for cardiac diseases.

4.3.2 Scale-Up and Durability Testing:

Future research should assess these modified MFCs in larger, continuous-flow reactors with real wastewater over extended periods. This will reveal whether the high power densities can be maintained and whether the polypyrrole and AuNP coatings remain stable under practical operating conditions. Strategies such as self-cleaning electrode surfaces or regenerative catalyst systems could be investigated to enhance longevity.

4.3.3 Optimization of Materials and Costs:

To make the technology economically viable, alternative materials should be explored. For example, cheaper metal nanoparticles or carbon-based nanostructures might replace gold, and optimized polymer formulations (perhaps doped or co-polymerized) could provide similar conductivity at lower doses. Process optimization to use minimal polypyrrole that still supports yeast viability will also be important. The electrodes should also be considered – felt or brush the material could be used as well as some kind of metal alloys. This could also lead to a cheaper alternative than thousands of carbon rods.

4.3.4 Genetic and Biochemical Enhancements:

Another promising direction is to use genetic engineering or metabolic engineering to enable *S. cerevisiae* to produce its own redox-active molecules. If the yeast could express endogenous mediators or conductive proteins, it might further improve electron transfer without external chemicals. Investigating this approach could lead to more robust bioelectrodes.

4.3.5 Integrated System Development:

Long-term, these modified yeast MFCs should be assessed in integrated settings. For instance, coupling them with microbial electrolysis cells or hybrid bio-solar systems could harvest more energy. Applications *in situ*, such as *in-situ* treatment of industrial effluents while generating power, should be piloted. Evaluating the system's performance in powering actual devices (sensors, LED lights, etc.) would demonstrate real-world feasibility.

4.3.6 Environmental and Economic Analysis:

A techno-economic analysis and life-cycle assessment would clarify the conditions under which this technology makes sense. Future work should quantify the net energy gain, material costs,[271] and environmental benefits compared to conventional treatment or power methods. Such analysis can guide design choices (e.g., how to reuse or recycle the AuNPs) and identify niche applications where the advantages of bio-based power are greatest.

5. CONCLUSIONS

In this dissertation, we examined a novel hybrid strategy to enhance electron transfer in *Saccharomyces cerevisiae*-based microbial fuel cells by modifying the yeast with a conductive polymer (polypyrrole) and incorporating 10 nm AuNPs as an additional conductive mediator. Prior to this we indicated that DCM atrium-derived hmMSCs are larger and exhibit reduced acetylation, MMP, and NAD^+ levels, along with a significant decrease in redox potential compared to healthy counterparts. HDAC inhibitor SAHA treatment enhanced these parameters, particularly in healthy hmMSCs, potentially improving atrial cell function. SECM effectively characterized redox potential differences between healthy and DCM atrium-derived hmMSCs, detecting changes in redox status influenced by therapeutic agents. The cell-impermeant mediator FcCOOH can monitor both extracellular and intracellular redox changes, proposing a benign method for assessing cellular reactions to therapies. Overall, SECM is a valuable tool for examining intracellular redox dynamics in cardiac cells. Future research will utilize advanced techniques to further explore energetic homeostasis in the heart and other cell types. In the later investigation, the research aimed to determine whether the fungal modifications could improve the power output of yeast MFCs, preserve cell viability, and enable effective operation with real-world substrates (e.g., wastewater sludge). As the results have shown modifications to be successful and the MFC adaptation for the wastewater treatment plant samples has been promising as well, the further investigation will be set for the future. The results our team has now will be a fascinating refferable topic over the upcoming MFC studies. The search for a perfect combination of living microorganisms, their modifications and electrode materials, sets ground for a promising interest in MFCs for th research community.

5.1 The key findings

5.1.1 The bioelectrochemical investigation with SECM

Human mesenchymal stem cells derived from DCM hearts were found to be larger and exhibited reduced levels of intracellular acetylated proteins, MMP, NAD^+ levels, and redox capacity compared to healthy hmMSCs. The HDAC inhibitor SAHA significantly enhanced acetylation and MMP in both healthy and pathological hmMSCs, with a more pronounced effect in the pathological cells. However, the increase in redox capacity was more substantial in healthy cells, indicating that pathological hmMSCs have

compromised NAD^+ biosynthetic pathways, making them less responsive to SAHA treatment.

The study utilized SECM as a non-invasive method to assess intracellular redox states and PMET activities, correlating well with biochemical measurements of NAD^+. The findings suggest that SECM can effectively monitor redox states in human myocardium-derived hmMSCs, with implications for evaluating therapeutic interventions aimed at enhancing cardiac regeneration. Overall, the research highlights the significance of intracellular redox status and PMET in cardiac health and the potential of HDAC inhibitors like SAHA to modulate these parameters for therapeutic benefits.

5.1.2 Enhanced Electrical Performance:

Yeast cells coated with polypyrrole showed a clear increase in current density compared to untreated cells (from roughly 3.76 to 5.01 mA/cm^2 under the same conditions), demonstrating that pPy improves the conductive interface at the cell wall. When both pPy and AuNPs were used, the MFC's power density rose dramatically. In a buffered glucose/$K_3[Fe(CN)_6]$ solution, the hybrid-modified yeast achieved a peak power density of about 61.1 mW/m^2 (using a 10 kΩ external resistor), far exceeding the values for unmodified yeast (9.2 mW/m^2) or yeast modified only with one additive. Especially, when actual diluted wastewater sludge was fed this AuNP-pPy-modified yeast MFC, it produced around 179 mW/m^2, verifying that the improvements transfer into substantially greater power production even in real world substrates. These results coincide with our theories that gold nanoparticles would close conductive network gaps and that polypyrrole coating of the cells would enable direct electron transmission.

5.1.3 Cell Viability and Mediator Strategy:

Throughout these modifications, the yeast cells remained metabolically active.[54] colony-forming unit assays indicated that a 50 mM pyrrole treatment did not decrease yeast viability, which is crucial for sustained MFC operation. The dual-mediator system (using both the hydrophilic ferricyanide and an organic mediator)[46] also appeared to benefit the MFC performance, supporting the idea that *S. cerevisiae* requires both types of mediators for optimal electron shuttling. In sum, the study confirms that *S. cerevisiae* can serve as a robust biocatalyst in MFCs and that our controlled modification approach enhances its electron-transfer capabilities without severely harming the cells.

5.1.4 Alignment with Objectives:

These findings directly address the goals stated in the Introduction. The Objectives were addressed in this manner:

- The electrochemical tests has shown that SECM's feed back mode effectiveness in monitoring redox states for therapeutic interventions in human heart stem cells regeneration is valid (Objective 1).
- Polypyrrole deposition on *S. cerevisiae* cell surface improves electron transfer (Objective 2).
- Gold nanoparticles integration into yeast solution before constructing MFC enhances charge transfer efficiency (Objective 3).
- Modified MFC has been tested with real wastewater sludge (Objective 4).

Each defendable statement posed at the outset was supported: SECM's ability to differentiate healthy and pathological cardiac stem cells through electrochemical methods was tested; the modifications on the selected fungus enhanced electron flow and power output in the MFC performance while experimenting in laboratory scale and during tests with actual wastewater.

5.1.5 Practical Implications:

First, the study demonstrates the practicality of SECM in distinguishing between healthy and pathological cardiac stem cells. By employing SECM, our team were able to bio-harmlessly assess intracellular redox states and PMET activities, which were compatible with biochemical estimations of NAD+ levels. The findings revealed that human mesenchymal stem cells from DCM hearts exhibited compromised redox capacity and altered acetylation compared to healthy cells. The application of the HDAC inhibitor SAHA showed enhanced acetylation and MMP in both cell types, but the response was more pronounced in pathological cells. This underscores SECM's utility in monitoring cellular responses to therapeutic interventions, highlighting its potential role in evaluating strategies for cardiac regeneration. Overall, SECM proves to be a valuable tool in understanding the electrochemical dynamics of cardiac health and disease.

Secondly, the enhanced yeast MFC demonstrated high practicality. The fact that we achieved a much higher power density with wastewater means that such systems could potentially be used for low-power applications like powering remote environmental sensors or providing supplemental energy in wastewater treatment plants. The use of waste sludge as fuel is especially

attractive, as it aligns with the vision of MFCs as sustainable, self-contained power sources. However, the results also highlight challenges. While 179 mW/m² is a substantial improvement, it remains a modest absolute power level, so real applications would likely require either large electrode areas or coupling with energy storage. For now, the need for glucose to be present in the system limits yeast-based MFC technology implementation only to food industry wastewater treatment. The durability of the AuNP–pPy coating in real environments is promising but must be assessed over longer timescales. Moreover, cost considerations arise: gold nanoparticles are effective but expensive, so future practical designs may need to explore cheaper alternatives or reuse of the catalyst materials. Nonetheless, this work shows that relatively simple bio-modification strategies can significantly boost MFC performance, bringing practical applications a step closer.

In conclusion, this study confirms the electrochemical capabilities of SECM to detect and evaluate different cardiac cell types as well as that bio-modifying *S. cerevisiae* with CPs and nanoparticles can significantly enhance MFC performance, validating the initial hypotheses. The technical advances demonstrated here (higher currents, improved power densities, and maintained cell viability) bring yeast-based MFCs closer to practical use. With further optimization and scaling, modified MFCs could find roles in sustainable energy harvesting from waste streams, aligning with the broader goals of renewable bioelectrochemical systems. The approaches and insights gained in this work provide a foundation for future interdisciplinary efforts [275,276] to develop scalable, efficient, and eco-friendly MFC technologies.

6. REFFERENCES

1. Sharif A, Mehmood U, Tiwari S. A step towards sustainable development: role of green energy and environmental innovation. *Environ Dev Sustain*. 2024;26(4):9603-9624. doi:10.1007/s10668-023-03111-5
2. Jones ER, Van Vliet MTH, Qadir M, Bierkens MFP. Country-level and gridded estimates of wastewater production, collection, treatment and reuse. *Earth Syst Sci Data*. 2021;13(2):237-254. doi:10.5194/essd-13-237-2021
3. Lazenby RA, White RJ. Advances and perspectives in chemical imaging in cellular environments using electrochemical methods. *Chemosensors*. 2018;6(2). doi:10.3390/chemosensors6020024
4. Giam LR, Massich MD, Hao L, Wong LS, Mader CC, Mirkin CA. Scanning probe-enabled nanocombinatorics define the relationship between fibronectin feature size and stem cell fate. *Proc Natl Acad Sci U S A*. 2012;109(12):4377-4382. doi:10.1073/pnas.1201086109
5. Kaya T, Torisawa Y suke, Oyamatsu D, Nishizawa M, Matsue T. Monitoring the cellular activity of a cultured single cell by scanning electrochemical microscopy (SECM). A comparison with fluorescence viability monitoring. *Biosens Bioelectron*. 2003;18(11):1379-1383. doi:10.1016/S0956-5663(03)00083-6
6. Liu B, Cheng W, Rotenberg SA, Mirkin M V. Scanning electrochemical microscopy of living cells - Part 2. Imaging redox and acid/basic reactivities. *Journal of Electroanalytical Chemistry*. 2001;500(1-2):590-597. doi:10.1016/S0022-0728(00)00436-8
7. Morkvenaite-Vilkonciene I, Ramanaviciene A, Ramanavicius A. 9,10-Phenanthrenequinone as a redox mediator for the imaging of yeast cells by scanning electrochemical microscopy. *Sens Actuators B Chem*. 2016;228:200-206. doi:10.1016/j.snb.2015.12.102
8. Murata T, Yasukawa T, Shiku H, Matsue T. Electrochemical single-cell gene-expression assay combining dielectrophoretic manipulation with secreted alkaline phosphatase reporter system. *Biosens Bioelectron*. 2009;25(4):913-919. doi:10.1016/j.bios.2009.09.001
9. Sun P, Laforge FO, Abeyweera TP, Rotenberg SA, Carpino J, Mirkin M V. Nanoelectrochemistry of mammalian cells. *Proc Natl Acad Sci U S A*. 2008;105(2):443-448. doi:10.1073/pnas.0711075105

10. Li Y, Ning X, Ma Q, Qin D, Lu X. Recent advances in electrochemistry by scanning electrochemical microscopy. *TrAC - Trends in Analytical Chemistry*. *Elsevier B.V.* 2016;80:242-254. doi:10.1016/j.trac.2016.02.002
11. Morkvenaite-Vilkonciene I, Ramanaviciene A, Genys P, Ramanavicius A. Evaluation of Enzymatic Kinetics of GOx-based Electrodes by Scanning Electrochemical Microscopy at Redox Competition Mode. *Electroanalysis*. 2017;29(6):1532-1542. doi:10.1002/elan.201700022
12. Rotenberg SA, Mirkin M V. Scanning electrochemical microscopy: Detection of human breast cancer cells by redox environment. *J Mammary Gland Biol Neoplasia*. 2004;9(4):375-382. doi:10.1007/s10911-004-1407-7
13. Yao L, Filice FP, Yang Q, Ding Z, Su B. Quantitative Assessment of Molecular Transport through Sub-3 nm Silica Nanochannels by Scanning Electrochemical Microscopy. *Anal Chem*. 2019;91(2):1548-1556. doi:10.1021/acs.analchem.8b04795
14. Bard AJ, Mirkin M V. *Scanning Electrochemical Microscopy*. Marcel Dekker; 2001.
15. Kranz C, Lötzbeyer T, Schmidt HL, Schuhmann W. Lateral visualization of direct electron transfer between microperoxidase and electrodes by means of scanning electrochemical microscopy. *Biosens Bioelectron*. 1997;12(4):257-266. doi:10.1016/S0956-5663(96)00056-5
16. Hengstenberg A, Kranz C, Schuhmann W. *Facilitated Tip-Positioning and Applications of Non-Electrode Tips in Scanning Electrochemical Microscopy Using a Shear Force Based Constant-Distance Mode*.
17. Ballesteros Katemann B, Schulte A, Schuhmann W. Constant-distance mode scanning electrochemical microscopy (SECM) - Part I: Adaptation of a non-optical shear-force-based positioning mode for SECM tips. *Chemistry - A European Journal*. 2003;9(9):2025-2033. doi:10.1002/chem.200204267
18. Yang N, Smirnov W, Kriele A, Hoffmann R, Nebel CE. Diamond nanotextured surfaces for enhanced protein redox activity. *physica status solidi (a)*. 2010;207(9):2069-2072. doi:10.1002/pssa.201000085
19. Kuznetsov YG, Malkin AJ, Mcpherson A. *Atomic Force Microscopy Studies of Living Cells: Visualization of Motility, Division, Aggregation, Transformation, and Apoptosis*. 1997.
20. Comstock DJ, Elam JW, Pellin MJ, Hersam MC. Integrated ultramicroelectrode-nanopipet probe for concurrent scanning electrochemical microscopy and scanning Ion conductance microscopy. *Anal Chem*. 2010;82(4):1270-1276. doi:10.1021/ac902224q

21. Lee JH, Lee J, Faccinto JA, et al. *To Cite This Article: P. I. James et Al*. Vol 145. 1998.
22. Ludwig M, Kranz C, Schuhmann W, Gaub HE. Topography feedback mechanism for the scanning electrochemical microscope based on hydrodynamic forces between tip and sample. *Review of Scientific Instruments*. 1995;66(4):2857-2860. doi:10.1063/1.1145568
23. Alpuche-Aviles MA, Wipf DO. Impedance feedback control for scanning electrochemical microscopy. *Anal Chem*. 2001;73(20):4873-4881. doi:10.1021/ac010581q
24. Eckhard K, Etienne M, Schulte A, Schuhmann W. Constant-distance mode AC-SECM for the visualisation of corrosion pits. *Electrochem commun*. 2007;9(7):1793-1797. doi:10.1016/j.elecom.2007.03.035
25. Shin H, Hesketh PJ, Mizaikoff B, Kranz C. Development of wafer-level batch fabrication for combined atomic force-scanning electrochemical microscopy (AFM-SECM) probes. *Sens Actuators B Chem*. 2008;134(2):488-495. doi:10.1016/j.snb.2008.05.039
26. Bard AJ, Mirkin M V, Unwin PR, Wipf DO. Scanning electrochemical microscopy. 12. Theory and experiment of the feedback mode with finite heterogeneous electron-transfer kinetics and arbitrary substrate size. *Journal of Physical Chemistry*. 1992;96(4):1861-1868. doi:10.1021/j100183a064
27. Cooper LT. Myocarditis. *New England Journal of Medicine*. 2009;360(15):1526-1538. doi:10.1056/nejmra0800028
28. Islam A, Abraham P, Hapner CD, Deuster PA, Chen Y. Tissue-specific upregulation of HSP72 in mice following short-term administration of alcohol. *Cell Stress Chaperones*. 2013;18(2):215-222. doi:10.1007/s12192-012-0375-x
29. Maisch B, Noutsias M, Ruppert V, Richter A, Pankuweit S. Cardiomyopathies: Classification, Diagnosis, and Treatment. *Heart Fail Clin*. 2012;8(1):53-78. doi:10.1016/j.hfc.2011.08.014
30. Dadson K, Hauck L, Billia F. Molecular mechanisms in cardiomyopathy. *Clin Sci*. 2017;131(13):1375-1392. doi:10.1042/CS20160170
31. Stoppel WL, Kaplan DL, Black LD. Electrical and mechanical stimulation of cardiac cells and tissue constructs. *Adv Drug Deliv Rev*. 2016;96:135-155. doi:10.1016/j.addr.2015.07.009
32. Gan T, Hu J, Aledan AKO, et al. Exploring the pathogenesis and immune infiltration in dilated cardiomyopathy complicated with atrial fibrillation by bioinformatics analysis. *Front Immunol*. 2023;14(January):1-15. doi:10.3389/fimmu.2023.1049351

33. Kolwicz SC, Purohit S, Tian R. Cardiac metabolism and its interactions with contraction, growth, and survival of cardiomyocytes. *Circ Res*. 2013;113(5):603-616. doi:10.1161/CIRCRESAHA.113.302095
34. Karwi QG, Uddin GM, Ho KL, Lopaschuk GD. Loss of Metabolic Flexibility in the Failing Heart. *Front Cardiovasc Med*. *Frontiers Media S.A.* 2018;5. doi:10.3389/fcvm.2018.00068
35. Xiao W, Wang RS, Handy DE, Loscalzo J. NAD(H) and NADP(H) Redox Couples and Cellular Energy Metabolism. *Antioxid Redox Signal*. *Mary Ann Liebert Inc.* 2018;28(3):251-272. doi:10.1089/ars.2017.7216
36. Carotenuto F, Manzari V, Nardo P Di. Cardiac Regeneration: the Heart of the Issue. doi:10.1007/s40472-021-00319-0/Published
37. Nesselmann C, Ma N, Bieback K, et al. Mesenchymal stem cells and cardiac repair. *J Cell Mol Med*. *Blackwell Publishing Inc.* 2008;12(5B):1795-1810. doi:10.1111/j.1582-4934.2008.00457.x
38. Camelliti P, Borg TK, Kohl P. Structural and functional characterisation of cardiac fibroblasts. *Cardiovasc Res*. 2005;65(1):40-51. doi:10.1016/j.cardiores.2004.08.020
39. Yacoub MH, Terrovitis J. CADUCEUS, SCIPIO, ALCADIA: Cell therapy trials using cardiac-derived cells for patients with post myocardial infarction LV dysfunction, still evolving. *Glob Cardiol Sci Pract*. 2013;2013(1):3. doi:10.5339/gcsp.2013.3
40. Ng SC, Ng HH. The metabolic programming of stem cells. Published online 2017. doi:10.1101/gad.293167
41. Shi X, Yin Y, Guo X, et al. The histone deacetylase inhibitor SAHA exerts a protective effect against myocardial ischemia/reperfusion injury by inhibiting sodium-calcium exchanger. *Biochem Biophys Res Commun*. 2023;671:105-115. doi:10.1016/j.bbrc.2023.05.120
42. Iyer A, Fenning A, Lim J, et al. Antifibrotic activity of an inhibitor of histone deacetylases in DOCA-salt hypertensive rats: Research paper. *Br J Pharmacol*. 2010;159(7):1408-1417. doi:10.1111/j.1476-5381.2010.00637.x
43. Xie M, Kong Y, Tan W, et al. Histone deacetylase inhibition blunts ischemia/reperfusion injury by inducing cardiomyocyte autophagy. *Circulation*. 2014;129(10):1139-1151. doi:10.1161/CIRCULATIONAHA.113.002416
44. Miksiunas R, Rucinskas K, Janusauskas V, Labeit S, Bironaite D. Histone deacetylase inhibitor suberoylanilide hydroxamic acid improves energetic status and cardiomyogenic differentiation of

human dilated myocardium-derived primary mesenchymal cells. *Int J Mol Sci*. 2020;21(14):1-20. doi:10.3390/ijms21144845

45. Mahto KU, Das S. Electroactive biofilm communities in microbial fuel cells for the synergistic treatment of wastewater and bioelectricity generation. *Crit Rev Biotechnol*. *Taylor and Francis Ltd.* Preprint posted online 2024. doi:10.1080/07388551.2024.2372070
46. Willner I, Willner B, Katz E. Biomolecule-nanoparticle hybrid systems for bioelectronic applications. *Bioelectrochemistry*. 2007;70(1):2-11. doi:10.1016/j.bioelechem.2006.03.013
47. Boas JV, Oliveira VB, Simões M, Pinto AMFR. Review on microbial fuel cells applications, developments and costs. *J Environ Manage*. *Academic Press*. 2022;307. doi:10.1016/j.jenvman.2022.114525
48. Kižys K, Zinovičius A, Jakštys B, et al. Microbial Biofuel Cells: Fundamental Principles, Development and Recent Obstacles. *Biosensors (Basel)*. 2023;13(2). doi:10.3390/bios13020221
49. Ramanavicius A, Andriukonis E, Stirke A, Mikoliunaite L, Balevicius Z, Ramanaviciene A. Synthesis of polypyrrole within the cell wall of yeast by redox-cycling of [Fe(CN)6]3−/[Fe(CN)6]4−. *Enzyme Microb Technol*. 2016;83:40-47. doi:10.1016/J.ENZMICTEC.2015.11.009
50. Ramanavicius S, Ramanavicius A. Conducting Polymers in the Design of Biosensors and Biofuel Cells. *Polymers (Basel)*. 2021;13(1):1-19. doi:10.3390/polym13010049
51. Bruzaite I, Rozene J, Morkvenaite-Vilkonciene I, Ramanavicius A. Towards microorganism-based biofuel cells: The viability of saccharomyces cerevisiae modified by multiwalled carbon nanotubes. *Nanomaterials*. 2020;10(5):1-14. doi:10.3390/nano10050954
52. Rozene J, Morkvenaite-Vilkonciene I, Bruzaite I, Dzedzickis A, Ramanavicius A. Yeast-based microbial biofuel cell mediated by 9,10-phenantrenequinone. *Electrochim Acta*. 2021;373:137918. doi:10.1016/j.electacta.2021.137918
53. Rozene J, Morkvenaite-Vilkonciene I, Bruzaite I, Zinovicius A, Ramanavicius A. Baker's yeast-based microbial fuel cell mediated by 2-methyl-1,4-naphthoquinone. *Membranes (Basel)*. 2021;11(3):1-10. doi:10.3390/membranes11030182
54. Kižys K, Pirštelis D, Morkvėnaitė-Vilkončienė I. Effect of Gold Nanoparticles in Microbial Fuel Cells Based on Polypyrrole-Modified Saccharomyces cerevisiae. *Biosensors (Basel)*. 2024;14(12). doi:10.3390/bios14120572
55. Adomaitė G, Virbickas P, Valiūnienė A. Modification of Saccharomyces cerevisiae Cells with Metal Hexacyanoferrates for the

Construction of a Yeast-Based Fuel Cell. *Molecules*. 2025;30(1). doi:10.3390/molecules30010137

56. Bashir S, Houf W, Liu JL, Mulvaney SP. 3D Conducting Polymeric Membrane and Scaffold Saccharomyces cerevisiae Biofilms to Enhance Energy Conversion in Microbial Fuel Cells. *ACS Appl Mater Interfaces*. 2022;14(18):20393-20403. doi:10.1021/acsami.1c20445
57. Moradian JM, Yang FQ, Xu N, et al. Enhancement of bioelectricity and hydrogen production from xylose by a nanofiber polyaniline modified anode with yeast microbial fuel cell. *Fuel*. 2022;326. doi:10.1016/j.fuel.2022.125056
58. Flimban SGA, Hassan SHA, Rahman MM, Oh SE. The effect of Nafion membrane fouling on the power generation of a microbial fuel cell. *Int J Hydrogen Energy*. 2020;45(25):13643-13651. doi:10.1016/j.ijhydene.2018.02.097
59. Rabaey K, Verstraete W. Microbial fuel cells: Novel biotechnology for energy generation. *Trends Biotechnol*. 2005;23(6):291-298. doi:10.1016/j.tibtech.2005.04.008
60. Babanova S, Hubenova Y, Mitov M. Influence of artificial mediators on yeast-based fuel cell performance. *J Biosci Bioeng*. 2011;112(4):379-387. doi:10.1016/j.jbiosc.2011.06.008
61. Schafer FQ, Buettner GR. *Review Article REDOX ENVIRONMENT OF THE CELL AS VIEWED THROUGH THE REDOX STATE OF THE GLUTATHIONE DISULFIDE/GLUTATHIONE COUPLE*. 2001.
62. Zhang Q, Piston DW, Goodman RH. Regulation of corepressor function by nuclear NADH. *Science (1979)*. 2002;295(5561):1895-1897. doi:10.1126/science.1069300
63. Hubenova Y, Mitov M. Extracellular electron transfer in yeast-based biofuel cells: A review. *Bioelectrochemistry*. 2015;106:177-185. doi:10.1016/j.bioelechem.2015.04.001
64. Shkil H, Schulte A, Guschin DA, Schuhmann W. Electron transfer between genetically modified Hansenula polymorpha yeast cells and electrode surfaces via os-complex modified redox polymers. *ChemPhysChem*. 2011;12(4):806-813. doi:10.1002/cphc.201000889
65. Williams J, Trautwein-Schult A, Jankowska D, Kunze G, Squire MA, Baronian K. Identification of uric acid as the redox molecule secreted by the yeast Arxula adeninivorans. *Appl Microbiol Biotechnol*. 2014;98(5):2223-2229. doi:10.1007/s00253-013-5487-4
66. Hubenova Y, Georgiev D, Mitov M. Enhanced phytate dephosphorylation by using Candida melibiosica yeast-based biofuel

cell. *Biotechnol Lett*. 2014;36(10):1993-1997. doi:10.1007/s10529-014-1571-9

67. Walker AL, Walker CW. Biological fuel cell and an application as a reserve power source. *J Power Sources*. 2006;160(1):123-129. doi:10.1016/j.jpowsour.2006.01.077
68. Szijgyarto Z, Garedew A, Azevedo C, Saiardi A. Influence of inositol pyrophosphates on cellular energy dynamics. *Science (1979)*. 2011;334(6057):802-805. doi:10.1126/science.1211908
69. Hubenova Y, Mitov M. Mitochondrial origin of extracelullar transferred electrons in yeast-based biofuel cells. *Bioelectrochemistry*. 2015;106:232-239. doi:10.1016/j.bioelechem.2014.06.005
70. Duarte KDZ, Frattini D, Kwon Y. High performance yeast-based microbial fuel cells by surfactant-mediated gold nanoparticles grown atop a carbon felt anode. *Appl Energy*. 2019;256(September):113912. doi:10.1016/j.apenergy.2019.113912
71. Duarte KDZ, Kwon Y. Enhanced extracellular electron transfer of yeast-based microbial fuel cells via one pot substrate-bound growth iron-manganese oxide nanoflowers. *J Power Sources*. 2020;474(January):228496. doi:10.1016/j.jpowsour.2020.228496
72. Sirinutsomboon B. Modeling of a membraneless single-chamber microbial fuel cell with molasses as an energy source. *International Journal of Energy and Environmental Engineering*. 2014;5(2-3):1-9. doi:10.1007/s40095-014-0093-5
73. Maron BJ, Towbin JA, Thiene G, et al. Contemporary definitions and classification of the cardiomyopathies: An American Heart Association Scientific Statement from the Council on Clinical Cardiology, Heart Failure and Transplantation Committee; Quality of Care and Outcomes Research and Functio. *Circulation*. 2006;113(14):1807-1816. doi:10.1161/CIRCULATIONAHA.106.174287
74. Raghavulu SV, Goud RK, Sarma PN, Mohan SV. Saccharomyces cerevisiae as anodic biocatalyst for power generation in biofuel cell: Influence of redox condition and substrate load. *Bioresour Technol*. 2011;102(3):2751-2757. doi:10.1016/j.biortech.2010.11.048
75. Ramanavicius A, Ramanaviciene A. Hemoproteins in Design of Biofuel Cells. *Fuel Cells*. 2009;9(1):25-36. doi:10.1002/fuce.200800052
76. Kisieliute A, Popov A, Apetrei RMM, et al. Towards microbial biofuel cells: Improvement of charge transfer by self-modification of microoganisms with conducting polymer – Polypyrrole. *Chemical Engineering Journal*. 2019;356:1014-1021. doi:10.1016/J.CEJ.2018.09.026

77. Davis F, Higson SPJ. Biofuel cells-Recent advances and applications. *Biosens Bioelectron*. Published online 2007. doi:10.1016/j.bios.2006.04.029
78. Liu Y, Zhang J, Cheng Y, Jiang SP. Effect of Carbon Nanotubes on Direct Electron Transfer and Electrocatalytic Activity of Immobilized Glucose Oxidase. Published online 2018. doi:10.1021/acsomega.7b01633
79. Kisieliute A, Popov A, Apetrei RM, et al. Towards microbial biofuel cells: Improvement of charge transfer by self-modification of microoganisms with conducting polymer – Polypyrrole. *Chemical Engineering Journal*. 2019;356:1014-1021. doi:10.1016/J.CEJ.2018.09.026
80. Sekrecka-Belniak A, Toczyłowska-Mamińska R. Fungi-based microbial fuel cells. *Energies (Basel)*. 2018;11(10):2827.
81. Babanova S, Hubenova Y, Mitov M. Influence of artificial mediators on yeast-based fuel cell performance. *J Biosci Bioeng*. Published online 2011. doi:10.1016/j.jbiosc.2011.06.008
82. Morkvenaite-Vilkonciene I, Ramanaviciene A, Ramanavicius A. 9,10-Phenanthrenequinone as a redox mediator for the imaging of yeast cells by scanning electrochemical microscopy. *Sens Actuators B Chem*. 2016;228:200-206. doi:10.1016/j.snb.2015.12.102
83. Ishioka T, Uchida T, Teramae N. Analysis of the redox reaction of 9,10-phenanthrenequinone on a gold electrode surface by cyclic voltammetry and time-resolved Fourier transform surface-enhanced Raman scattering spectroscopy. *Anal Chim Acta*. 2001;449(1-2):253-260. doi:10.1016/S0003-2670(01)01352-6
84. Le Comte A, Chhin D, Gagnon A, Retoux R, Brousse T, Bélanger D. Spontaneous grafting of 9,10-phenanthrenequinone on porous carbon as an active electrode material in an electrochemical capacitor in an alkaline electrolyte. *J Mater Chem A Mater*. 2015;3(11):6146-6156. doi:10.1039/c4ta05536e
85. Genys P, Aksun E, Tereshchenko A, Valiūnienė A, Ramanaviciene A, Ramanavicius A. Electrochemical deposition and investigation of poly-9,10-phenanthrenequinone layer. *Nanomaterials*. 2019;9(5). doi:10.3390/nano9050702
86. Hossain MS, Tryk D, Yeager E. The electrochemistry of graphite and modified graphite surfaces: the reduction of O2. *Electrochim Acta*. 1989;34(12):1733-1737. doi:10.1016/0013-4686(89)85057-1
87. Brousse T, Cougnon C, Bélanger D. Grafting of quinones on carbons as active electrode materials in electrochemical capacitors. *J Braz*

Chem Soc. Sociedade Brasileira de Quimica. 2018;29(5):989-997. doi:10.21577/0103-5053.20180015

88. Rodriguez CE, Sobol Z, Schiestl RH. 9, 10-Phenanthrenequinone induces DNA deletions and forward mutations via oxidative mechanisms in the yeast Saccharomyces cerevisiae. *Toxicology in Vitro*. 2008;22(2):296-300.
89. Yamashoji S. Different characteristics between menadione and menadione sodium bisulfite as redox mediator in yeast cell suspension. *Biochem Biophys Rep*. Published online 2016. doi:10.1016/j.bbrep.2016.03.007
90. Hubenova Y V, Rashkov RS, Buchvarov VD, Arnaudova MH, Babanova SM, Mitov MY. Improvement of yeast− biofuel cell output by electrode modifications. *Ind Eng Chem Res*. 2010;50(2):557-564.
91. Morkvenaite-Vilkonciene I, Ramanaviciene A, Ramanavicius A. 9,10-Phenanthrenequinone as a redox mediator for the imaging of yeast cells by scanning electrochemical microscopy. *Sens Actuators B Chem*. 2016;228. doi:10.1016/j.snb.2015.12.102
92. Kisieliute A, Popov A, Apetrei RM, et al. Towards microbial biofuel cells: Improvement of charge transfer by self-modification of microoganisms with conducting polymer – Polypyrrole. *Chemical Engineering Journal*. 2019;356:1014-1021. doi:10.1016/j.cej.2018.09.026
93. Petroniene J, Morkvenaite-Vilkonciene I, Miksiunas R, et al. Scanning electrochemical microscopy for the investigation of redox potential of human myocardium-derived mesenchymal stem cells grown at 2D and 3D conditions. *Electrochim Acta*. 2020;360. doi:10.1016/j.electacta.2020.136956
94. Petroniene J, Morkvenaite-Vilkonciene I, Miksiunas R, et al. Evaluation of redox activity of human myocardium-derived mesenchymal stem cells by scanning electrochemical microscopy. *Electroanalysis*. Published online February 14, 2020:elan.201900723. doi:10.1002/elan.201900723
95. Rodriguez CE, Sobol Z, Schiestl RH. 9, 10-Phenanthrenequinone induces DNA deletions and forward mutations via oxidative mechanisms in the yeast Saccharomyces cerevisiae. *Toxicology in Vitro*. 2008;22(2):296-300. doi:10.1016/j.tiv.2007.09.001
96. Yamashoji S. Different characteristics between menadione and menadione sodium bisulfite as redox mediator in yeast cell suspension. *Biochem Biophys Rep*. 2016;6:88-93. doi:10.1016/j.bbrep.2016.03.007
97. Morkvenaite-Vilkonciene I, Ramanaviciene A, Ramanavicius A. 9,10-Phenanthrenequinone as a redox mediator for the imaging of yeast

cells by scanning electrochemical microscopy. *Sens Actuators B Chem*. 2016;228. doi:10.1016/j.snb.2015.12.102

98. Zinovicius A, Rozene J, Merkelis T, Bruzaitė I, Ramanavicius A, Morkvenaite-Vilkonciene I. Evaluation of a Yeast–Polypyrrole Biocomposite Used in Microbial Fuel Cells. *Sensors*. 2022;22(1). doi:10.3390/s22010327
99. Rozene J, Morkvenaite-Vilkonciene I, Bruzaite I, Dzedzickis A, Ramanavicius A. Yeast-based microbial biofuel cell mediated by 9,10-phenantrenequinone. *Electrochim Acta*. 2021;373:137918. doi:10.1016/j.electacta.2021.137918
100. Hubenova Y V, Rashkov RS, Buchvarov VD, Arnaudova MH, Babanova SM, Mitov MY. Improvement of Yeast− Biofuel Cell Output by Electrode Modifications. *Ind Eng Chem Res*. 2010;50(2):557-564.
101. O'Brien PJ. Molecular mechanisms of quinone cytotoxicity. *Chem Biol Interact*. 1991;80(1):1-41. doi:10.1016/0009-2797(91)90029-7
102. Brunmark A, Cadenas E. Redox and addition chemistry of quinoid compounds and its biological implications. *Free Radic Biol Med*. 1989;7(4):435-477. doi:10.1016/0891-5849(89)90126-3
103. Monks TJ, Lau SS. Toxicology of quinone-thioethers. *Crit Rev Toxicol*. 1992;22(5-6):243-270. doi:10.3109/10408449209146309
104. Bolton JL, Trush MA, Penning TM, Dryhurst G, Monks TJ. Role of quinones in toxicology. *Chem Res Toxicol*. 2000;13(3):135-160. doi:10.1021/tx9902082
105. Rozene J, Morkvenaite-Vilkonciene I, Bruzaite I, Zinovicius A, Ramanavicius A. Baker's yeast-based microbial fuel cell mediated by 2-methyl-1,4-naphthoquinone. *Membranes (Basel)*. 2021;11(3):1-10. doi:10.3390/membranes11030182
106. Rozene J, Morkvenaite-Vilkonciene I, Bruzaite I, Dzedzickis A, Ramanavicius A. Yeast-based microbial biofuel cell mediated by 9,10-phenantrenequinone. *Electrochim Acta*. 2021;373:137918. doi:10.1016/j.electacta.2021.137918
107. Ramanavicius A, Morkvenaite-Vilkonciene I, Kisieliute A, Petroniene J, Ramanaviciene A. Scanning electrochemical microscopy based evaluation of influence of pH on bioelectrochemical activity of yeast cells − Saccharomyces cerevisiae. *Colloids Surf B Biointerfaces*. 2017;149:1-6. doi:10.1016/j.colsurfb.2016.09.039
108. Emir G, Dilgin Y, Ramanaviciene A, Ramanavicius A. Amperometric nonenzymatic glucose biosensor based on graphite rod electrode

modified by Ni-nanoparticle/polypyrrole composite. *Microchemical Journal*. 2021;161. doi:10.1016/j.microc.2020.105751

109. Ramanavicius A, Oztekin Y, Ramanaviciene A. Electrochemical formation of polypyrrole-based layer for immunosensor design. *Sens Actuators B Chem*. 2014;197:237-243. doi:10.1016/j.snb.2014.02.072
110. Long YZ, Li MM, Gu C, et al. Recent advances in synthesis, physical properties and applications of conducting polymer nanotubes and nanofibers. *Prog Polym Sci*. 2011;36(10):1415-1442. doi:10.1016/J.PROGPOLYMSCI.2011.04.001
111. Ramanavicius S, Ramanavicius A. Conducting Polymers in the Design of Biosensors and Biofuel Cells. *Polymers 2021, Vol 13, Page 49*. 2020;13(1):49. doi:10.3390/POLYM13010049
112. Rahman MA, Kumar P, Park DS, Shim YB. Electrochemical sensors based on organic conjugated polymers. *Sensors*. 2008;8(1):118-141. doi:10.3390/s8010118
113. Bredas JL, Street GB. Polarons, Bipolarons, and Solitons in Conducting Polymers. *Acc Chem Res*. 1985;18(10):309-315. doi:10.1021/ar00118a005
114. Le THH, Kim Y, Yoon H. Electrical and electrochemical properties of conducting polymers. *Polymers (Basel)*. 2017;9(4):150. doi:10.3390/polym9040150
115. Ratautaite V, Topkaya SN, Mikoliunaite L, et al. Molecularly Imprinted Polypyrrole for DNA Determination. *Electroanalysis*. 2013;25(5):1169-1177. doi:10.1002/elan.201300063
116. Ramanavicius S, Ramanavicius A. Charge Transfer and Biocompatibility Aspects in Conducting Polymer-Based Enzymatic Biosensors and Biofuel Cells. *Nanomaterials*. 2021;11(2):371. doi:10.3390/nano11020371
117. Ramanaviciene A, Ramanavicius A. Pulsed amperometric detection of DNA with an ssDNA/polypyrrole-modified electrode. *Anal Bioanal Chem*. 2004;379(2):287-293. doi:10.1007/s00216-004-2573-6
118. Ramanavicius A, Kausaite A, Ramanaviciene A. Self-encapsulation of oxidases as a basic approach to tune the upper detection limit of amperometric biosensors. *Analyst*. 2008;133(8):1083. doi:10.1039/b801501e
119. Bai S, Hu Q, Zeng Q, Wang M, Wang L. Variations in Surface Morphologies, Properties, and Electrochemical Responses to Nitro-Analyte by Controlled Electropolymerization of Thiophene Derivatives. *ACS Appl Mater Interfaces*. 2018;10(13):11319-11327. doi:10.1021/acsami.8b00554

120. Stewart S, Ivy MA, Anslyn E V. The use of principal component analysis and discriminant analysis in differential sensing routines. *Chem Soc Rev*. 2014;43(1):70-84. doi:10.1039/c3cs60183h
121. Jiang JX, Su F, Trewin A, et al. Conjugated Microporous Poly(aryleneethynylene) Networks. *Angewandte Chemie*. 2007;119(45):8728-8732. doi:10.1002/ange.200701595
122. Lete C, Lakard B, Hihn JY, del Campo FJ, Lupu S. Use of sinusoidal voltages with fixed frequency in the preparation of tyrosinase based electrochemical biosensors for dopamine electroanalysis. *Sens Actuators B Chem*. 2017;240(C):801-809. doi:10.1016/j.snb.2016.09.045
123. Patois T, Lakard B, Martin N, Fievet P. Effect of various parameters on the conductivity of free standing electrosynthesized polypyrrole films. *Synth Met*. 2010;160(19-20):2180-2185. doi:10.1016/j.synthmet.2010.08.005
124. Leonavicius K, Ramanaviciene A, Ramanavicius A. Polymerization Model for Hydrogen Peroxide Initiated Synthesis of Polypyrrole Nanoparticles. *Langmuir*. 2011;27(17):10970-10976. doi:10.1021/la201962a
125. Pankratova G, Hederstedt L, Gorton L. Extracellular electron transfer features of Gram-positive bacteria. *Anal Chim Acta*. 2019;1076:32-47. doi:10.1016/j.aca.2019.05.007
126. Pankratova G, Pankratov D, Milton RD, Minteer SD, Gorton L. Following Nature: Bioinspired Mediation Strategy for Gram-Positive Bacterial Cells. *Adv Energy Mater*. 2019;9(16):1-6. doi:10.1002/aenm.201900215
127. Güven G, Lozano-Sanchez P, Güven A. Power Generation from Human Leukocytes/Lymphocytes in Mammalian Biofuel Cell. *International Journal of Electrochemistry*. 2013;2013:1-11. doi:10.1155/2013/706792
128. Ayato Y, Sakurai K, Fukunaga S, et al. A simple biofuel cell cathode with human red blood cells as electrocatalysts for oxygen reduction reaction. *Biosens Bioelectron*. 2014;55:14-18. doi:10.1016/j.bios.2013.11.063
129. Apetrei RM, Carac G, Bahrim G, Ramanaviciene A, Ramanavicius A. Modification of Aspergillus niger by conducting polymer, Polypyrrole, and the evaluation of electrochemical properties of modified cells. *Bioelectrochemistry*. 2018;121:46-55. doi:10.1016/J.BIOELECHEM.2018.01.001
130. Apetrei RM, Carac G, Ramanaviciene A, Bahrim G, Tanase C, Ramanavicius A. Cell-assisted synthesis of conducting polymer – polypyrrole – for the improvement of electric charge transfer through fungal cell wall. *Colloids Surf B Biointerfaces*. 2019;175:671-679. doi:10.1016/J.COLSURFB.2018.12.024

131. Vaitkuviene A, Kaseta V, Voronovic J, et al. Evaluation of cytotoxicity of polypyrrole nanoparticles synthesized by oxidative polymerization. *J Hazard Mater*. 2013;250-251:167-174. doi:10.1016/j.jhazmat.2013.01.038
132. Vaitkuviene A, Ratautaite V, Mikoliunaite L, et al. Some biocompatibility aspects of conducting polymer polypyrrole evaluated with bone marrow-derived stem cells. *Colloids Surf A Physicochem Eng Asp*. 2014;442:152-156. doi:10.1016/j.colsurfa.2013.06.030
133. Magennis EP, Fernandez-Trillo F, Sui C, et al. Bacteria-instructed synthesis of polymers for self-selective microbial binding and labelling. *Nat Mater*. 2014;13(7):748-755. doi:10.1038/nmat3949
134. German N, Ramanaviciene A, Ramanavicius A. Formation and electrochemical evaluation of polyaniline and polypyrrole nanocomposites based on glucose oxidase and gold nanostructures. *Polymers (Basel)*. 2020;12(12):1-20. doi:10.3390/polym12123026
135. Van der Zee FP, Cervantes FJ. Impact and application of electron shuttles on the redox (bio)transformation of contaminants: A review. *Biotechnol Adv*. 2009;27(3):256-277. doi:10.1016/j.biotechadv.2009.01.004
136. Niu J, Lunn DJ, Pusuluri A, et al. Engineering live cell surfaces with functional polymers via cytocompatible controlled radical polymerization. *Nat Chem*. 2017;9(6):537-545. doi:10.1038/nchem.2713
137. Apetrei RM, Carac G, Bahrim G, Ramanaviciene A, Ramanavicius A. Modification of Aspergillus niger by conducting polymer, Polypyrrole, and the evaluation of electrochemical properties of modified cells. *Bioelectrochemistry*. 2018;121(2017):46-55. doi:10.1016/j.bioelechem.2018.01.001
138. Stirke A, Apetrei RM, Kirsnyte M, et al. Synthesis of polypyrrole microspheres by Streptomyces spp. *Polymer (Guildf)*. 2016;84:99-106. doi:10.1016/j.polymer.2015.12.029
139. Zhao M., Li M., Tian X., Tan. Ch., McDaniel C. T., Hassett D. J. GT. Microbial fuel cell (MFC) power performance improvement through enhanced microbial electrogenicity. *Biotechnol Adv*. 2018;36(4):1316-1327.
140. Van der Zee FP, Cervantes FJ. Impact and application of electron shuttles on the redox (bio)transformation of contaminants: A review. *Biotechnol Adv*. 2009;27(3):256-277. doi:10.1016/j.biotechadv.2009.01.004
141. Ramanaviciene A, Nastajute G, Snitka V, et al. Spectrophotometric evaluation of gold nanoparticles as red-ox mediator for glucose oxidase. *Sensors and Actuators B-Chemical*. 2009;137(2):483-489. doi:DOI 10.1016/j.snb.2009.01.021
142. Zhao M., Li M., Tian X., Tan. Ch., McDaniel C. T., Hassett D. J. GT. Microbial fuel cell (MFC) power performance improvement through

enhanced microbial electrogenicity. *Biotechnol Adv*. 2018;36(4):1316-1327.
143. Rudra R. Chapter 8 Conducting Polymer-Based Microbial Fuel Cells. 2019;(January). doi:10.21741/9781644900079
144. Higham T.E. Author ' s personal copy Automatica Author ' s personal copy. *Encyclopedia of Toxicology*. 2014;50(January 2014):952-961.
145. Rawson FJ, Downard AJ, Baronian KH. Electrochemical detection of intracellular and cell membrane redox systems in Saccharomyces cerevisiae. *Sci Rep*. 2014;4.
146. Holmes DE, Ueki T, Tang H yan, et al. A Membrane-Bound Cytochrome Enables from Extracellular Electron Transfer. *American society for Microbiology*. 2019;10(4):1-12.
147. Okamoto A, Kalathil S, Deng X, Hashimoto K, Nakamura R, Nealson KH. Cell-secreted flavins bound to membrane cytochromes dictate electron transfer reactions to surfaces with diverse charge and pH. *Sci Rep*. 2014;4:1-8. doi:10.1038/srep05628
148. Andriukonis E, Ramanaviciene A, Ramanavicius A. Synthesis of polypyrrole induced by [Fe(CN)6]3- and redox cycling of [Fe(CN)6]4-/[Fe(CN)6]3-. *Polymers (Basel)*. 2018;10(7):12-16. doi:10.3390/polym10070749
149. Pontié M, Jaspard E, Friant C, et al. A sustainable fungal microbial fuel cell (FMFC) for the bioremediation of acetaminophen (APAP) and its main by-product (PAP) and energy production from biomass. *Biocatal Agric Biotechnol*. 2019;22(October). doi:10.1016/j.bcab.2019.101376
150. Mbokou SF, Tonle IK, Pontié M. Development of a novel hybrid biofuel cell type APAP/O2 based on a fungal bioanode with a Scedosporium dehoogii biofilm. *J Appl Electrochem*. 2017;47(2):273-280. doi:10.1007/s10800-016-1030-5
151. Wang W, Zhang B, Liu Q, Du P, Liu W, He Z. Biosynthesis of palladium nanoparticles using: Shewanella loihica PV-4 for excellent catalytic reduction of chromium(VI). *Environ Sci Nano*. 2018;5(3):730-739. doi:10.1039/c7en01167a
152. Wu X, Xiong X, Owens G, et al. Anode modification by biogenic gold nanoparticles for the improved performance of microbial fuel cells and microbial community shift. *Bioresour Technol*. 2018;270:11-19. doi:10.1016/j.biortech.2018.08.092
153. de Oliveira AHP, Alcaraz-Espinoza JJ, da Costa MM, Nascimento MLF, Swager TM, de Oliveira HP. Improvement of Baker's yeast-based fuel cell power output by electrodes and proton exchange

membrane modification. *Materials Science and Engineering C*. 2019;105(May):110082. doi:10.1016/j.msec.2019.110082

154. Duarte KDZ, Kwon Y. Enhanced extracellular electron transfer of yeast-based microbial fuel cells via one pot substrate-bound growth iron-manganese oxide nanoflowers. *J Power Sources*. 2020;474(January):228496. doi:10.1016/j.jpowsour.2020.228496
155. Duarte KDZ, Frattini D, Kwon Y. High performance yeast-based microbial fuel cells by surfactant-mediated gold nanoparticles grown atop a carbon felt anode. *Appl Energy*. 2019;256(September):113912. doi:10.1016/j.apenergy.2019.113912
156. Christwardana M, Kwon Y. Yeast and carbon nanotube based biocatalyst developed by synergetic effects of covalent bonding and hydrophobic interaction for performance enhancement of membraneless microbial fuel cell. *Bioresour Technol*. 2017;225:175-182. doi:10.1016/j.biortech.2016.11.051
157. Coman V, Gustavsson T, Finkelsteinas A, Von Wachenfeldt C, Hägerhäll C, Gorton L. Electrical wiring of live, metabolically enhanced Bacillus subtilis cells with flexible osmium-redox polymers. *J Am Chem Soc*. 2009;131(44):16171-16176. doi:10.1021/ja905442a
158. Christwardana M, Frattini D, Duarte KDZ, Accardo G, Kwon Y. Carbon felt molecular modification and biofilm augmentation via quorum sensing approach in yeast-based microbial fuel cells. *Appl Energy*. 2019;238(October 2018):239-248. doi:10.1016/j.apenergy.2019.01.078
159. Jiang X, Hu J, Lieber AM, et al. Nanoparticle facilitated extracellular electron transfer in microbial fuel cells. *Nano Lett*. 2014;14(11):6737-6742. doi:10.1021/nl503668q
160. Sharma T, Mohana Reddy AL, Chandra TS, Ramaprabhu S. Development of carbon nanotubes and nanofluids based microbial fuel cell. *Int J Hydrogen Energy*. 2008;33(22):6749-6754. doi:10.1016/j.ijhydene.2008.05.112
161. Zhao CE, Chen J, Ding Y, et al. Chemically Functionalized Conjugated Oligoelectrolyte Nanoparticles for Enhancement of Current Generation in Microbial Fuel Cells. *ACS Appl Mater Interfaces*. 2015;7(26):14501-14505. doi:10.1021/acsami.5b03990
162. Cui Q, Wang X, Yang Y, Li S, Li L, Wang S. Binding-Directed Energy Transfer of Conjugated Polymer Materials for Dual-Color Imaging of Cell Membrane. *Chemistry of Materials*. 2016;28(13):4661-4669. doi:10.1021/acs.chemmater.6b01424

163. De M, Ghosh PS, Rotello VM. Applications of nanoparticles in biology. *Advanced Materials*. 2008;20(22):4225-4241. doi:10.1002/adma.200703183
164. Stark WJ, Stoessel PR, Wohlleben W, Hafner A. Industrial applications of nanoparticles. *Chem Soc Rev*. 2015;44(16):5793-5805. doi:10.1039/c4cs00362d
165. Luo X, Morrin A, Killard AJ, Smyth MR. Application of nanoparticles in electrochemical sensors and biosensors. *Electroanalysis*. *Wiley-VCH Verlag*. 2006;18(4):319-326. doi:10.1002/elan.200503415
166. Yang Y, Li C, Yin L, et al. Enhanced charge transfer by gold nanoparticle at DNA modified electrode and its application to label-free DNA detection. *ACS Appl Mater Interfaces*. 2014;6(10):7579-7584. doi:10.1021/am500912m
167. Han TH, Khan MM, Kalathil S, Lee J, Cho MH. Simultaneous enhancement of methylene blue degradation and power generation in a microbial fuel cell by gold nanoparticles. *Ind Eng Chem Res*. 2013;52(24):8174-8181. doi:10.1021/ie4006244
168. Pan Y, Neuss S, Leifert A, et al. Size-dependent cytotoxicity of gold nanoparticles. *Small*. 2007;3(11):1941-1949. doi:10.1002/smll.200700378
169. Woźniak A, Malankowska A, Nowaczyk G, et al. Size and shape-dependent cytotoxicity profile of gold nanoparticles for biomedical applications. *J Mater Sci Mater Med*. 2017;28(6). doi:10.1007/s10856-017-5902-y
170. Zinovicius A, Rozene J, Merkelis T, Bruzaitė I, Ramanavicius A, Morkvenaite-Vilkonciene I. Evaluation of a Yeast–Polypyrrole Biocomposite Used in Microbial Fuel Cells. *Sensors*. 2022;22(1). doi:10.3390/s22010327
171. Andriukonis E, Ramanaviciene A, Ramanavicius A. Synthesis of polypyrrole induced by [Fe(CN)6]3- and redox cycling of [Fe(CN)6]4-/[Fe(CN)6]3-. *Polymers (Basel)*. 2018;10(7):12-16. doi:10.3390/polym10070749
172. Zhang RB, Wu Y, Lin ZQ, et al. Living and Conducting: Coating Individual Bacterial Cells with In Situ Formed Polypyrrole. *Angewandte Chemie*. 2017;129(35):10652-10656. doi:10.1002/ange.201704729
173. Apetrei RM, Cârâc G, Bahrim G, Camurlu P. Sensitivity enhancement for microbial biosensors through cell Self-Coating with polypyrrole. *International Journal of Polymeric Materials and Polymeric Biomaterials*. 2019;68(17):1058-1067. doi:10.1080/00914037.2018.1525548

174. Ramanavičius A, Kaušaite A, Ramanavičiene A. Polypyrrole-coated glucose oxidase nanoparticles for biosensor design. *Sens Actuators B Chem*. 2005;111-112(SUPPL.):532-539. doi:10.1016/j.snb.2005.03.038
175. Olea D, Viratelle O, Faure C. Polypyrrole-glucose oxidase biosensor. Effect of enzyme encapsulation in multilamellar vesicles on analytical properties. *Biosens Bioelectron*. 2008;23(6):788-794. doi:10.1016/j.bios.2007.08.018
176. Mazur M, Krywko-Cendrowska A, Krysiński P, Rogalski J. Encapsulation of laccase in a conducting polymer matrix: A simple route towards polypyrrole microcontainers. *Synth Met*. 2009;159(17-18):1731-1738. doi:10.1016/j.synthmet.2009.05.018
177. Ramanavicius A, Kausaite A, Ramanaviciene A, Acaite J, Malinauskas A. Redox enzyme - glucose oxidase - initiated synthesis of polypyrrole. *Synth Met*. 2006;156(5-6):409-413. doi:10.1016/j.synthmet.2005.12.018
178. Apetrei RM, Cârâc G, Bahrim G, Camurlu P. Utilization of enzyme extract self-encapsulated within polypyrrole in sensitive detection of catechol. *Enzyme Microb Technol*. 2019;128(February):34-39. doi:10.1016/j.enzmictec.2019.04.015
179. Ramanavičius A, Kaušaite A, Ramanavičiene A. Polypyrrole-coated glucose oxidase nanoparticles for biosensor design. *Sens Actuators B Chem*. 2005;111-112(SUPPL.):532-539. doi:10.1016/j.snb.2005.03.038
180. Sherman HG, Hicks JM, Jain A, et al. Mammalian-Cell-Driven Polymerisation of Pyrrole. *ChemBioChem*. 2019;20(8):1008-1013. doi:10.1002/cbic.201800630
181. Apetrei RM, Cârâc G, Bahrim G, Camurlu P. Sensitivity enhancement for microbial biosensors through cell Self-Coating with polypyrrole. *International Journal of Polymeric Materials and Polymeric Biomaterials*. 2019;68(17):1058-1067. doi:10.1080/00914037.2018.1525548
182. Bennett MR, Gurnani P, Hill PJ, Alexander C, Rawson FJ. Iron-Catalysed Radical Polymerisation by Living Bacteria. *Angewandte Chemie*. 2020;132(12):4780-4785. doi:10.1002/ange.201915084
183. Sherman HG, Hicks JM, Jain A, et al. Mammalian-Cell-Driven Polymerisation of Pyrrole. *ChemBioChem*. 2019;20(8):1008-1013. doi:10.1002/cbic.201800630
184. Ramanaviciene A, Kausaite A, Tautkus S, Ramanavicius A. Biocompatibility of polypyrrole particles: an in-vivo study in mice. *Journal of Pharmacy and Pharmacology*. 2010;59(2):311-315. doi:10.1211/jpp.59.2.0017

185. Liu SR, Cai LF, Wang LY, et al. Polydopamine coating on individual cells for enhanced extracellular electron transfer. *Chemical Communications*. 2019;55(71):10535-10538. doi:10.1039/c9cc03847g
186. Yu YY, Wang YZ, Fang Z, et al. Single cell electron collectors for highly efficient wiring-up electronic abiotic/biotic interfaces. *Nat Commun*. 2020;11(1). doi:10.1038/s41467-020-17897-9
187. Yang C, Aslan H, Zhang P, et al. Carbon dots-fed Shewanella oneidensis MR-1 for bioelectricity enhancement. *Nat Commun*. 2020;11(1):1-11. doi:10.1038/s41467-020-14866-0
188. Liu S, Yi X, Wu X, Li Q, Wang Y. Internalized Carbon Dots for Enhanced Extracellular Electron Transfer in the Dark and Light. *Small*. 2020;16(44):1-7. doi:10.1002/smll.202004194
189. Aslan S, Conghaile P, Leech D, Gorton L, Timur S, Anik U. Development of an Osmium Redox Polymer Mediated Bioanode and Examination of its Performance in Gluconobacter oxydans Based Microbial Fuel Cell. *Electroanalysis*. 2017;29(6):1651-1657. doi:10.1002/elan.201600727
190. Yuan Y, Shin H, Kang C, Kim S. Wiring microbial biofilms to the electrode by osmium redox polymer for the performance enhancement of microbial fuel cells. *Bioelectrochemistry*. 2016;108:8-12. doi:10.1016/j.bioelechem.2015.11.001
191. Timur S, Haghighi B, Tkac J, Pazarlioğlu N, Telefoncu A, Gorton L. Electrical wiring of Pseudomonas putida and Pseudomonas fluorescens with osmium redox polymers. *Bioelectrochemistry*. 2007;71(1):38-45. doi:10.1016/j.bioelechem.2006.08.001
192. Hasan K, Çevik E, Sperling E, Packer MA, Leech D, Gorton L. Photoelectrochemical Wiring of Paulschulzia pseudovolvox (Algae) to Osmium Polymer Modified Electrodes for Harnessing Solar Energy. *Adv Energy Mater*. 2015;5(22). doi:10.1002/aenm.201501100
193. Aslan S, Conghaile P, Leech D, Gorton L, Timur S, Anik U. Development of an Osmium Redox Polymer Mediated Bioanode and Examination of its Performance in Gluconobacter oxydans Based Microbial Fuel Cell. *Electroanalysis*. 2017;29(6):1651-1657. doi:10.1002/elan.201600727
194. Andriukonis E, Celiesiute-germaniene R, Ramanavicius S, Viter R, Ramanavicius A. From microorganism-based amperometric biosensors towards microbial fuel cells. *Sensors*. 2021;21(7):1-23. doi:10.3390/s21072442

195. Kižys K, Zinovičius A, Jakštys B, et al. Microbial Biofuel Cells: Fundamental Principles, Development and Recent Obstacles. *Biosensors (Basel)*. 2023;13(2):221. doi:10.3390/bios13020221
196. Sayed ET, Tsujiguchi T, Nakagawa N. Catalytic activity of baker's yeast in a mediatorless microbial fuel cell. *Bioelectrochemistry*. 2012;86:97-101.
197. Mbokou SF, Tonle IK, Pontié M. Development of a novel hybrid biofuel cell type APAP/O2 based on a fungal bioanode with a Scedosporium dehoogii biofilm. *J Appl Electrochem*. 2017;47(2):273-280. doi:10.1007/s10800-016-1030-5
198. Wu W, Niu H, Yang D, et al. Polyaniline/Carbon nanotubes composite modified anode via graft polymerization and self-assembling for microbial fuel cells. *Polymers (Basel)*. 2018;10(7). doi:10.3390/polym10070759
199. Pontié M, Jaspard E, Friant C, et al. A sustainable fungal microbial fuel cell (FMFC) for the bioremediation of acetaminophen (APAP) and its main by-product (PAP) and energy production from biomass. *Biocatal Agric Biotechnol*. 2019;22(October). doi:10.1016/j.bcab.2019.101376
200. Marshall CW, May HD. Electrochemical evidence of direct electrode reduction by a thermophilic Gram-positive bacterium, Thermincola ferriacetica. *Energy Environ Sci*. 2009;2(6):699-705. doi:10.1039/b823237g
201. Christwardana M, Frattini D, Duarte KDZ, Accardo G, Kwon Y. Carbon felt molecular modification and biofilm augmentation via quorum sensing approach in yeast-based microbial fuel cells. *Appl Energy*. 2019;238(October 2018):239-248. doi:10.1016/j.apenergy.2019.01.078
202. Herrero-Hernandez E, Smith TJ, Akid R. Electricity generation from wastewaters with starch as carbon source using a mediatorless microbial fuel cell. *Biosens Bioelectron*. 2013;39(1):194-198. doi:10.1016/j.bios.2012.07.037
203. Babanova S, Hubenova Y, Mitov M. Influence of artificial mediators on yeast-based fuel cell performance. *J Biosci Bioeng*. 2011;112(4):379-387. doi:10.1016/j.jbiosc.2011.06.008
204. He Z, Liu J, Qiao Y, Li CM, Thatt T, Tan Y. Nano Lett._2012_12_4738_4.pdf. Published online 2012:10-13.
205. Mardiana U, Innocent C, Cretin M, et al. Applicability of Alginate Film Entrapped Yeast for Microbial Fuel Cell. *Russian Journal of Electrochemistry*. 2019;55(2):78-87. doi:10.1134/S1023193519010075
206. Cornut R, Lefrou C. New analytical approximation of feedback approach curves with a microdisk SECM tip and irreversible kinetic

reaction at the substrate. *Journal of Electroanalytical Chemistry*. 2008;621(2):178-184. doi:10.1016/j.jelechem.2007.09.021
207. Andriukonis E, Stirkė A, Mikoliunaite L, Balevicius Z, Ramanavičiene A, Ramanavičius A. Pyrrole bio-polymerization using redox mediator, Patent No. LT6239B. Published online 2016.
208. Bard AJ., Faulkner LR. *Electrochemical Methods : Fundamentals and Applications*. John Wiley & Sons, Inc.; 2001.
209. Trevor Henderson. Review of the Metrohm Autolab PGSTAT302N_ Features, Performance, and Applications. *LabX.com*. Published online September 9, 2024.
210. Mafi P, Hindocha S, Mafi R, Griffin M, Khan WS. *Adult Mesenchymal Stem Cells and Cell Surface Characterization-A Systematic Review of the Literature*. Vol 5. 2011.
211. Miksiunas R, Aldonyte R, Vailionyte A, et al. Cardiomyogenic differentiation potential of human dilated myocardium-derived mesenchymal stem/stromal cells: The impact of HDAC inhibitor SAHA and biomimetic matrices. *Int J Mol Sci*. 2021;22(23). doi:10.3390/ijms222312702
212. Yin N, Lu R, Lin J, Zhi S, Tian J, Zhu J. Islet-1 promotes the cardiac-specific differentiation of mesenchymal stem cells through the regulation of histone acetylation. *Int J Mol Med*. 2014;33(5):1075-1082. doi:10.3892/ijmm.2014.1687
213. Lu H, Li Y, Wang Y, et al. Wnt-promoted Isl1 expression through a novel TCF/LEF1 binding site and H3K9 acetylation in early stages of cardiomyocyte differentiation of P19CL6 cells. *Mol Cell Biochem*. 2014;391(1-2):183-192. doi:10.1007/s11010-014-2001-y
214. Yang J, He J, Ismail M, et al. HDAC inhibition induces autophagy and mitochondrial biogenesis to maintain mitochondrial homeostasis during cardiac ischemia/reperfusion injury. *J Mol Cell Cardiol*. 2019;130:36-48. doi:10.1016/j.yjmcc.2019.03.008
215. Wang YJ, Matter CM. Histone deacetylase 6 suppression protects from myocardial ischaemia-reperfusion injury in diabetes: insights from genetic deletion and pharmacological inhibition. *Cardiovasc Res*. *Oxford University Press*. 2024;120(12):1369-1371. doi:10.1093/cvr/cvae145
216. Chen W, Liu S, Yang Y, Zhang Z, Zhao Y. Spatiotemporal monitoring of NAD+ metabolism with fluorescent biosensors. *Mech Ageing Dev*. *Elsevier Ireland Ltd*. 2022;204. doi:10.1016/j.mad.2022.111657

217. Kiledjian M. Eukaryotic RNA 5′-End NAD+ Capping and DeNADding. *Trends Cell Biol*. *Elsevier Ltd*. 2018;28(6):454-464. doi:10.1016/j.tcb.2018.02.005
218. Tanno M, Kuno A, Yano T, et al. Induction of manganese superoxide dismutase by nuclear translocation and activation of SIRT1 promotes cell survival in chronic heart failure. *Journal of Biological Chemistry*. 2010;285(11):8375-8382. doi:10.1074/jbc.M109.090266
219. Katsyuba E, Mottis A, Zietak M, et al. De novo NAD+ synthesis enhances mitochondrial function and improves health. *Nature*. 2018;563(7731):354-359. doi:10.1038/s41586-018-0645-6
220. Lang J, Li Y, Ye Z, et al. Investigating the Effect of Substrate Stiffness on the Redox State of Cardiac Fibroblasts Using Scanning Electrochemical Microscopy. *Anal Chem*. 2021;93(14):5797-5804. doi:10.1021/acs.analchem.0c05284
221. Rapino S, Marcu R, Bigi A, et al. Scanning electro-chemical microscopy reveals cancer cell redox state. *Electrochim Acta*. 2015;179:65-73. doi:10.1016/j.electacta.2015.04.053
222. Koch-Nolte F, Fischer S, Haag F, Ziegler M. Compartmentation of NAD+-dependent signalling. *FEBS Lett*. 2011;585(11):1651-1656. doi:10.1016/j.febslet.2011.03.045
223. Berridge M V, Tan AS. *Forum Original Research Communication Cell-Surface NAD(P)H-Oxidase: Relationship to Trans-Plasma Membrane NADH-Oxidoreductase and a Potential Source of Circulating NADH-Oxidase*. Vol 2. Mary Ann Liebert, Inc; 2000.
224. Bruzzone S, Guida L, Zocchi E, Franco L, Flora A De. Connexin 43 hemichannels mediate Ca2+-regulated transmembrane NAD+ fluxes in intact cells. *The FASEB Journal*. 2001;15(1):10-12. doi:10.1096/fj.00-0566fje
225. Poderyte M, Ramanavicius A, Valiūnienė A. Scanning electrochemical microscopy based irreversible destruction of living cells. *Biosens Bioelectron*. 2022;216. doi:10.1016/j.bios.2022.114621
226. Li Y, Hu K, Yu Y, Rotenberg SA, Amatore C, Mirkin M V. Direct Electrochemical Measurements of Reactive Oxygen and Nitrogen Species in Nontransformed and Metastatic Human Breast Cells. *J Am Chem Soc*. 2017;139(37):13055-13062. doi:10.1021/jacs.7b06476
227. Liu B, Rotenberg SA, Mirkin M V. *Scanning Electrochemical Microscopy of Living Cells: Different Redox Activities of Nonmetastatic and Metastatic Human Breast Cells*. 2000. www.pnas.org

228. Petroniene J, Morkvenaite-Vilkonciene I, Miksiunas R, et al. Scanning electrochemical microscopy for the investigation of redox potential of human myocardium-derived mesenchymal stem cells grown at 2D and 3D conditions. *Electrochim Acta*. 2020;360. doi:10.1016/j.electacta.2020.136956
229. Mikšiūnas R, Labeit S, Bironaite D. Class I and II Histone Deacetylase Inhibitors as Therapeutic Modulators of Dilated Cardiac Tissue-Derived Mesenchymal Stem/Stromal Cells. *Int J Mol Sci*. 2024;25(12). doi:10.3390/ijms25126758
230. Ying W. NAD+/NADH and NADP+/NADPH in cellular functions and cell death: Regulation and biological consequences. *Antioxid Redox Signal*. 2008;10(2):179-206. doi:10.1089/ars.2007.1672
231. Stein LR, Imai SI. The dynamic regulation of NAD metabolism in mitochondria. *Trends in Endocrinology and Metabolism*. 2012;23(9):420-428. doi:10.1016/j.tem.2012.06.005
232. Frederick L. Crane DJMHEL. *Oxidoreduction at the Plasma Membranerelation to Growth and Transport*. Vol 2. CRC Press; 1991.
233. Herst PM, Petersen T, Jerram P, Baty J, Berridge M V. The antiproliferative effects of phenoxodiol are associated with inhibition of plasma membrane electron transport in tumour cell lines and primary immune cells. *Biochem Pharmacol*. 2007;74(11):1587-1595. doi:10.1016/j.bcp.2007.08.019
234. Lambeth JD. NOX enzymes and the biology of reactive oxygen. *Nat Rev Immunol*. *Nature Publishing Group*. 2004;4(3):181-189. doi:10.1038/nri1312
235. Villalba JM, Navarro F, G6mez-Diaz C, Arroyo A, Belle RI, Navas P. *Role of Cytochrome B5 Reductase on the Antioxidant Function of Coenzyme Q in the Plasma Membrane*. Vol 18. 1997.
236. Gray JP, Eisen T, Cline GW, Smith PJS, Heart E. Plasma membrane electron transport in pancreatic β-cells is mediated in part by NQO1. *Am J Physiol Endocrinol Metab*. 2011;301(1). doi:10.1152/ajpendo.00673.2010
237. Zhu H, Qiu H, Won H, Yoon P, Huang S, Bunn HF. *The Scripps Research Institute*. 1999. www.ncbi.nlm.nih.gov.
238. James D, Brightman AO. *MINI-REVIEW NADH Oxidase of Plasma Membranes*. Vol 23. 1991.
239. Franco R, Cidlowski JA. Apoptosis and glutathione: Beyond an antioxidant. *Cell Death Differ*. 2009;16(10):1303-1314. doi:10.1038/cdd.2009.107

240. Logan BE, Hamelers B, Rozendal R, et al. *Microbial Fuel Cells: Methodology and Technology*. Vol 40. 2006. doi:10.1021/es0605016
241. Zhao F, Slade RCT, Varcoe JR. Techniques for the study and development of microbial fuel cells: An electrochemical perspective. *Chem Soc Rev*. 2009;38(7):1926-1939. doi:10.1039/b819866g
242. Quintero-Jaime AF, Conzuelo F, Cazorla-Amorós D, Morallón E. Pyrroloquinoline quinone-dependent glucose dehydrogenase bioelectrodes based on one-step electrochemical entrapment over single-wall carbon nanotubes. *Talanta*. 2021;232. doi:10.1016/j.talanta.2021.122386
243. Sairaman Saikrithika, Yesudas K. Yashly, Annamalai Senthil Kumar. Quinones and Organic Dyes Based Redox-Active Organic Molecular Compounds Immobilized Surfaces for Electrocatalysis and Bioelectrocatalysis Applications. In: Gupta RK, ed. *Organic Electrodes*. Engineering Materials. Springer International Publishing; 2022. doi:10.1007/978-3-030-98021-4
244. Hernández-Fernández FJ, Pérez De Los Ríos A, Salar-García MJ, et al. Recent progress and perspectives in microbial fuel cells for bioenergy generation and wastewater treatment. *Fuel Processing Technology*. *Elsevier B.V.* 2015;138:284-297. doi:10.1016/j.fuproc.2015.05.022
245. Ramírez-Vargas CA, Prado A, Arias CA, Carvalho PN, Esteve-Núñez A, Brix H. Microbial Electrochemical Technologies for Wastewater Treatment: Principles and Evolution from Microbial Fuel Cells to Bioelectrochemical-Based Constructed Wetlands. *Water (Basel)*. 2018;10(9). doi:10.20944/preprints201807.0369.v1
246. Scholz F. Thermodynamics of electrochemical reactions. In: *Electroanalytical Methods: Guide to Experiments and Applications*. Springer Berlin Heidelberg; 2010:11-31. doi:10.1007/978-3-642-02915-8_2
247. Ramanavicius A, German N, Ramanaviciene A. Evaluation of Electron Transfer in Electrochemical System Based on Immobilized Gold Nanoparticles and Glucose Oxidase. *J Electrochem Soc*. 2017;164(4):G45-G49. doi:10.1149/2.0691704jes
248. Chen M, Zhou X, Liu X, et al. Facilitated extracellular electron transfer of Geobacter sulfurreducens biofilm with in situ formed gold nanoparticles. *Biosens Bioelectron*. 2018;108:20-26. doi:10.1016/j.bios.2018.02.030
249. Zhou M, Wang H, Hassett DJ, Gu T. Recent advances in microbial fuel cells (MFCs) and microbial electrolysis cells (MECs) for wastewater treatment, bioenergy and bioproducts. *Journal of Chemical*

Technology and Biotechnology. 2013;88(4):508-518. doi:10.1002/jctb.4004

250. Bergman LW. Growth and Maintenance of Yeast. In: *Two-Hybrid Systems: Methods and Protocols*. Vol 177. Springer Nature; 2001:9-14. doi:https://doi.org/10.1385/1-59259-210-4:009
251. Aguilar-Uscanga B, François JM. A study of the yeast cell wall composition and structure in response to growth conditions and mode of cultivation. *Lett Appl Microbiol*. 2003;37(3):268-274. doi:10.1046/j.1472-765X.2003.01394.x
252. Sampermans S, Mortier J, Soares E V. Flocculation onset in Saccharomyces cerevisiae: The role of nutrients. *J Appl Microbiol*. 2005;98(2):525-531. doi:10.1111/j.1365-2672.2004.02486.x
253. Trebiaine JH, Miller JJ. Effect of yeast extract, peptone, and certain nitrooen compounds on sporulation of Saccharomyces cerevisiae. *Mycopathol Mycol Appl*. 1956;7:241-250. doi:https://doi.org/10.1007/BF02249074
254. Lin T, Bai X, Hu Y, et al. Synthetic Saccharomyces cerevisiae-Shewanella oneidensis consortium enables glucose-fed high-performance microbial fuel cell. *AIChE Journal*. 2017;63(6):1830-1838. doi:10.1002/aic.15611
255. Shirpay A. Effects of electrode size on the power generation of the microbial fuel cell by Saccharomyces cerevisiae. *Ionics (Kiel)*. 2021;27(9):3967-3973. doi:10.1007/s11581-021-04162-2
256. Christwardana M, Frattini D, Accardo G, Yoon SP, Kwon Y. Optimization of glucose concentration and glucose/yeast ratio in yeast microbial fuel cell using response surface methodology approach. *J Power Sources*. 2018;402:402-412. doi:10.1016/j.jpowsour.2018.09.068
257. Aguilera A, Benítez T. Relationship between growth, fermentation, and respiration rates in Saccharomyces cerevisiae: A study based on the analysis of the yield Ypx. *Biotechnol Bioeng*. 1988;32(2):240-244. doi:10.1002/bit.260320215
258. Lodato P, Segovia De Huergo M, Buera MP. Viability and thermal stability of a strain of Saccharomyces cerevisiae freeze-dried in different sugar and polymer matrices. *Appl Microbiol Biotechnol*. 1999;52:215-220.
259. Powell CD, Van Zandycke SM, Quain DE, Smart KA. *Replicative Ageing and Senescence in Saccharomyces Cerevisiae and the Impact on Brewing Fermentations*. Vol 146. 2000.

260. Abd-Elrahman NK, Al-Harbi N, Basfer NM, Al-Hadeethi Y, Umar A, Akbar S. Applications of Nanomaterials in Microbial Fuel Cells: A Review. *Molecules*. 2022;27(21). doi:10.3390/molecules27217483
261. Duarte KDZ, Frattini D, Kwon Y. High performance yeast-based microbial fuel cells by surfactant-mediated gold nanoparticles grown atop a carbon felt anode. *Appl Energy*. 2019;256(September):113912. doi:10.1016/j.apenergy.2019.113912
262. Hu M, Li X, Xiong J, et al. Nano-Fe3C@PGC as a novel low-cost anode electrocatalyst for superior performance microbial fuel cells. *Biosens Bioelectron*. 2019;142. doi:10.1016/j.bios.2019.111594
263. Duarte KDZ, Kwon Y. Enhanced extracellular electron transfer of yeast-based microbial fuel cells via one pot substrate-bound growth iron-manganese oxide nanoflowers. *J Power Sources*. 2020;474:228496. doi:10.1016/J.JPOWSOUR.2020.228496
264. Salar-Garcia MJ, Montilla F, Quijada C, Morallon E, Ieropoulos I. Improving the power performance of urine-fed microbial fuel cells using PEDOT-PSS modified anodes. *Appl Energy*. 2020;278. doi:10.1016/j.apenergy.2020.115528
265. Rajendran J, Shetty BH, Ganapathy D, et al. Thermally Expanded Graphite Incorporated with PEDOT:PSS Based Anode for Microbial Fuel Cells with High Bioelectricity Production. *J Electrochem Soc*. 2022;169(1):017515. doi:10.1149/1945-7111/ac4b23
266. Tarasov S, Plekhanova Y, Kashin V, et al. Gluconobacter Oxydans-Based MFC with PEDOT:PSS/Graphene/Nafion Bioanode for Wastewater Treatment. *Biosensors (Basel)*. 2022;12(9). doi:10.3390/bios12090699
267. Wu X, Xiong X, Owens G, et al. Anode modification by biogenic gold nanoparticles for the improved performance of microbial fuel cells and microbial community shift. *Bioresour Technol*. 2018;270:11-19. doi:10.1016/j.biortech.2018.08.092
268. Truong DH, Dam MS, Bujna E, et al. In situ fabrication of electrically conducting bacterial cellulose-polyaniline-titanium-dioxide composites with the immobilization of Shewanella xiamenensis and its application as bioanode in microbial fuel cell. *Fuel*. 2021;285:119259. doi:10.1016/J.FUEL.2020.119259
269. Hemdan BA, El-Taweel GE, Naha S, Goswami P. Bacterial community structure of electrogenic biofilm developed on modified graphite anode in microbial fuel cell. *Sci Rep*. 2023;13(1). doi:10.1038/s41598-023-27795-x

270. Christwardana M, Kwon Y. Yeast and carbon nanotube based biocatalyst developed by synergetic effects of covalent bonding and hydrophobic interaction for performance enhancement of membraneless microbial fuel cell. *Bioresour Technol*. 2017;225:175-182. doi:10.1016/j.biortech.2016.11.051
271. Shetty BH, Sundramoorthy AK, Annamalai J, et al. Fabrication of High-Performance MgCoO2/PEDOT:PSS@Nickel Foam Anode for Bioelectricity Generation by Microbial Fuel Cells. *J Nanomater*. 2022;2022. doi:10.1155/2022/6358852
272. Huang L, Li X, Ren Y, Wang X. In-situ modified carbon cloth with polyaniline/graphene as anode to enhance performance of microbial fuel cell. *Int J Hydrogen Energy*. 2016;41(26):11369-11379. doi:10.1016/J.IJHYDENE.2016.05.048
273. Pu KB, Ma Q, Cai WF, Chen QY, Wang YH, Li FJ. Polypyrrole modified stainless steel as high performance anode of microbial fuel cell. *Biochem Eng J*. 2018;132:255-261. doi:10.1016/j.bej.2018.01.018
274. Wang Y, Zhu L, An L. Electricity generation and storage in microbial fuel cells with porous polypyrrole-base composite modified carbon brush anodes. *Renew Energy*. 2020;162:2220-2226. doi:10.1016/j.renene.2020.10.032
275. Chakma R, Hossain MK, Paramasivam P, et al. Recent Applications, Challenges, and Future Prospects of Microbial Fuel Cells: A Review. *Global Challenges*. *John Wiley and Sons Inc*. Preprint posted online 2025. doi:10.1002/gch2.202500004
276. Jadhav DA, Carmona-Martínez AA, Chendake AD, Pandit S, Pant D. Modeling and optimization strategies towards performance enhancement of microbial fuel cells. *Bioresour Technol*. *Elsevier Ltd*. 2021;320. doi:10.1016/j.biortech.2020.124256

7. SANTRAUKA

Dokumente pateikiama išsami mikrobinių kuro elementų (MFC) analizė ir jų potencialas sprendžiant energetikos ir aplinkosaugos problemas, ypač nuotekų valymo ir širdies audinių regeneracijos kontekste.

7.1 Įvadas ir kontekstas

Didėjantis tvarios energetikos poreikis kartu su būtinybe efektyviai valyti nuotekas skatina kurti technologijas, galinčias vienu metu spręsti abi šias problemas. Viena perspektyviausių krypčių – mikrobiniai kuro elementai (ang. MFC – microbial fuel cell), kurie leidžia tiesiogiai paversti organiniuose substratuose sukauptą cheminę energiją elektros energija švelniomis eksploatacinėmis sąlygomis. Tokia dviguba funkcija sudaro prielaidas energijos išgavimui iš atliekų srautų ir kartu mažina nuotekų poveikį aplinkai, todėl MFC laikomi patrauklia žiedinės bioekonomikos sistemų dalimi. Nepaisant intensyvių tyrimų, jų praktinį taikymą vis dar riboja mažas galios tankis ir nepakankamas ilgalaikis stabilumas, daugiausia susiję su neefektyviu ekstraląsteliniu elektronų perdavimu (EEP).

Eukariotiniuose mikroorganizmuose EEP efektyvumą smarkiai riboja izoliuojančios ląstelės sienelės ir plazminės membranos savybės. Dėl to mielių pagrindu veikiančiuose MFC elektronų pernaša dažniausiai vyksta dalyvaujant tirpiems redokso mediatoriams. Nors tokios sistemos gali generuoti elektros srovę, jos tampa sudėtingesnės, brangesnės ir gali neigiamai veikti ląstelių gyvybingumą bei sistemos tvarumą. Todėl laidžios, stabilios ir biologiškai suderinamos ląstelės–elektrodo sąsajos formavimas yra vienas svarbiausių uždavinių siekiant padidinti mielių pagrindu veikiančių MFC efektyvumą.

Skirtingai nei elektroaktyvios bakterijos, *Saccharomyces cerevisiae* yra nepatogeniškas, genetiškai gerai apibūdintas, aplinkos sąlygoms atsparus ir plačiai biotechnologijoje naudojamas mikroorganizmas. Dėl paprasto kultivavimo, gebėjimo augti aerobinėmis ir anaerobinėmis sąlygomis bei technologinio pritaikomumo jis yra patrauklus bioelektrocheminių sistemų mastelio didinimui. Vis dėlto mažas natūralus EEP efektyvumas riboja jo tiesioginį taikymą didelio našumo MFC, todėl būtinos inžinerinės strategijos, leidžiančios pagerinti krūvio pernašą nepakenkiant ląstelių metabolizmui ir gyvybingumui.

Viena perspektyviausių EEP gerinimo krypčių – ląstelės ir elektrodo sąsajos modifikavimas naudojant laidžias ir biologiškai suderinamas medžiagas. Laidūs polimerai, tokie kaip polipirolis, gali būti formuojami

119

ekstraląsteliniu būdu ir sudaryti puslaidininkinį bei redokso aktyvų sluoksnį, kuris pagerina elektronų pernašą ir mikroorganizmų adheziją bei biofilmo stabilumą. Aukso nanodalelės dėl didelio elektrinio laidumo, cheminio stabilumo ir nanometrinio dydžio gali sudaryti lokalius laidžius kelius ir palengvinti tiesioginį elektronų perdavimą per menkai laidžias ląstelės struktūras. Šių komponentų derinimas sudaro sinerginę strategiją efektyviai bioelektrocheminei sąsajai formuoti. Tačiau jų bendras poveikis mielių pagrindu veikiančių MFC veikimui, ypač realioms nuotekų valymo sąlygoms artimoje terpėje, iki šiol nėra išsamiai ištirtas.

Plėtojant MFC technologiją svarbus ir pažangių elektrocheminių metodų taikymas gyvų ląstelių redokso procesams tirti. Skenuojanti elektrocheminė mikroskopija (SECM) leidžia neinvaziniu būdu gauti erdviškai lokalizuotą elektrocheminio aktyvumo informaciją mikro- ir nanometriniu masteliu. Taikant šį metodą galima įvertinti viduląstelinę redokso būseną ir plazminės membranos elektronų perdavimo procesus fiziologiškai artimomis sąlygomis. Šiame darbe SECM buvo taikoma kaip metodologinė platforma žmogaus prieširdžių mezenchiminių stromos ląstelių redokso aktyvumui tirti ir vėliau pritaikyta bioelektrocheminių sistemų analizei.

Siekiant praktinio MFC pritaikymo, būtina vertinti jų veikimą ne tik modelinėmis laboratorinėmis sąlygomis, bet ir sudėtingose realiose terpėse. Nuotekų dumblas yra tinkamas substratas, nes jame yra biologiškai skaidžių organinių medžiagų ir natūralių redokso mediatorių, galinčių palaikyti mikroorganizmų metabolizmą ir elektronų pernašą. Modifikuotų mielių pagrindu veikiančių MFC integravimas į tokią terpę yra svarbus žingsnis kuriant praktiškai pritaikomas energijos išgavimo iš atliekų sistemas.

Šios disertacijos mokslinis naujumas – dvigubos bioelektrodo sąsajos formavimo strategijos sukūrimas, derinant ekstraląstelinį polipirolio sluoksnį ir aukso nanodaleles, siekiant suaktyvinti tiesioginį elektronų perdavimą išlaikant ląstelių gyvybingumą. Taip pat pirmą kartą modifikuotų sistemų veikimas vertinamas naudojant realų nuotekų dumblą. Darbe parodoma ir SECM taikymo galimybė kaip neardomojo metodo gyvų ląstelių redokso procesams tirti.

Disertacijos tikslas – padidinti ekstraląstelinio elektronų perdavimo efektyvumą *Saccharomyces cerevisiae* pagrindu veikiančiuose mikrobinio kuro elementuose formuojant laidžią ir biologiškai suderinamą ląstelės–elektrodo sąsają polipirolo ir aukso nanodalelių pagrindu bei įvertinti modifikuotų sistemų veikimą realių nuotekų terpėje.

Disertacijoje keliami uždaviniai:

1. Įvertinti skenuojančios elektrocheminės mikroskopijos tinkamumą gyvų ląstelių redokso aktyvumui ir plazminės membranos elektronų perdavimo procesams tirti.
2. Suformuoti ekstraląstelinį polipirolio sluoksnį ant *Saccharomyces cerevisiae* ląstelių paviršiaus ir nustatyti jo įtaką tiesioginiam elektronų perdavimui bei ląstelių gyvybingumui.
3. Nustatyti aukso nanodalelių įterpimo į mielių sistemą įtaką krūvio pernašos efektyvumui ir mikrobinio kuro elemento elektrinėms charakteristikoms.
4. Įvertinti modifikuotų sistemų veikimą laboratorinėmis ir realių nuotekų sąlygomis.

Darbo uždavinių pagrindu iškeliamos šios hipotezės:

– Skenuojanti elektrocheminė mikroskopija leidžia diferencijuoti gyvas ląsteles pagal jų redokso aktyvumą ir plazminės membranos elektronų perdavimą.
– Ekstraląstelinis polipirolio sluoksnis suformuoja laidžią ir biologiškai suderinamą sąsają, kuri sustiprina tiesioginį elektronų perdavimą mielių pagrindu veikiančiuose MFC.
– Aukso nanodalelės sudaro papildomus laidžius krūvio pernašos kelius ir padidina generuojamą srovę bei galios tankį.
– Modifikuotos sistemos gali efektyviai veikti realių nuotekų terpėje neprarasdamos našumo.

7.2 Literatūros apžvalga

Šioje pastraipoje pateikiama išsami literatūros apžvalga keliomis tarpusavyje susijusiomis temomis, daugiausia dėmesio skiriant skenuojančiajai elektrocheminei mikroskopijai (SECM) praplėčiant elektrocheminių žinių sritį; MFC, kaip pagrindiniam tyrimo objektui; kardiomiopatijai, jos diagnostikai bei svarbai ją tirti elektrochemiškai; ir bioelektrocheminių sistemų pažangai bei ateičiai.

7.2.1 SECM tyrimo principai:

Ultramikroelektrodas (UME) yra pagrindinis SECM elementas, kuris kartu su etaloniniu ir priešpriešiniu elektrodais atlieka mobilaus darbinio elektrodo funkciją elektrocheminėse ląstelėse. Dokumente paaiškinami UME veikimo režimai, įskaitant pastovaus aukščio ir pastovaus atstumo režimus, išsamiai

aprašant UME srovės, koncentracijos ir artumo prie mėginio paviršiaus ryšius. Šlyties jėgos metodų integravimas padidina matavimo tikslumą, naudojant vibracijas ir fazės poslinkius, kad būtų palaikomi tinkami atstumai tarp elektrodo ir mėginių, taip pagerinant elektrocheminių stebėjimų tikslumą.

7.2.2 MFC architektūra ir veikimo principai:

MFC sudaro anodas ir katodo kamera, kurioje mikrobiniai procesai paverčia organinius substratus elektros energija. Anaerobinėmis sąlygomis mikroorganizmai generuoja protonus ir elektronus, kurie, prasiskverbdami pro protonų mainų membraną (PEM), reaguoja katode ir galiausiai gamina vandenį. Apžvalgoje pabrėžiama anodinių medžiagų, ypač nanostruktūrinio anglies veltinio, svarba optimaliam galios tankiui ir mikrobų prilipimui. Paprastieji cukrūs, tokie kaip gliukozė, pabrėžiami kaip pagrindiniai MFC degalai. Dokumente taip pat aptariama potenciali galia ir pažangių medžiagų, sukurtų siekiant padidinti elektronų perdavimo efektyvumą, vaidmuo, susiejant kuro tipus su MFC efektyvumu.

7.2.3 Kardiopatijos ir žmogaus širdies regeneracija:

Kardiomiopatijos, ypač išsiplėtusi kardiomiopatija (DKM), nagrinėjamos atsižvelgiant į jų poveikį širdies funkcijai ir struktūriniam vientisumui. Apžvalgoje apibūdinami gydymo iššūkiai, pabrėžiant standartinius farmakologinius metodus ir regeneracinių gebėjimų žmogaus širdies audiniuose ribotumą. Naujausi tyrimai rodo, kad stimuliuojant mezenchimines kamienines ląsteles (hmMSC) ir taikant naujas epigenetines strategijas, skirtas pagerinti jų funkcinį atsistatymą, galima skatinti širdies ląstelių regeneraciją. Diagnostikai pritaikoma ir SECM metodika.

7.2.4 Nauji bioelektrocheminiai pasiekimai:

Dokumente apžvelgiami reikšmingi bioelektrocheminių sistemų pasiekimai, ypač palengvinant elektronų perdavimą mikrobų ir elektrodų sąsajose. Nanomedžiagų, dvigubų mediatorių sistemų, įskaitant lipofilinius ir hidrofilinius mediatorius, ir laidžių polimerų integravimo strategijų naudojimas aptariamas kaip novatoriškos metodikos, gerinančios mikrobinių kuro elementų efektyvumą ir našumą. Dėmesys skiriamas tyrimams, kuriuose nagrinėjama biocheminė sąveika šiose sąsajose ir kaip modifikacijos gali padidinti bendrą MFC produkciją.

7.2.5 Nanomedžiagų ir polimerų integravimas:

Apžvalgoje išsamiai aprašoma, kaip nanomedžiagos, laidūs polimerai, tokie kaip polipirolas (pPy), ir kapsuliavimo metodai gali padidinti mikrobų ląstelių efektyvumą bioelektrocheminėse sistemose. Tyrimas iliustruoja, kad redokso aktyviųjų mediatorių integravimas į gyvas ląsteles padidina krūvio perdavimo galimybes, sudarydamas sąlygas efektyvesniam energijos konversijos procesui tarp MFC.

Santraukoje aprašoma tvirta biologinių substratų, mikrobų elektronikos ir chemijos inžinerijos sąveika kaip pagrindinės dabartinių tyrimų sritys, kuriomis siekiama geriau suprasti bioelektrochemines sistemas ir jas taikyti įvairiose pramonės ir su sveikata susijusiose srityse.

7.3 Metodai

7.3.1 hmMSC paruošimas ir patvirtinimas

Tyrimo tikslas buvo išskirti hmMSC iš pacientų, neturinčių mitralinio vožtuvo sutrikimų, dešiniojo prieširdžio miokardo biopsijų, lyginant mėginius iš sveikų asmenų ir tų, kuriems operacijos metu buvo išsiplėtę prieširdžiai. Buvo gautas etinis sutikimas, o biopsijos buvo apdorotos naudojant modifikuotą protokolą, apimantį tripsino virškinimą ir kultivavimą fibronektinu padengtose plokštelėse IMDM terpėje su vaisiaus galvijų serumu (FBS) ir antibiotikais iki susiliejimo.

Ląstelių dydis buvo įvertintas mikroskopija ir kompiuterinėmis programomis, o paviršiaus žymekliai buvo analizuojami srauto citometrijos metodu po tripsino panaudojimo ir antikūnų inkubacijos. hmMSC acetilinimo lygiai buvo matuojami po apdorojimo HDAC inhibitoriumi, o mitochondrijų potencialas įvertintas naudojant JC-1 dažus ir fluorescencijos santykį. NAD+ lygiai buvo kiekybiškai įvertinti kolorimetriniu tyrimu pagal standartinį protokolą. Be to, ląstelės buvo kultivuojamos ant želatina padengtų dengiamųjų stiklelių elektrocheminiams eksperimentams, siekiant užtikrinti metabolinį aktyvumą. Tyrimas atitiko etikos standartus, gavus institucijos etikos komiteto pritarimą ir visų pacientų informuotą sutikimą.

7.3.2 Mielių tirpalo paruošimas

S. cerevisiae buvo kultivuojama YPD sultinyje, naudojant specialią metodiką standartizuotam mielių tirpalui gauti. Parametrai užtikrino medžiagų apykaitos efektyvumą ir ląstelių gyvybingumą visų eksperimentinių fazių metu.

7.3.3 Elektrodų paruošimas

Grafito elektrodai buvo poliruoti, išvalyti ir modifikuoti, siekiant pagerinti elektrocheminę sąveiką, naudojant įvairius tarpininkų tirpalus efektyviam elektronų perdavimui.

7.3.4 SECM metodai

hmMSC redokso aktyvumui įvertinti skenuojančios elektrocheminės mikroskopijos (SECM) eksperimentams buvo naudojamas disko formos Au pagrindu pagamintas ultramikroelektrodas (UME), prieš tai kruopščiai išvalytas ir kondicionuotas. Matavimai buvo atlikti trijų elektrodų sistemoje, naudojant potenciostatą, o HDAC inhibitoriaus SAHA poveikis elektrocheminiam elgesiui buvo įvertintas įvairiose terpėse. Artėjimo kreivės parodė ląstelėms nelaidžio redokso tarpininko ($[FcCOOH]^+$) sumažėjimą šalia ląstelių membranų, o tai paaiškina srovės ir atstumo nuo mėginio ryšį. Šių kreivių pritaikymas naudojant matematinius modelius leido išskirti su laidžiais ir izoliuojančiais paviršiais susijusius parametrus, galiausiai nustatant kinetinę konstantą λ. Buvo atlikta statistinė analizė, siekiant užtikrinti 95 % patikimumo lygį išvestuose parametruose.

7.3.5 Elektrocheminių matavimų parametrai

Buvo naudojama trijų elektrodų sistema, kurią sudarė mielėmis modifikuotas grafitas MFC kaip darbinis elektrodas, Ag/AgCl etaloninis elektrodas ir platinos priešpriešinis elektrodas. Elektrocheminė celė buvo užpildyta fosfatiniu buferiniu tirpalu (PBS), kuriame yra 20 mM kalio fericianido ir gliukozės, siekiant palengvinti elektronų perdavimą ir biologinį aktyvumą. Prieš bandymą buvo atliktas 20 minučių stabilizavimo laikotarpis, siekiant užtikrinti pusiausvyrą tarp elektrodo paviršiaus, elektrolito ir biologinių komponentų. Elektrocheminiai matavimai buvo atlikti naudojant potenciostatą („Autolab PGSTAT302N“), taikant ciklinę voltamperometriją (CV), keičiant potencialą nuo -0,6 V iki +0,6 V esant 50 mV/s greičiui, kas leido gauti įžvalgų apie redokso procesus ir elektrodų kinetiką. Ši konfigūracija buvo skirta pagerinti modifikuotos elektrodų sistemos bioelektrocheminės energijos konversijos efektyvumą.

7.3.6 Galios tankio matavimai

Eksperimentiniuose įrenginiuose grafito strypų elektrodai veikė kaip anodai arba katodai, o MFC buvo vertinami tiek laboratorinėmis sąlygomis,

tiek komunalinėse nuotekose, siekiant įvertinti galios tankį esant įvairioms varžoms.

7.4 Rezultatai

7.4.1 hmMSC tyrimas

Iš sveiko ir išsiplėtusio prieširdžio miokardo, naudojant eksplantacinį ataugų metodą, buvo išskirtos iš žmogaus prieširdžių gautos hmMSC ir kultivuojamos pilnoje IMDM augimo terpėje. Tiek sveikos, tiek patologinės hmMSC pasižymėjo verpstės formos morfologija. Tačiau iš išsiplėtusio miokardo išskirtos hmMSC (10B pav.) atrodė didesni, palyginti su iš sveikų audinių išskirtomis hmMSC (10A pav.). Kiekybinė ląstelių prisitvirtinimo ploto analizė naudojant „ImageJ“ programinę įrangą patvirtino, kad patologinės hmMSC pasižymėjo žymiai didesniu prisitvirtinimo plotu (4000–5000 μm²), palyginti su sveikomis hmMSC (1000–2000 μm²) (10C pav.).

Tiek sveikos, tiek patologinės hmMSC ekspresavo tipinius mezenchiminių kamieninių ląstelių paviršiaus žymenis (CD29, CD44, CD90, CD73 ir CD105), tačiau neturėjo hematopoetinių ir imuninių žymenų (CD34, CD45, CD14 ir CD40) ekspresijos, patvirtindamos jų mezenchiminę kilmę (10E pav.). Šie duomenys rodo, kad iš išsiplėtusio prieširdžių miokardo gautos hmMSC pasižymi padidėjusia morfologija, palyginti su gautomis iš neišsiplėtusio miokardo, išlaikant būdingą MSC paviršiaus žymenų profilį. Tačiau, nepaisant to, kad MSC gali būti naudojamos audinių inžinerijoje, genų terapijoje, transplantacijoje ir audinių sužalojimuose, jų identifikavimas skirtinguose audiniuose vis dar yra iššūkis.[210]

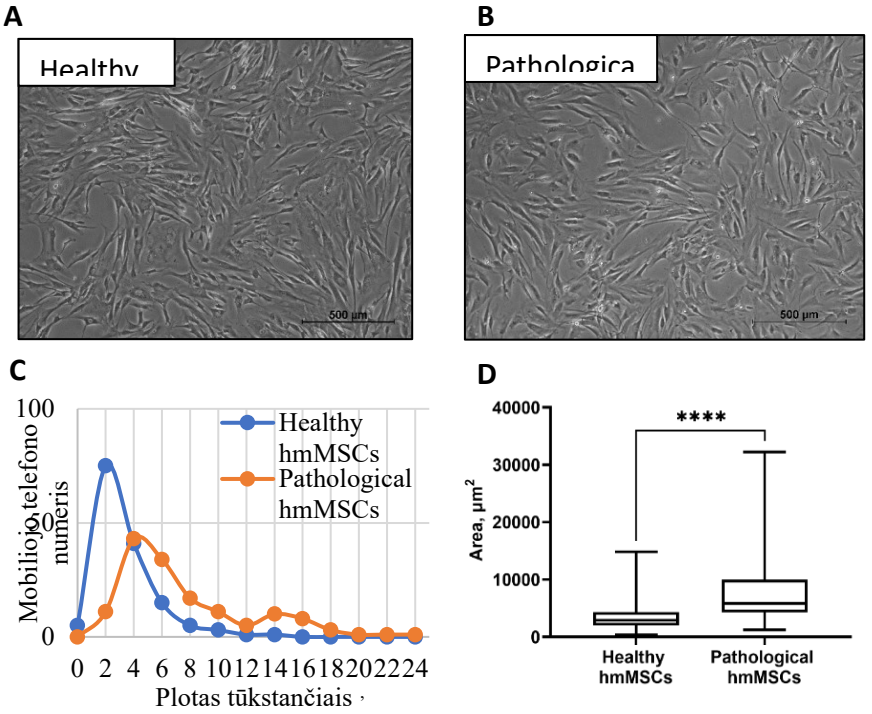

E

	CD29	CD44	CD90	CD73	CD105	CD34	CD45	CD14	CD40
Healthy hmMSCs	96.4±0.6	91.6±2.6	79±11	86±5.6	90.5±5.6	2.3±0.4	1.3±0.3	1.5±0.2	4.7±1.2
Pathological hmMSCs	96.1±2.2	75.7±7.3	73±5.8	82±2.4	70.4±4.7	0.5±0.2	0.7±0.1	1.1±0.7	1.6±0.5

1 paveikslas. Iš sveiko ir išsiplėtusio/patologinio prieširdžių miokardo išskirtų hmMSC fenotipinis palyginimas. (A) Iš sveiko, neišsiplėtusio prieširdžių audinio gautų hmMSC morfologija. (B) Iš patologinio, išsiplėtusio prieširdžių audinio gautų hmMSC morfologija. Mastelio juosta = 500 µ m. (C) Ląstelių prisitvirtinimo ploto pasiskirstymas sveikose ir patologinėse hmMSC; n = 150 ląstelių iš trijų mikrografijų. (D) Kiekybinis sveikų ir patologinių hmMSC prisitvirtinimo ploto palyginimas; n = 150 ląstelių iš trijų mikrografijų. (E) Sveikų ir patologinių hmMSC paviršiaus baltymų lygio profiliai. Duomenys pateikiami kaip vidurkis ± SD. Skirtumai buvo laikomi reikšmingais, kai $p \leq 0{,}05$.

Kadangi SAHA yra histono deacetilazės (HDAC) inhibitorius, buvo įvertintas jo poveikis bendram acetilintų baltymų kiekiui tiek sveikose, tiek patologinėse hmMSC (2A pav.). Sveikos (neišsiplėtusios) ir patologinės (išsiplėtusios) iš prieširdžių miokardo gautos hmMSC buvo kultivuojamos 3 dienas pilnoje augimo terpėje (IMDM su 10 % FBS) arba kardiomiogeninėje diferenciacijos terpėje (DMEM/F12 su 2 % FBS), su arba be 1 arba 2. µM SAHA. Pradinio tyrimo metu patologinėse prieširdžių hmMSC buvo nustatytas mažesnis baltymų acetilinimo lygis, palyginti su sveikomis

ląstelėmis. Abi SAHA koncentracijos skatino baltymų acetilinimą, o patologinėse hmMSC poveikis buvo ryškesnis (padidėjimas iki 2 kartų), o sveikose ląstelėse poveikis buvo silpnesnis (iki 1,5 karto), palyginti su negydytomis kontrolinėmis grupėmis (11 pav.).

Panašūs rezultatai buvo gauti ankstesniame mūsų tyrime, kuriame lyginome iš sveiko ir išsiplėtusio žmogaus skilvelių miokardo gautas hmMSC ir vertinome SAHA poveikį jų kardiomiogeninės diferenciacijos potencialui (Miksiunas ir kt., 2021) . Kiti tyrimai taip pat parodė, kad histonų acetilinimo/deacetilinimo reguliavimas vaidina svarbų vaidmenį pelių MSC linijų, tokių kaip C3H10T1/2 (Yin ir kt., 2014) ir P19CL6 ląstelės, kardiomiogeninėje diferenciacijoje, padidinant Isl1 ekspresiją. [213]Tačiau paskelbtų mokslinių tyrimų, kuriuose nagrinėjamas iš žmogaus miokardo gautų hmMSC regeneracinis potencialas epigenetinės moduliacijos būdu, skaičius išlieka mažas.

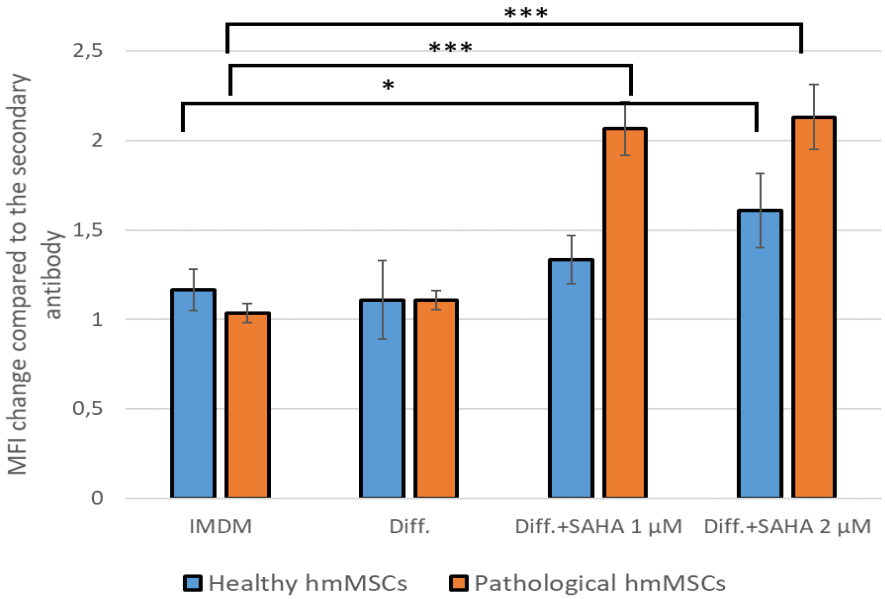

2 paveikslas. Bendras baltymų acetilinimo lygis sveikose ir patologinėse hmMSC. Ląstelės buvo kultivuojamos 3 dienas pilnoje augimo terpėje (IMDM su 10 % FBS), širdies diferenciacijos terpėje (Diff) (DMEM/F12 su 2 % FBS) arba širdies diferenciacijos terpėje, papildytoje 1 arba 2. µM SAHA. Baltymų acetilinimo lygiai buvo įvertinti srauto citometrijos metodu, kaip aprašyta skyriuje „Metodai“. Duomenys pateikiami kaip vidurkiai. ± SD. Statistinis reikšmingumas buvo apibrėžtas kaip *$p \leq 0,05$ ir ***$p \leq 0,01$.

Be to, mitochondrijų membranos potencialas (MMP) buvo įvertintas srauto citometrijos metodu, naudojant JC-1 dažus (12 pav.). Pradinio tyrimo metu patologinės hmMSC parodė žymiai mažesnį MMP, palyginti su sveikomis ląstelėmis. SAHA gydymas sustiprino MMP abiejų tipų ląstelėse, atspindėdamas acetilinimo duomenis. Tiksliau, MMP padidėjo maždaug 2 kartus patologinėse ląstelėse ir 1,4 karto sveikose ląstelėse, palyginti su kontrolinėmis grupėmis, kultivuojamomis standartinėje IMDM terpėje (11 pav.). Ankstesnis mūsų darbas [44]taip pat parodė, kad SAHA pagerina mitochondrijų funkciją tiek sveikose, tiek išsiplėtusiose žmogaus skilvelių miokardo hmMSC. Papildomi tyrimai parodė, kad SAHA apsaugo naujagimių žiurkių skilvelių miocitus ir žmogaus embrioninių kamieninių ląstelių kardiomiocitus nuo išemijos / reperfuzijos pažeidimo, išsaugodama mitochondrijų homeostazę . [214]Panašiai ir HDAC6 inhibitorius tubastatinas A, kaip įrodyta, apsaugo pelių širdis nuo TNF-α sukelto mitochondrijų pažeidimo.[215]

Šie duomenys patvirtina HDAC inhibitorių svarbą reguliuojant mitochondrijų funkciją ir gyvybingumą hmMSC, gautose tiek iš sveikų, tiek iš sergančių žmogaus prieširdžių miokardo.

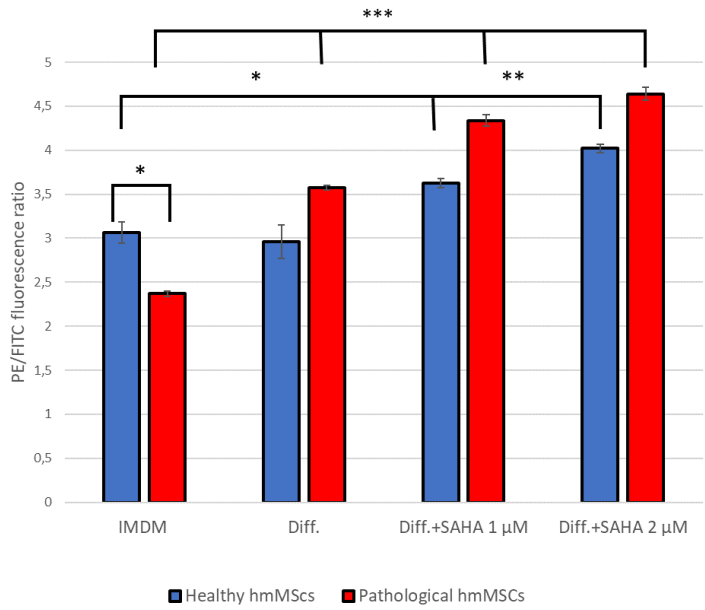

3 paveikslas. Sveikų ir patologinių hmMSC mitochondrijų membranos (MMP) potencialas. Ląstelės 3 dienas buvo kultivuojamos pilnoje augimo terpėje (IMDM su 10 % FBS), širdies diferenciacijos terpėje (Diff.) (DMEM/F12 su 2 % FBS) arba širdies diferenciacijos terpėje, papildytoje 1 arba 2. µM SAHA. MMP buvo matuojama srauto citometrija naudojant JC-1 dažymą, kaip aprašyta skyriuje „Metodai“. Duomenys pateikiami kaip vidurkiai. ± SD. Statistinis reikšmingumas

nustatytas ties * $p \leq 0{,}05$. Matavimai atlikti su mėginiais iš mažiausiai trijų nepriklausomų kiekvieno tipo iš pacientų gautų ląstelių linijų.

bendras tarpląstelinis NAD^+ kiekis (13 pav.). Patologinėse hmMSC NAD^+ kiekis buvo žymiai mažesnis – beveik dvigubai mažesnis – palyginti su sveikomis ląstelėmis kontrolinėmis sąlygomis. Įdomu tai, kad SAHA turėjo didesnį poveikį NAD^+ kiekiui sveikose ląstelėse nei patologinėse. Tai rodo, kad NAD^+ išsaugojimo ir sintezės keliai sveikose prieširdžių hmMSC yra mažiau sutrikę ir labiau reaguoja į HDAC slopinimą, palyginti su patologinėmis ląstelėmis.

Apibendrinus šiuos rezultatus, galima teigti, kad SAHA veiksmingiau sustiprina acetilinimą ir mitochondrijų aktyvumą patologinėse prieširdžių hmMSC, palyginti su sveikomis. Tačiau NAD^+ biosintezės sistema patologinėse ląstelėse atrodo labiau pažeista ir mažiau reaguoja į SAHA, o tai pabrėžia NAD^+ reguliavimo sudėtingumą sergančiose ląstelėse. Norint geriau suprasti šiuos skirtumus ir optimizuoti HDAC taikinius dilatacinei kardiomiopatijai (DKM) gydyti, reikia atlikti tolesnius tyrimus.

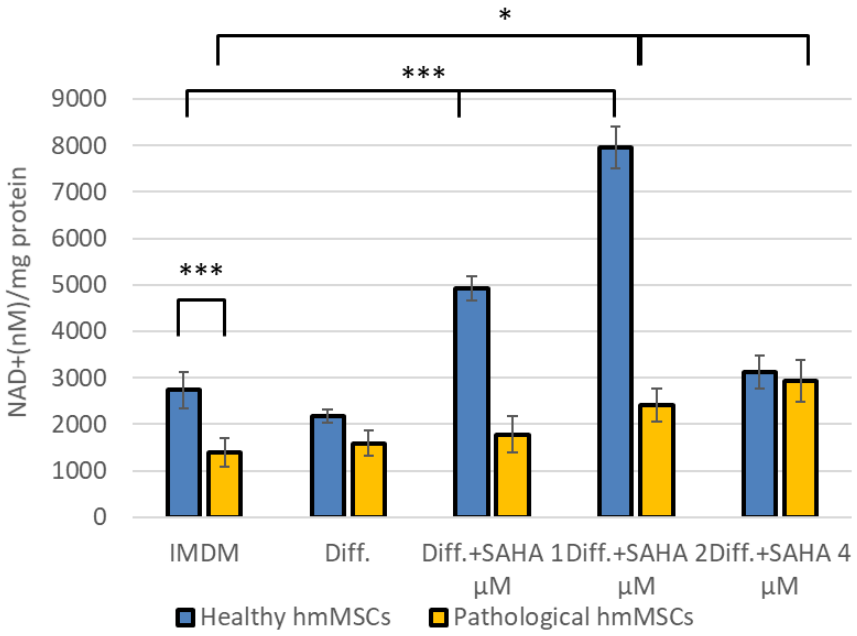

4 paveikslas. Bendras NAD^+ kiekis sveikose ir patologinėse hmMSC. Ląstelės 3 dienas buvo kultivuojamos pilnoje augimo terpėje (IMDM su 10 % FBS), širdies diferenciacijos terpėje (Diff) (DMEM/F12 su 2 % FBS) arba širdies diferenciacijos terpėje, papildytoje 1 arba 2. µM SAHA. Bendras NAD^+ kiekis buvo matuojamas spektrofotometriškai, kaip aprašyta skyriuje „Metodai“. Duomenys pateikiami kaip

vidurkis. ± SD. Statistinis reikšmingumas nustatytas ties $p \leq 0,\ 05$. Matavimai buvo atlikti naudojant bent tris nepriklausomas kiekvieno tipo iš pacientų gautas ląstelių linijas.

Kitame etape įvertinome sveikų ir patologinių prieširdžių hmMSC tarpląstelinę redokso būseną prieš ir po SAHA gydymo, naudodami skenuojančiąją elektrocheminę mikroskopiją (SECM) su ląstelėms nepralaidžiu redokso tarpininku ferocenokarboksirūgštimi (FcCOOH) . Tikslas buvo palyginti redokso atsakus tarp ląstelių tipų, matuojant NAD^+ lygius tiek biochemiškai (lizatuose), tiek elektrochemiškai (neinvaziškai). Šie rezultatai gali praplėsti SECM taikymą vertinant tarpląstelinę redokso dinamiką žmogaus prieširdžių kilmės hmMSC.

7.4.2 SECM metodo intervencija

Skenuojančios elektrocheminės mikroskopijos (SECM) eksperimentuose srovė registruojama ultramikroelektrodu (UME), esančiu įvairiais atstumais nuo imobilizuotų ląstelių. Srovės ir atstumo priklausomybės matuojamos grįžtamojo ryšio režimu vertikaliai (z kryptimi) artėjant prie ląstelės paviršiaus. SECM matavimams buvo pasirinktas ląstelei nepralaidus redokso tarpininkas ferocenokarboksirūgštis (FcCOOH). 14 paveiksle pateikta schema iliustruoja, kad vieno tarpininko sistemoje FcCOOH gali pranešti apie dviejų tipų redokso aktyvumą: (A) ląstelėse esančių redukuojančių junginių (pvz., GSH, NADH, NADPH ir kt.) išsiskyrimą iš pažeistų arba mirštančių ląstelių po toksinio poveikio, kuris pažeidžia membranos vientisumą; ir (B) su membrana susijusį elektronų perdavimą iš gyvybingų ląstelių per plazminės membranos surištas arba transmembranines NAD(H)/NAD(P)H oksidoreduktazes.

Remiantis 14A paveiksle parodytu modeliu, buvo įrodyta, kad Ras transformacija, naudojama kaip vėžio modelis in vitro, pažeidžia žmogaus naviko nesukeliančias krūties epitelio ląsteles (MCF10A), dėl ko išsiskiria redukuotas glutationas (GSH), kuris savo ruožtu sumažina tarpląstelinio FcCOOH kiekį, kaip nustatyta SECM metodu. 14B paveiksle pateikta schema rodo alternatyvų mechanizmą, kai FcCOOH redukuojamas ląstelės paviršiuje gyvybingų ląstelių būdu per plazminės membranos elektronų pernašą (PMET).

Ankstesni mūsų atlikti tyrimai su žmogaus širdies skilvelių hmMSC parodė, kad subtoksinės SAHA koncentracijos (1–2 μM 3 dienas) pagerino mitochondrijų funkciją ir pagerino tiek sveikų, tiek išsiplėtusių ląstelių energetinę būklę, palengvindamos kardiomiogeninę diferenciaciją.[211,228,229] Šie rezultatai paskatino mus toliau tirti tarpląstelinę redokso būseną ,

naudojant du vienas kitą papildančius metodus: elektrocheminius matavimus sveikose, nelizuotose ląstelėse naudojant SECM ir biocheminius tyrimus lizuotose ląstelėse.

Necitotoksinio SAHA gydymo poveikį sveikų ir patologinių iš prieširdžių gautų hmMSC tarpląsteliniam redokso potencialui , daugiausia dėmesio skirdami jo aptikimui per plazminės membranos elektronų pernašos (PMET) sistemą, naudojant ląstelėms nepralaidų mediatorių FcCOOH.

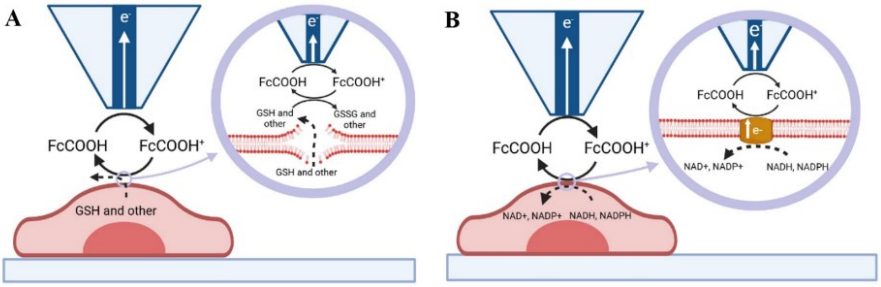

5 paveikslas. Išsiskyrusių ir viduląstelinių redokso junginių SECM matavimai naudojant ląstelėms nepralaidų mediatorių FcCOOH. A. FcCOOH redukcija išsiskyrusiais viduląsteliniais redokso junginiais ląstelės pažeidimo metu. B. FcCOOH redukcija pasiekiama naudojant membraną surištas ir (arba) transmembranines NAD(H)/NAD(P)H fermentų sistemas, kai ląstelės nėra pažeistos ir redukuojantys junginiai neišsiskiria užląsteliniu būdu.

NAD^+ / NADH ir $NADP^+$ / NADPH redokso poros atlieka esminį vaidmenį palaikant tarpląstelinę redokso būseną, remiant ląstelių energijos metabolizmą, mitochondrijų funkciją, genų ekspresiją, signalizacijos kelius ir kitus fiziologinius procesus. [35,230]Iš jų NAD^+ /NADH pora yra ypač svarbi širdies audiniuose, kur oksidacinis fosforilinimas yra pagrindinis ATP generavimo kelias.[231]

Plazminės membranos elektronų pernašos (PMET) sistema pirmą kartą buvo identifikuota pastebėjus, kad nepažeistos ląstelės gali sumažinti membranai nelaidžių oksidantų kiekį. [232] Nuo tada PMET buvo pripažintas pagrindiniu redokso homeostazės, ląstelių proliferacijos ir išgyvenimo reguliatoriumi. [223,233,234] Elektrocheminių matavimų kontekste, naudojant ląstelėms nelaidų redokso tarpininką FcCOOH , žmogaus prieširdžių hmMSC PMET sistemą galima schematiškai pavaizduoti taip:

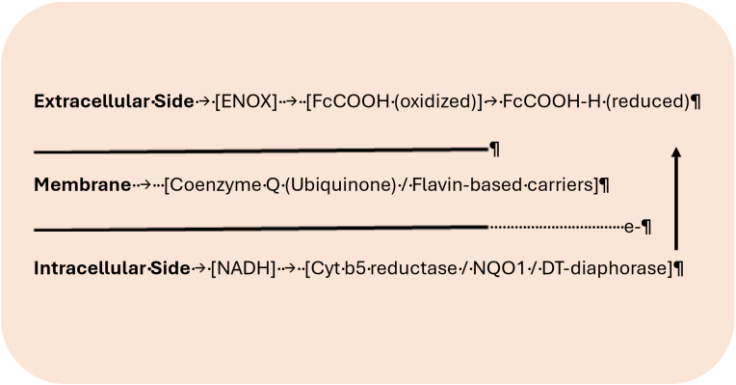

6 paveikslas. PMET schema žmogaus širdies prieširdžių ląstelėse elektrocheminiams redokso tyrimams, naudojant ląstelėms nepralaidžią FcCOOH. ENOX – exto-NOX arba ląstelės paviršiaus NADH oksidazė.

Citozolinis NADH daugiausia susidaro glikolizės (ypač GAPDH etapo), malato-aspartato pernašos (MAS) , laktatdehidrogenazės (LDH) ir alkoholio dehidrogenazės būdu. Šis NADH telkinys gali atiduoti elektronus PMET per tarpines reduktazes, tokias kaip: NADH-citochromo b5 oksidoreduktazė (CYB5R3), dar žinoma kaip citochromo b5 reduktazė, kuri egzistuoja tiek citozolinėje, tiek membranoje susijungusioje formoje, kuri taip pat redukuoja kofermentą Q (CoQ) ir askorbatą, palaikydama antioksidacinę apsaugą ir apsaugodama nuo lipidų peroksidacijos; [235]ir NAD(P)H:chinono oksidoreduktazė 1 (NQO1) , daugiausia citozolinis fermentas, kuris redukuoja chinonus, bet taip pat gali sąveikauti su membranoje susijungusiu ubichinonu ir perkelti elektronus į plazminę membraną. [236,237]Abu fermentai yra pagrindiniai citozoliniai NADH transporteriai į plazminę membraną.

Apibendrinant galima teigti, kad žmogaus prieširdžių kilmės hmMSC PMET sistema funkciškai geba sumažinti ląstelėms nelaidžių mediatorių, tokių kaip FcCOOH , kiekį, todėl ji tinka neinvaziniam elektrocheminiam stebėjimui naudojant SECM (skenuojančiąją elektrocheminę mikroskopiją). Šis redokso reaguojantis aktyvumas atspindi ląstelės viduje esančio NADH prieinamumą ir gali būti moduliuojamas metabolinėmis intervencijomis, tokiomis kaip gydymas HDAC inhibitoriais, tokiais kaip SAHA . Tiek sveikos, tiek patologinės/išsiplėtusios žmogaus širdies kilmės mezenchiminės kamieninės ląstelės (hmMSC) turi aktyvią plazminės membranos elektronų pernašos (PMET) sistemą, kuri atspindi širdies ląstelių ląstelėse esantį redokso potencialą, pagrįstą NAD^+ / NADH santykiu, ir gali būti įvertinta elektrochemiškai.

Kai ultramikroelektrodo (UME) zondas yra toli nuo ląstelės membranos, tirpale išmatuota srovė atsiranda dėl FcCOOH+ redukcijos, kurią sukelia redokso aktyvūs produktai, kurie difunduoja arba išsiskiria iš ląstelių. Šiuo

atveju mėginys veikia kaip bipolinis elektrodas , redukuojantis $[FcCOOH]^+$ iki FcCOOH arba, tiksliau, redukuojantis ferocenio joną ($[FcCOOH]^+$) iki FcCOOH. Šis procesas padidina vietinę FcCOOH koncentraciją šalia elektrodo, todėl atitinkamai padidėja išmatuota srovė.[3]

Tyrimo rezultatai rodo, kad SAHA padidina ne tik mitochondrijų aktyvumą ir membranos potencialą , kaip buvo parodyta anksčiau, bet ir bendrą tarpląstelinį redokso pajėgumą tiek sveikose, tiek sergančiose prieširdžių miokardo hmMSC. Be to, SECM matavimai su ląstelėms nepralaidžiu tarpininku FcCOOH yra vertinga, neinvazinė elektrocheminė priemonė, skirta tirti tarpląstelinį redokso ir PMET aktyvumą įvairiomis fiziologinėmis ir patologinėmis sąlygomis. Reikalingi tolesni tyrimai, siekiant išsamiau išaiškinti molekulinius mechanizmus, kuriais grindžiamas SAHA poveikis prieširdžių ląstelių funkcijai, redoksui ir PMET reguliavimui.

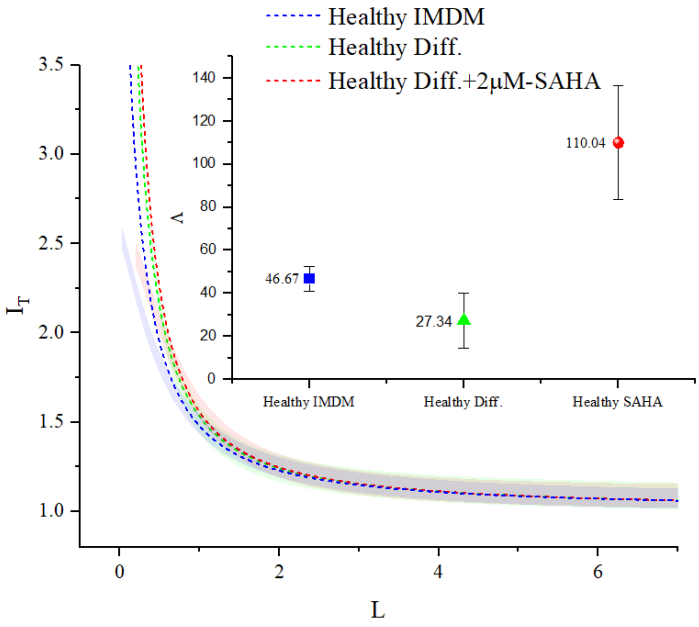

7 paveikslas. Sveikų (neišplėstų) hmMSC SECM UME metodo kreivės. Mėlyna – sveikos hmMSC pilnoje IMDM augimo terpėje; žalia – sveikos hmMSC kardiomiogeninėje diferenciacijos terpėje (Diff.); raudona – sveikos hmMSC Diff. terpėje, papildytoje 2 μM SAHA, 3 dienas. Matavimai atlikti esant +400 mV potencialo poslinkiui Ag/AgCl atžvilgiu, naudojant 6 μM FcCOOH kaip redokso tarpininką. Eksperimentiniai duomenys buvo pritaikyti naudojant matematinį modelį, pagrįstą Cornuto ir Lefrou aproksimacijomis, siekiant nustatyti reakcijos greičio kinetiką, įvertinant kinetinį parametrą λ (lambda). Duomenys pateikiami kaip vidurkis ± SD iš mažiausiai trijų nepriklausomų matavimų, naudojant ląsteles iš trijų skirtingų donorų. Skaidrios kreivės rodo eksperimentinius duomenis su 95 % patikimumo intervalu. Punktyrinės linijos rodo teorinį atitikimą, pagrįstą taikomu modeliu.

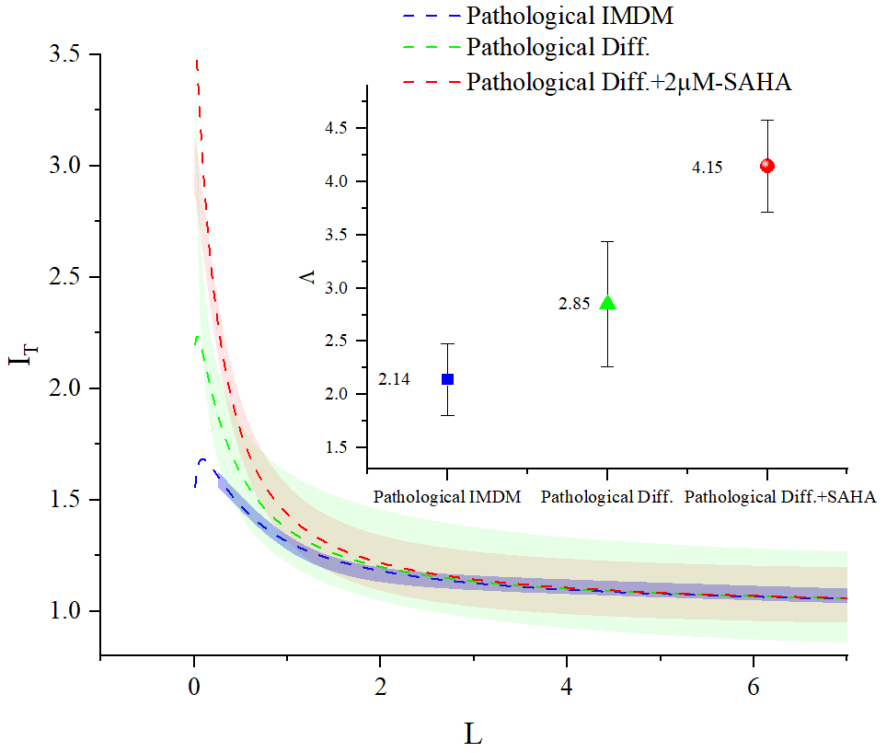

8 paveikslas. Patologinių (išsiplėtusių) prieširdžių hmMSC kreivės, gautos naudojant SECM UME metodą. Mėlyna – patologinės hmMSC IMDM terpėje; žalia – patologinės hmMSC kardiomiogeninės diferenciacijos terpėje (Diff.); raudona – patologinės hmMSC Diff. terpėje, papildytoje 2 μM SAHA, 3 dienas. Matavimai atlikti esant +400 mV potencialo poslinkiui Ag/AgCl atžvilgiu, naudojant 6 μM FcCOOH kaip redokso tarpininką. Eksperimentiniai duomenys buvo pritaikyti naudojant matematinį modelį, pagrįstą Cornuto ir Lefrou aproksimacijomis, siekiant nustatyti reakcijos greičio kinetiką, įvertinant kinetinį parametrą λ. Duomenys pateikiami kaip vidurkis ± SD iš mažiausiai trijų ląstelių, gautų iš trijų skirtingų pacientų. Skaidrios kreivės rodo eksperimentinius duomenis su 95 % patikimumo intervalu. Punktyrinės linijos atitinka teorinį atitikimą, gautą iš matematinio modelio.

Taigi, mūsų tyrimų rezultatai rodo, kad sveikų žmogaus širdies hmMSC turi aktyvesnį PMET nei patologinių, o gydymas SAHA sustiprino tiek sveikų, tiek iš išsiplėtusių prieširdžių gautų hmMSC redokso ir PMET aktyvumą, vertinant pagal tarpląstelinį FcCOOH sumažėjimą. Tai rodo pagerėjusią tarpląstelinę redokso būseną, kurią greičiausiai lemia padidėjęs NADH prieinamumas ir (arba) su membrana susijusių NADH oksidoreduktazių, tokių kaip cyt b5 reduktazė arba NQO1, aktyvacija. Šie rezultatai atitinka žinomą SAHA vaidmenį moduliuojant mitochondrijų funkciją ir NAD^+ metabolizmą , ir pabrėžia PMET kaip funkcinį ląstelių

redokso pajėgumo rodmenį žmogaus miokardo kamieninėse / stromos ląstelėse.

7.4.3 Pradiniai MFC elektrocheminiai matavimai

Siekiant nustatyti pPy poveikį mielėms, buvo atlikti ciklinės voltamperometrijos eksperimentai (18 pav.) be mielių (A), su nemodifikuotomis mielėmis (B) ir su mielėmis, kurių ląstelės sienelė buvo modifikuota (C) naudojant 200 mM pirolį. Matavimai buvo atlikti prieš ir po mielių inkubacijos 20 min. darbiniame tirpale. PQ smailės išliko beveik tokios pačios, o kalio ferocianido smailės per nurodytą laiką padidėjo, o tai rodo, kad gliukozės metabolizmas mielėse veikia tik redokso proceso pradžią ferocianide. Remiantis užregistruotais variacijos koeficientais (18 pav.), srovės tankis padidėjo naudojant pPy modifikuotas mieles, palyginti su nemodifikuotomis arba kontroline grupe (be mielių). Lyginant fero/feri redokso smailes (18D pav.) darbiniame tirpale tarp tuščio elektrodo ir įprasto mielių MFC, oksidacinio smailės srovės tankis padidėjo du kartus su mielėmis – nuo 1,806 mA/cm² iki 3,759 mA/cm², o redukcinio smailės – nuo 1,680 mA/cm² iki 3,258 mA/cm². Palyginus grynų mielių ir polipirolu modifikuotų mielių MFC, modifikuotų elektrodų oksidacinių smailių srovės tankis padidėjo 33 % ir iš viso pasiekė 5,008 mA/cm² (18C pav.). Redukciniai smailės pasiekė 3,606 mA/cm² , t. y. padidėjo, palyginti su tuščio elektrodo (18A pav.) ir nemodifikuoto mielių elektrodo (18B pav.) variacijos koeficiento smailėmis.

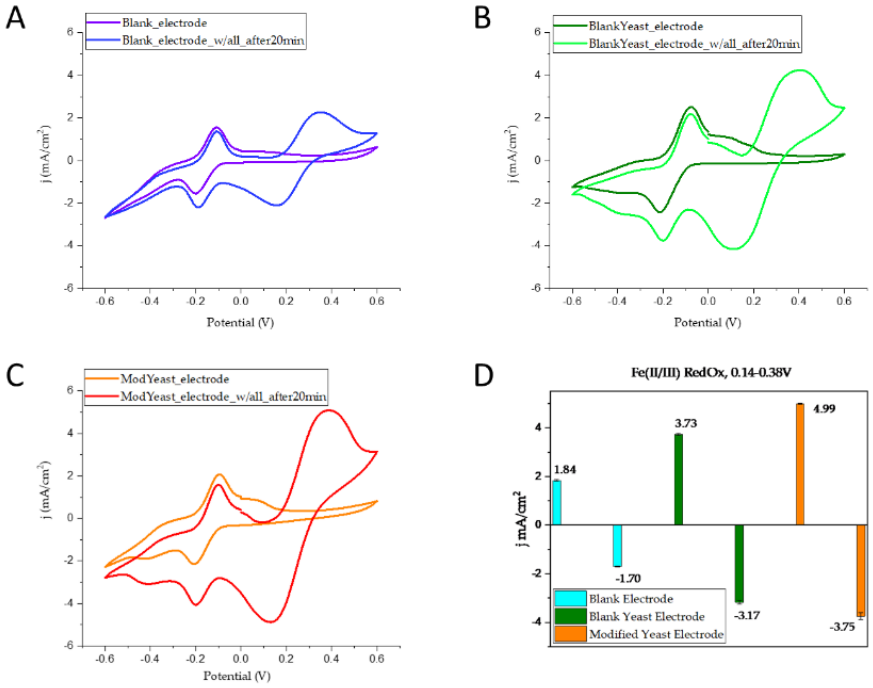

9 paveikslas. Trijų tipų PQ padengtų grafito elektrodų ciklinė voltamperometrija: A. Tuščias, be kitų priedų; B. Tuščias-mielės, tik su plikomis *S. cerevisiae* ir PCTE membrana su 3 µm poromis; ir C. Mod-mielės, 200 mM polipirolu modifikuotos *S. cerevisiae* su ta pačia PCTE membrana. D. Diagrama vaizduoja CV pikus arba ferocianido redukciją ir oksidaciją. Matavimai buvo atlikti keičiant potencialą nuo -0,6 V iki +0,6 V, 50 mV/s greičiu, naudojant Ag/AgCl etaloninį elektrodą KCl 3M tirpale ir Pt priešpriešinį elektrodą. Darbinis tirpalas: 20 mM gliukozės ir 20 mM ferocianido PBS tirpale.

Apibendrinus rezultatus, matyti, kad mielių paviršiaus chemijos pakeitimas gali gerokai pagerinti mikrobinių kuro elementų bioelektrocheminį efektyvumą, net ir sumažinus substrato afinitetą. Tai atkreipia dėmesį į didelę laidžių polimerų modifikuotų biokatalizatorių, kaip pakaitalų, galimybę pagerinti mikrobinių kuro elementų efektyvumą, ypač situacijose, kai reikia didesnės galios. Būsimuose tyrimuose reikėtų siekti patobulinti modifikavimo procesą, taip užtikrinant harmoningą pusiausvyrą tarp laidumo ir afiniteto, kad būtų pasiektas didžiausias įmanomas našumas.

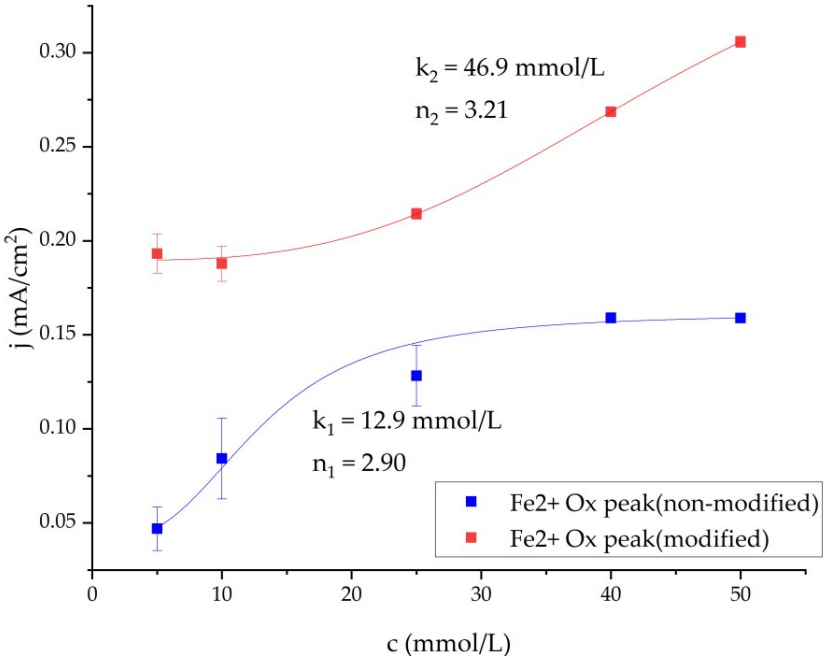

10 paveikslas. Srovės tankio priklausomybės nuo Iš $[Fe(CN)_6]^4$ ekstrahuotos gliukozės koncentracijos piko variacijos koeficiente (CV) duomenys. Eksperimentuose naudotos 200 mM pirolu modifikuotos ir nemodifikuotos mielės, pritaikytos naudojant Hilo lygtį (2 lygtis).

Be to, mielės buvo modifikuotos naudojant 50 mM pirolo ir 10 nm aukso nanodaleles, sujungtas mielių ir nanodalelių tirpalo santykiu du su vienu, nes šis koncentracijos santykis buvo ištirtas, bet nebuvo dokumentuotas jokiuose leidiniuose. Tas pats variacijos koeficiento metodas buvo naudojamas geriausiam našumui nustatyti. Tada buvo atlikti galios tankio matavimai. 20A paveiksle pavaizduota potenciali priklausomybė nuo varžos.

Didžiausias galios tankis buvo gautas naudojant 10 kΩ apkrovą 0 min., kaip parodyta 20B paveiksle. Šiame eksperimente grynos mielės parodė mažiausią galios tankį – esant 10 kΩ apkrovai, MFC pasiekė 73,7 mW/m² (20B paveikslas, geltona Sc dalis). Palyginimui, 50 mM pirolo polimerizuoto *S. cerevisiae ląstelės sienelės MFC (tas pats grafikas, oranžinis, Sc + pPy dalis) tuo pačiu matavimo momentu* pasiekė 86,5 mW/m² galios tankio piką esant tai pačiai apkrovai · Pridėjus 10 nm aukso nanodalelių prie MFC sudėtyje, padidėjo potencialas, o skaičiavimais nustatyta, kad grynų mielių MFC galios tankis su tokiu priedu siekia 122,8 mW/m² · tai yra 66,6 % daugiau nei be nanodalelių (pilka, Sc + AuNP). Tuomet tokiu pačiu būdu buvo tirta polipirolu modifikuota mielių ląstelių sienelė su tomis pačiomis

nanodalelėmis MFC, galios tankis pasiekė 147,8 mW/m² , dvigubai didesnį nei gryno mielių anodo didžiausias galios tankis.

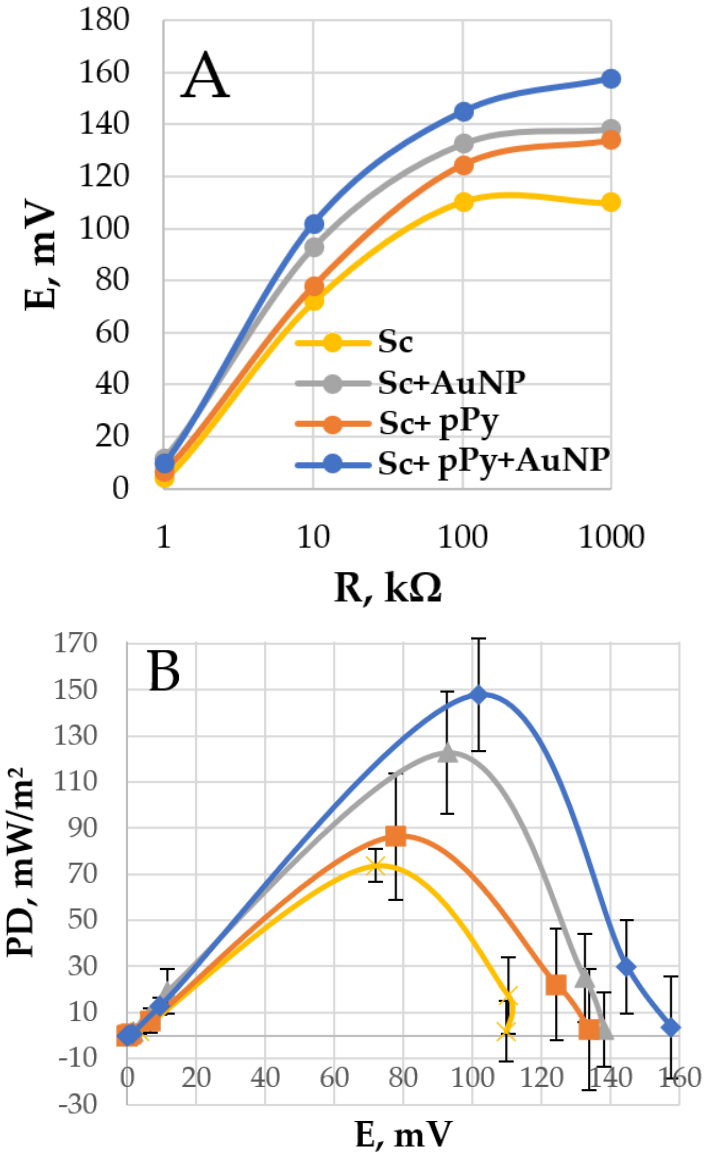

11 paveikslas. A. Potencialų priklausomybės nuo apkrovos. B. Galios tankio (PD) priklausomybės nuo potencialo. Matavimai atlikti PBS tirpale su gliukoze (20 mM) ir K3 [Fe(CN) 6] (20 mM). Naudoti elektrodai buvo padengti PQ ir *S. cerevisiae* su įvairiais pakeitimais, parodytais 8 paveiksle.

MFC galios tankio priklausomybės nuo skirtingų apkrovų buvo matuojamos kas minutę 3 minučių laikotarpiu (21 pav.). Nustatyta, kad galios tankis mažėjo su kiekviena minute. Tačiau matyti, kad didžiausias galios tankis buvo stebimas, kai mielės buvo modifikuotos pPy ir aukso nanodalelėmis. Ši tendencija turėtų būti interpretuojama kaip geriausia šioje disertacijoje nustatyta modifikacija.

Palyginti su ankstesniais tyrimais, pateiktais išvadų skyriaus 3 lentelėje, mūsų MFC su visiškai modifikuota grafito strypo anodo struktūra pasiekia geriausią momentinį galios tankį šioje kategorijoje. Tai gali reikšti, kad ateityje būtų galima naudoti skirtingas anodų medžiagas, pavyzdžiui, didžiausią galios tankį pasiekiantį anglies veltinį ir anglies šepetėlius, taip pat tirti kitas inercines medžiagas ar lydinius, naudojamus MFC elektrodams.

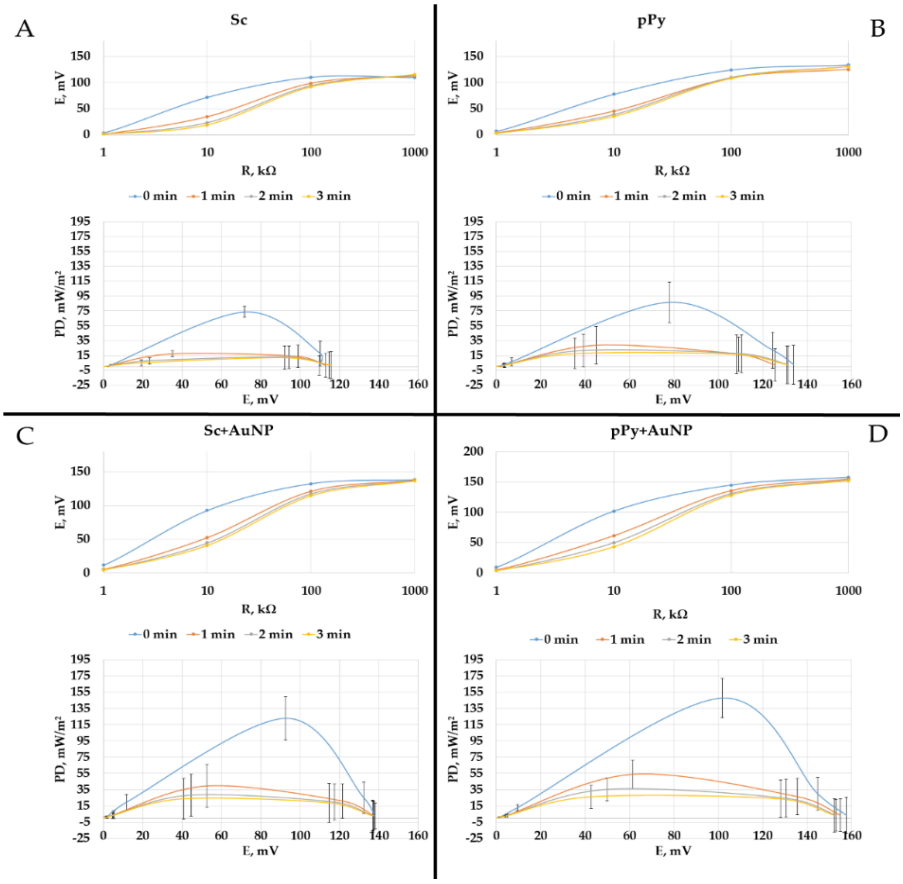

12 paveikslas. Potencialo ir apkrovos bei galios tankio (PD) ir potencialo priklausomybės, išmatuotos laike su gliukoze (20 mM) ir kalio fericianidu (20 mM) PBS tirpale. A. Grynas mielių MFC. B. Polimerizuotas mielių ląstelių sienelių MFC. C. Mielės, modifikuotos nanodalelėmis. D. Mielės, modifikuotos pPy ir nanodalelėmis.

Geriausiai veikianti MFC konfigūracija nustatyta su 50 mM pirolo polimerizuotų mielių ląstelių sienele su 10 nm Au nanosferos dalelių priedu ant poliruoto grafito strypo, padengto PQ, ir 3 µm porų PCTE membrana, dengiančia visą paviršių. Ši konfigūracija buvo naudojama matavimams atlikti realiose nuotekose, esant 10 kΩ apkrovai. Po 3 minučių trukmės vertinimo galios tankis pasiekė stulbinančią 179,2 mW/m² vertę (22 pav., raudonas taškas). Palyginimui, ankstesnių eksperimentų galios tankio rezultatai po 3 minučių ir esant 10 kΩ apkrovai buvo 9,2 mW/m² $^{\text{grynų}}$ mielių MFC atveju, 20,6 mW/m² polipirolo mielių MFC atveju, 24,6 mW/m² grynų mielių su nanodalelėmis atveju ir 61,1 mW/m² $^{\text{su}}$ MFC PBS su gliukozės ir kalio fericianido tirpalu po to paties laikotarpio.

Šie eksperimentai rodo, kad visapusiškas mielių tarpląstelinės ir tarpląstelinės aplinkos manipuliavimas yra optimalus mikrobiniams kuro elementams, nes ateities prognozės rodo, kad tokios modifikacijos naudojant aukso nanodaleles galiausiai gali būti ekonomiškai perspektyvios. Pagrindinis pakeitimas čia gali būti pagrindinio anodo medžiagos pakeitimas ir įrenginio mastelio keitimas tinkamam naudojimui.

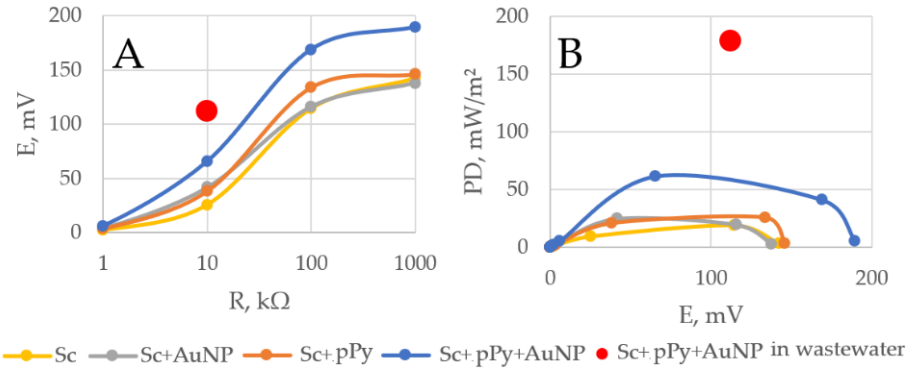

13 paveikslas. A. Potencialų priklausomybės nuo apkrovos. B. Galios tankio (PD) priklausomybės nuo potencialo. Matavimai atlikti gliukozės (20 mM) ir K3 [Fe(CN)$_6$] (20 mM) tirpale. Raudonas taškas žymi UAB „Vilniaus vandenys“ nuotekų valymo įrenginio mėginį. Jo matavimas buvo pakartotas 3 kartus ir įvestas vidurkis, tačiau paklaidos per mažos matyti paveikslėlyje.

7.4.4 Mielių ląstelių gyvybingumo įvertinimas

S. cerevisiae mielių augimui ir proliferacijai , buvo atlikti kolonijas formuojančių vienetų (ang. CFU – collony forming units) tyrimai, naudojant skirtingos koncentracijos polipirolo tirpalus. CFU kiekybiniai įvertinimai pateikti 2 lentelėje.

2 lentelė.CFU skaičiaus priklausomybė nuo polipirolio tirpalo koncentracijos

Pavyzdys	CFU/ml
Mielių ląstelės, apdorotos 8 mM koncentracijos polipirolio tirpalu	$2{,}5\cdot 10^{-7} \pm 5\cdot 10^{-2}$
Mielių ląstelės, apdorotos 25 mM koncentracijos polipirolio tirpalu	$1{,}6\cdot 10^{-7} \pm 5\cdot 10^{-2}$
Mielių ląstelės, apdorotos 50 mM koncentracijos polipirolio tirpalu	$1{,}0\cdot 10^{-7} \pm 5\cdot 10^{-2}$
Mielių ląstelės, apdorotos 100 mM koncentracijos polipirolio tirpalu	$0{,}6\cdot 10^{-7} \pm 5\cdot 10^{-2}$
Neapdorotos mielių ląstelės (kontrolė)	$5{,}0\cdot 10^{-7} \pm 5\cdot 10^{-2}$

Pateikta juostinė diagrama (14 pav.) ant agarizuotos YPD terpės rodo, kaip polipirolo modifikacija veikia *S. cerevisiae* kolonijų vystymąsi. 100 mM polipirolo tirpalo koncentracija turėjo didžiausią įtaką mielių ląstelių proliferacijai ir augimui, naudojant CFU/ml polipirolu apdorotų mielių ląstelių, kurių vertė buvo 0,6 x $107^{\pm}5\cdot 10\text{-}2$.

14 paveiksle pavaizduota, kaip polipirolio tirpalai riboja mielių kolonijų augimą. Skirtingai nuo kontrolinės grupės, visos eksperimente naudotos polipirolio koncentracijos aiškiai paveikė mielių ląstelių proliferaciją. Padidėjusi polipirolio koncentracija galėjo sukelti oksidacinį stresą ir pH disbalansą mielėse, todėl pakenkė ląstelių vystymuisi ir proliferacijai.

Jų gyvybingumas buvo įvertintas, nes tik gyvos *S. cerevisiae* ląstelės gali vykdyti medžiagų apykaitos veiklą, generuodamos elektronus. Šie elektronai yra būtini energijos gamybai MFC. Jei mielių ląstelės yra negyvybingos, kuro elemento efektyvumas sumažėja, nes jos negali prisidėti prie elektros srovės generavimo. Gyvybingumo testavimas užtikrina aktyvius mikroorganizmus ir tai, kad sistema veikia taip, kaip turėtų.

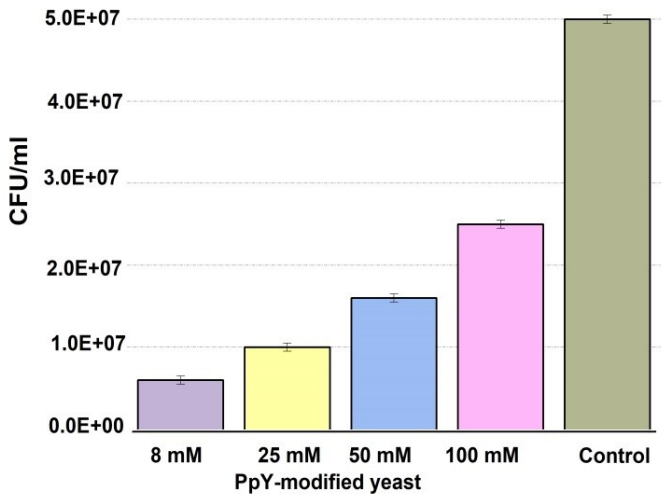

14 paveikslas. Polipirolo koncentracijos įtaka *Saccharomyces cerevisiae* mielių ląstelių gyvybingumui.

7.4.5 Ekonomiškesnio MFC voltammetrijos, DPV ir galios tankio matavimai

Siekiant nustatyti pPy poveikį mielių ląstelių, naudojamų projektuojant mieles ir PQ modifikuotą elektrodą, modifikacijai, buvo atlikti ciklinės voltamperometrijos matavimai (15A pav.). Gautos feri/fero redokso poros didžiausios srovės tankio vertės buvo pavaizduotos pagal mielių ląstelių modifikavimui naudojamą pPy koncentraciją, kaip parodyta 15B paveiksle. Naudojant 100 mM pirolo mielių ląstelių modifikavimui, buvo stebėtas maksimalus srovės tankis – 2,949 mA/cm2 (oksidacinėje smailėje) ir -2,504 mA/cm2 (redukcinėje smailėje). Be to, modifikuojant mieles naudojant mažas pirolo koncentracijas (8 ir 25 mM), srovės tankis yra mažesnis, palyginti su nemodifikuotomis mielių ląstelėmis, naudojamomis elektrodų konstrukcijoje.

Šis mažų duotųjų laidžių polimerų koncentracijų rezultatas gali rodyti slopinamąjį pPy poveikį mielių kataliziniam aktyvumui. Mano komanda ir aš rekomenduojame ateityje atlikti daugiau tyrimų apie mikroplastiko poveikį mielėms ar kitiems mikroorganizmams, naudojamiems MFC. Tai galėtų paskatinti naują laidžių polimerų naudojimo kryptį ateinančiais dešimtmečiais – ląstelių metabolizmo slopinimas taip pat yra išradinga tema.

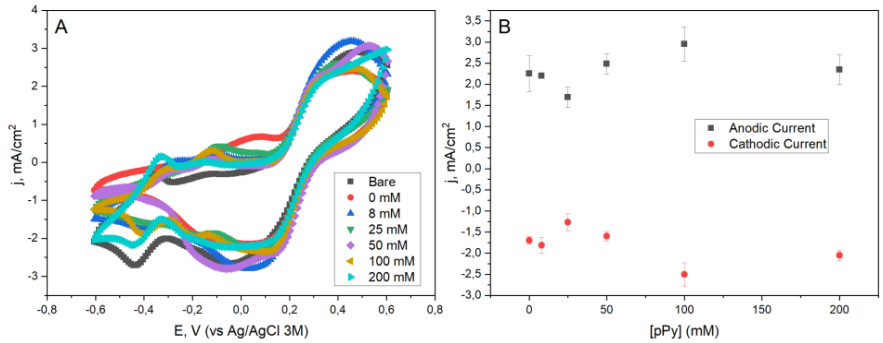

15 paveikslas. A - Skirtingų PQ ir modifikuotų mielių ląstelių elektrodų ciklinės voltamperinės kreivės. Matavimai atlikti keičiant potencialą nuo -0,6 V iki +0,6 V, 50 mV/s greičiu, naudojant Ag/AgCl etaloninį elektrodą KCl 3M tirpale ir Pt priešpriešinį elektrodą. Plikas – PQ modifikuotas grafito elektrodas be mielių ląstelių, 0 mM – PQ modifikuotas grafito elektrodas su nemodifikuotomis mielių ląstelėmis, 8–200 mM – pirolo, naudojamo mielių ląstelėms, kurios naudojamos elektrodo konstrukcijoje, modifikavimui, koncentracija. B – srovės tankis, užregistruotas oksidaciniam (0,32 V) ir redukciniam (0,11 V) fero/geležies redokso poros potencialams, esant skirtingoms pirolo, naudojamo mielių ląstelių modifikavimui, koncentracijoms.

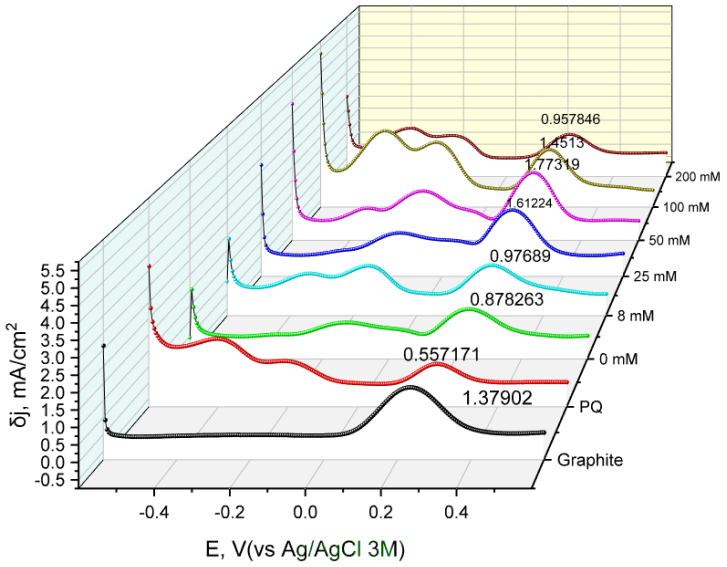

16 paveikslas. Įvairių modifikuotų darbinių elektrodų pavyzdžių, naudojamų elektrocheminėje sistemoje, diferencinės srovės tankio kreivės. Matavimai atlikti keičiant potencialą nuo -0,6 V iki +0,6 V, esant 5 mV žingsniniam potencialui, 50 mV impulso amplitudei 20 ms trukmei, skenavimo greičiui 50 mV/s, naudojant Ag/AgCl etaloninį elektrodą KCl 3M tirpale ir Pt kaip priešpriešinį elektrodą. Grafitas – nemodifikuotas grafito elektrodas, PQ – PQ modifikuotas grafito elektrodas, 0 mM – nemodifikuotos mielės ir PQ modifikuotas grafito elektrodas, 8–200 mM – PQ ir pPy modifikuotos mielės ant grafitinių darbinių elektrodų.

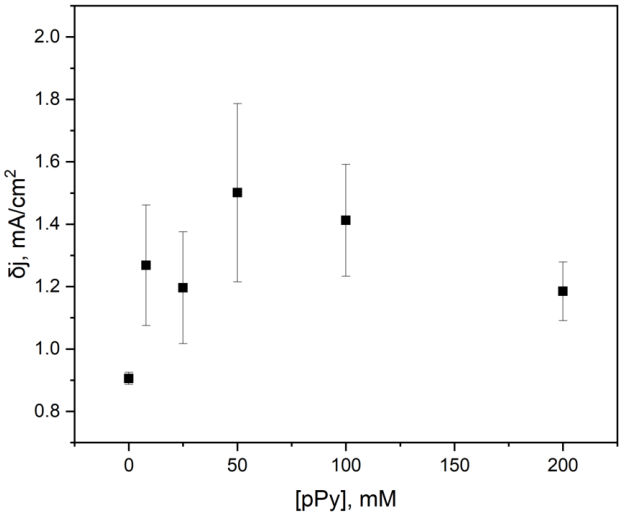

17 paveikslas. Diferencinio srovės tankio priklausomybė nuo pPy koncentracijos, naudojamos mielių ląstelių modifikavimui, naudojant PQ-pPy mielių-grafito elektrodo konstrukcijoje. Vertės buvo paimtos kaip $Fe2^{+}$ oksidacinio piko δj vertės.

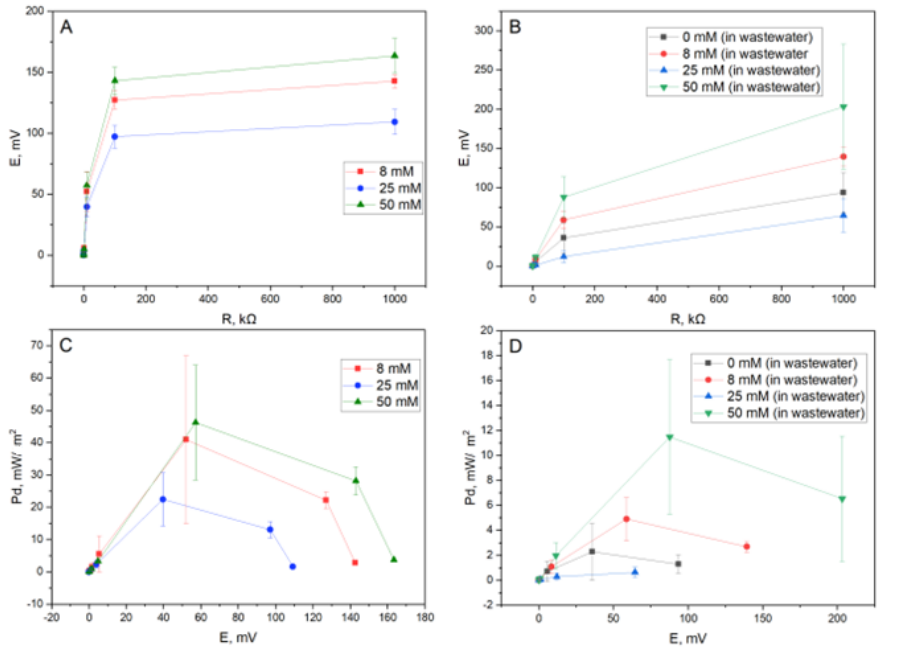

18 paveikslas. Galios tankio matavimai. A – MFC potencialo ir apkrovos priklausomybė 50 mM gliukozės ir 20 mM $K_3[Fe(CN_6)]$ tirpale PBS, naudojant mieles, modifikuotas skirtingomis pPy koncentracijomis. B – sistemos potencialo ir apkrovos priklausomybė nuotekų mėginiuose, esant skirtingoms pPy koncentracijoms, naudojamoms mielių modifikavimui. C – MFC galios tankio ir potencialo priklausomybė gliukozės/$K_3[Fe(CN_6)]$ mėginiuose. D – MFC galios tankio ir potencialo priklausomybė nuotekų mėginiuose.

Atsižvelgiant į didžiausią potencialą/galią, buvo nustatyta, kad ideali pPy dozė, naudojama mielių ląstelių sienelėms pakeisti, abiejų terpių mėginiams buvo 50 mM. Šis atradimas papildo anksčiau atliktą tyrimą. Nepaisant to, naudojant nuotekų terpę vietoj gliukozės ir K3[Fe(CN6)] mėginio, pastebimas aiškus tiek potencialo, tiek galios tankio verčių sumažėjimas ; šį rezultatą galima sieti su gyvybingo substrato mielių metabolizmui trūkumu arba optimalaus redokso tarpininko trūkumu nuotekų dumblo tirpale, ir jis gali smarkiai skirtis dėl koncentracijų, pH, temperatūros ir kitų veiksnių.

Dėl citotoksinio arba bendro slopinamojo poveikio ši arba mažesnė koncentracija gali sumažinti grybelių energijos gamybą. Be to, modifikuojant mielių ląsteles naudojant 25 mM pPy, pastebimas staigus energijos sumažėjimas, kaip buvo pastebėta atliekant voltamperometrijos matavimus. Tai gali reikšti, kad mielių ląstelės modifikuojamos taip, kad jos gamina mažiau energijos. Dar kartą iškeliama mintis atlikti mikroplastiko tyrimus.

7.5 Išvados

Šioje disertacijoje buvo sukurta nauja hibridinė strategija, skirta pagerinti elektronų perdavimą *Saccharomyces cerevisiae* pagrindu sukurtose MFC. Modifikuojant mieles laidžiu polimeru (polipirolu) ir įtraukiant 10 nm aukso nanodaleles kaip papildomą laidų tarpininką, tyrimo tikslas buvo pagerinti energijos gamybą, išlaikyti ląstelių gyvybingumą ir palengvinti efektyvų veikimą su realiais substratais, tokiais kaip nuotekų dumblas.

Svarbiausi tyrimai parodė, kad iš DCM širdies gautų hmMSC ląstelėse buvo sumažėjęs acetilintų baltymų, MMP, NAD^+ kiekis ir redokso pajėgumas, palyginti su sveikomis hmMSC. Gydymas HDAC inhibitoriumi SAHA pagerino acetilinimą ir MMP tiek sveikose, tiek patologinėse ląstelėse, o patologinėse hmMSC padidėjo labiau, o tai rodo sutrikusius NAD^+ signalo perdavimo kelius.

Tyrime efektyviai panaudota SECM redokso potencialo skirtumams apibūdinti, parodant jos gebėjimą neinvaziškai stebėti redokso būsenas ir biocheminį aktyvumą širdies kamieninėse ląstelėse, tokiu būdu palaikant galimas terapines intervencijas širdies regeneracijai.

Polipirolu modifikuotų mielių elektrinės charakteristikos žymiai padidėjo, srovės tankiui padidėjus nuo maždaug 3,76 iki 5,01 mA/cm^2. Kai buvo naudojamas ir polipirolas, ir AuNP, buferiniuose gliukozės tirpaluose galios tankis pasiekė apie 61,1 mW/m^2, viršydamas nemodifikuotų mielių sukuriamą galią (9,2 mW/m^2). Bandymuose su praskiestu nuotekų dumblu modifikuotų mielių MFC pagamino maždaug 179 mW/m^2, o tai patvirtina, kad šie patobulinimai realiomis sąlygomis lėmė didelę energijos gamybą.

Lyginamoji analizė su ankstesne literatūra parodė, kad AuNP įtraukimas žymiai padidino galią, o tai rodo sinergetinį poveikį su polipirolu gerinant krūvio perdavimą. Nors ankstesni tyrimai parodė mažesnį galios tankį panašioms MFC konfigūracijoms, čia pateiktas dvigubos modifikacijos metodas davė santykinį dviejų–trijų kartų našumo pagerėjimą.

Šie rezultatai tiesiogiai susiję su įvade nurodytais tikslais. Uždaviniai buvo įgyvendinti tokiu būdu:

- Elektrocheminiai bandymai parodė, kad SECM veiksmingumas stebint redokso būsenas, skirtas terapinėms intervencijoms žmogaus širdies sveikumo diagnostikos metu, yra pagrįstas (1 tikslas).
- Polipirolo nusodinimas *S. cerevisiae* ląstelės sienelės-membranos tarpsluoksnyje pagerina MFC elektronų perdavimo efektyvumą (2 tikslas).
- Aukso nanodalelių integravimas į mielių tirpalą prieš dengiant anodą pagerina MFC krūvio perdavimo efektyvumą (3 tikslas).

- Modifikuotas MFC, išbandytas su tikru nuotekų dumblu (4 tikslas).

Kiekviena pradžioje iškelta hipotezė buvo patvirtinta: buvo patikrintas ir patvirtintas SECM gebėjimas diferencijuoti sveikas ir patologines širdies kamienines ląsteles elektrocheminiais metodais; mielių ląstelių modifikacijos pagerino elektronų srautą ir galią, o sukonstruota MFC testuota bei įvertinta kaip veikianti su nuotekų dumblu.

Galop disertacijoje daroma išvada, kad SECM yra vertinga priemonė tiriant ląstelės vidinę redokso dinamiką, ir pabrėžiama reikšminga mielių pagrindu sukurtos MFC technologijos pažanga, skatinanti tvarų mikrobų populiacijų gyvybingumą ir kartu pasiekianti praktinį pritaikymą. Būsimos tyrimų kryptys siūlo ištirti platesnes SECM galimybes regeneracinėje medicinoje, didinti MFC naudojimą nuolatinio srauto reaktoriams, gerinti medžiagų sąnaudų efektyvumą, siekti genetinių mielių patobulinimų ir integruoti MFC į tvarius energijos sprendimus. Šios bendros įžvalgos atveria kelią tolesnėms tarpdisciplininėms pastangoms, būtinoms kuriant keičiamo mastelio ir ekologiškas bioelektrochemines sistemas.

8. ARTIFICIAL INTELIGENCE USAGE DECLARATION

I hereby declare that the information provided below is accurate and complete to the best of my knowledge. I understand that transparency in the use of AI tools is essential for research integrity.

During the preparation of this work, the author used OpenAI ChatGPT, Quillbot and Grammarly programs and sites for English Language Editing / Grammar / Style proofing.

The author subsequently reviewed and edited all content and take full responsibility for the published work's content.

9. CURRICULUM VITAE

Education and Qualification:

2020 y. – now:	VMTI FTMC, Vilnius, doctoral studies, Electrochemical technology department. Work with Scanning ElectroChemical Microscopy (SECM) and yeast-graphite biofuel cell modification. Obtained knowledge about galvanostatic and potentiostatic measurement techniques, as well as impedance spectrometry, and used that on microbial fuel cells and other biomaterials, such as human stem cells.
2015 y. – 2018 y.:	Chemistry at Faculty of Chemistry in Vilnius University, master studies, Polymer Chemistry Department, thesis in protein chromatography. Obtained knowledge about HPLC and sorbents used in soluble wheat protein purification.
2011 y. – 2015 y.:	Nanomaterial chemistry at Faculty of Chemistry in Vilnius University, bachelor studies, Organic Chemistry Department, thesis in synthesis of pyrrole pyrimidines. Obtained knowledge of the basic laboratory environment management.
2007 y. – 2011 y.	Secondary education at Pakruojis "Atžalynas" Gymnasium, Šiauliai region.

Additional Education:

2023 y. a. – 2024 y. spr.	Incubation and Acceleration program with Baltic Sandbox Ventures (BSV) as "#hitEnergy" founder. Gathered a group of enthusiast scientists, learned how to manage a startup and lead the team. Head: Self and BSV
2023 y. smr. (2 days)	Entrepreneurship workshop with Baltic Sandbox Ventures (BSV), FTMC, Vilnius, Lithuania. 1st place, learned the details about making a startup from my basic idea of doctoral studies. Head: Karolis Stašys.

2022 y. smr. (1 week)	e-Spark: International Summer School on Experimental Electrochemistry, IChF PAS, Warsaw, Poland. Learned about basic and advanced electrochemistry in practical usage. Head: Dr. Wojciech Nogala.
2021 y. a.	Erasmus practice in IChF PAS, Warsaw, Poland. Obtained knowledge about operating scanning electrochemical microscope. Head: Dr. Wojciech Nogala.
2014 y. smr. – 2014 y. a.:	An intern at Laboratory of Organic Synthesis at VMTI FTMC, Department of Organic Chemistry. Obtained knowledge about benzylation of polyethylene glycols and modification of perylene compounds. Head: Dr. Habil. proc. Linas Labanauskas, tutor: Dr. Jurgis Sūdžius.
2013 y. – 2015 y.:	Organometallic chemistry laboratory at Department of Organic Chemistry. Obtained knowledge about synthesis of fluorescent compounds of pyrrole[2,3-d]pyrimidine and acquired knowledge about Stille and Sonogashira cross coupling reactions. Head: Prof. Dr. Habil. Sigitas Tumkevičius, tutor: Dr. Jonas Bucevičius.
2006 y. – 2011 y.:	Mathematics and Informatics School at Šiauliai University, Department of Social Sciences. Learned the major part of my computer skills and improved my mathematical competences.
Volunteering:	
2015 y. a.:	An intern at AB "Amilina" (http://www.amilina.com/) Learned about purification techniques in production scale.
2011 y. – 2015 y.:	Chemists Students' Club "LP", member of Scientific Student Fellowship subunit and help in students' representation.

Contributed in Chemists' Days arrangement for 4 years, learned the basics of event establishment and improved my communicating skills.

10. ATTENDANCE

The results obtained during the doctoral studies were presented at the following scientific conferences, including international ones:

1) Conference “Open Readings 2021”, Vilnius “Microbial biofuel cell based on baker’s yeast treated by 9, 10-phenanthrenequinone”, Timas Merkelis; Kasparas Kižys; Antanas Zinovičius; Justė Rožėnė; Inga Morkvėnaitė-Vilkončienė; Arūnas Ramanavičius, 2021-03-16, attended virtually.
2) “23rd Advanced Materials and Technologies”, conference-school, Palanga “Using of polypyrrole-modified graphite electrode as biofuel cell anode”, Kasparas Kižys; Joris Juška; Inga Morkvėnaitė-Vilkončienė, 2021-08-27, poster presentation.
3) Conference “Open Readings 2022”, Vilnius “Electrochemical imaging of saccharomyces cerevisiae by scanning electrochemical microscopy”, Kasparas Kižys, 2022-03-15, attended virtually, oral presentation.
4) “24th Advanced Materials and Technologies”, conference-school, Palanga “Electrochemical studies of modified Saccharomyces cerevisiae”, Kasparas Kižys; Wojciech Nogala; Inga Morkvėnaitė-Vilkončienė, 2022-08-26, poster presentation.
5) FTMC conference for PhD students, Vilnius “Studies of stem cells by scanning electrochemical microscopy”, Kasparas Kižys, 2022-10-19, attended virtually, oral presentation.
6) Conference “Open Readings 2023”, Vilnius “Imaging Of Glucose Oxidase Activity By Scanning Electrochemical Microscopy”, Tomas Mockaitis; Wojciech Nogala; Agnė Boguševičė; Kasparas Kižys; Inga Morkvėnaitė-Vilkončienė, 2023-04-21, FTMC, poster presentation.
7) Conference “74th Annual Meeting of International Society of Electrochemistry”, France, Lyon “Human Myocardium-Derived Mesenchymal Stem/Stromal Cells Investigation by Scanning Electrochemical Microscopy”, Kasparas Kizys; Inga Morkvenaite-Vilkonciene; Jurate Petroniene; Antanas Zinovicius; Daiva Bironaite; Rokas Miksiunas; Arunas Ramanavicius, 2023-09-04, poster presentation.
8) Exhibition “LifeSciencesBaltics”, Vilnius, Litexpo, FTMC developed scaled-up microbial fuel cell presented, participated in StartupPitchBattle, won the main prize for investment in the idea, Kasparas Kižys, Pamela Rivera, 2023-09-21, oral presentation.

Conferences where the doctoral student was a co-author:

1) Conference “Open Readings 2021”, Vilnius “Microbial biofuel cell based on baker’s yeast treated by 9, 10-phenanthrenequinone”, Timas Merkelis; Kasparas Kižys; Antanas Zinovičius; Justė Rožėnė; Inga Morkvėnaitė-Vilkončienė; Arūnas Ramanavičius, 2021-03-16, attended virtually.
2) “23rd Advanced Materials and Technologies”, conference-school, Palanga “Using of polypyrrole-modified graphite electrode as biofuel cell anode”, Kasparas Kižys; Joris Juška; Inga Morkvėnaitė-Vilkončienė, 2021-08-27, poster presentation.
3) “24th Advanced Materials and Technologies”, conference-school, Palanga “Electrochemical studies of modified Saccharomyces cerevisiae”, Kasparas Kižys; Wojciech Nogala; Inga Morkvėnaitė-Vilkončienė, 2022-08-26, poster presentation.
4) Conference “Open Readings 2023”, Vilnius “Imaging Of Glucose Oxidase Activity By Scanning Electrochemical Microscopy”, Tomas Mockaitis; Wojciech Nogala; Agnė Boguševičė; Kasparas Kižys; Inga Morkvėnaitė-Vilkončienė, 2023-04-21, FTMC, poster presentation.
5) Conference “74th Annual Meeting of International Society of Electrochemistry”, France, Lyon “Human Myocardium-Derived Mesenchymal Stem/Stromal Cells Investigation by Scanning Electrochemical Microscopy”, Kasparas Kizys; Inga Morkvenaite-Vilkonciene; Jurate Petroniene; Antanas Zinovicius; Daiva Bironaite; Rokas Miksiunas; Arunas Ramanavicius, 2023-09-04, poster presentation.
6) Conference “Open Readings 2024”, Vilnius “Polypyrrole-modified saccharomyces cerevisiae used in microbial fuel cell”, Domas Pirštelis; Kasparas Kižys; Inga Morkvėnaitė-Vilkončienė, 2024-04-23-26, poster presentation.

Internships in which the doctoral student participated:

1) Erasmus internship in Poland, Warsaw, PAS IFCh institute, 2021-10-04 – 2021-12-18.
2) eSPARK International Summer School on Experimental Electrochemistry, 2022-06-11, Warsaw, Poland.
3) 23rd and 24th Advanced Materials and Technologies, conference-school, 2021-08-27 and 2022-08-26, Palanga, Lithuania.

11. ACKOWLEDGEMENTS

I would like to deliver my sincere “thank you” to my supervisor and friend, dr. Inga Morkvėnaitė-Vilkončienė – without your call for these studies, such a friendship and such a dissertation would have reached daylight. Thank you, Aistė, my fiancé, for the dedication all the way to the finish line. Thank you, Domas Pirštelis, for your time and effort to help this happen – I believe this dissertation made us friends for a long time. Thank you, Antanas Zinovičius, for being a wonderful expert and collegue in the electrochemical field – without your wisdom this could have been a very long and tiring achievement. And my biggest sympathy goes to the laboratory environment, delivered by all the colleagues I have met there day by day – I am glad we have the opportunity to work together.

For the work gadgets and biomes, I would like to thank FTMC and Vilnius Tech collaborative Bioelectrochemical Technology laboratory from Nanotechnology department. For this I need to deliver a “thank you” for two Arūnas – dr. habil. Ramanavičius and dr. Stirkė – without your encouragement the dissertation would not have such a heart inspiring topic.

Also, thank you, the members of the defense committee and the reviewers. I hope this document had made you enjoy your time while reading about the exciting world of microbial fuel cells and scanning electrochemical microscopy.

And the last big thank you goes to Innovation department, dr. Karolis Stašys and Mantas Skaržinskas – your efforts to keep me on topic and even spread it nationally was driving me forward through all the journeys.

Thank you, friends, colleagues, loves and companions. I hope this dissertation will brighten your research and the upcoming days.

biosensors

MDPI

Review

Microbial Biofuel Cells: Fundamental Principles, Development and Recent Obstacles

Kasparas Kižys [1], Antanas Zinovičius [1,2], Baltramiejus Jakštys [3], Ingrida Bružaitė [1,4], Evaldas Balčiūnas [1], Milda Petrulevičienė [1], Arūnas Ramanavičius [1,5] and Inga Morkvėnaitė-Vilkončienė [1,2,*]

[1] Laboratory of Electrochemical Energy Conversion, State Research Institute Centre for Physical Sciences and Technology, Saulėtekio Ave. 3, LT-10257 Vilnius, Lithuania
[2] Faculty of Mechanics, Vilnius Gediminas Technical University, LT-10223 Vilnius, Lithuania
[3] Faculty of Natural Sciences, Vytautas Magnus University, LT-44248 Kaunas, Lithuania
[4] Faculty of Fundamental Sciences, Vilnius Gediminas Technical University, LT-10223 Vilnius, Lithuania
[5] Faculty of Chemistry and Geosciences, Vilnius University, LT-01513 Vilnius, Lithuania
* Correspondence: inga.morkvenaite-vilkonciene@vilniustech.lt; Tel.: +370-683-61345

Abstract: This review focuses on the development of microbial biofuel cells to demonstrate how similar principles apply to the development of bioelectronic devices. The low specificity of microorganism-based amperometric biosensors can be exploited in designing microbial biofuel cells, enabling them to consume a broader range of chemical fuels. Charge transfer efficiency is among the most challenging and critical issues while developing biofuel cells. Nanomaterials and particular redox mediators are exploited to facilitate charge transfer between biomaterials and biofuel cell electrodes. The application of conductive polymers (CPs) can improve the efficiency of biofuel cells while CPs are well-suitable for the immobilization of enzymes, and in some specific circumstances, CPs can facilitate charge transfer. Moreover, biocompatibility is an important issue during the development of implantable biofuel cells. Therefore, biocompatibility-related aspects of conducting polymers with microorganisms are discussed in this review. Ways to modify cell-wall/membrane and to improve charge transfer efficiency and suitability for biofuel cell design are outlined.

Biosensors **2023**, *13*(2), 221; **https://doi.org/10.3390/bios13020221**

biosensors

MDPI

Article

Effect of Gold Nanoparticles in Microbial Fuel Cells Based on Polypyrrole-Modified *Saccharomyces cerevisiae*

Kasparas Kižys, Domas Pirštelis and Inga Morkvėnaitė-Vilkončienė *

Department of Nanotechnology, State Research Institute Center for Physical Sciences and Technology, 02300 Vilnius, Lithuania; kasparas.kizys@ftmc.lt (K.K.); domas.pirstelis@ftmc.lt (D.P.)
* Correspondence: inga.vilkonciene@ftmc.lt; Tel.: +370-68361345

Abstract: Microbial fuel cells (MFCs) are a candidate for green energy sources due to microbes' ability to generate charge in their metabolic processes. The main problem in MFCs is slow charge transfer between microorganisms and electrodes. Several methods to improve charge transfer have been used until now: modification of microorganisms by conductive polymers, use of lipophilic mediators, and conductive nanomaterials. We created an MFC with a graphite anode, covering it with 9,10-phenatrenequinone and polypyrrole-modified *Saccharomyces cerevisiae* with and without 10 nm sphere gold nanoparticles. The MFC was evaluated using cyclic voltammetry and power density measurements. The peak current from cyclic voltammetry measurements increased from 3.76 mA/cm^2 to 5.01 mA/cm^2 with bare and polypyrrole-modified yeast, respectively. The MFC with polypyrrole- and nanoparticle-modified yeast reached a maximum power density of 150 mW/m^2 in PBS with 20 mM Fe(III) and 20 mM glucose, using a load of 10 kΩ. The same MFC with the same load in wastewater reached 179.2 mW/m^2. These results suggest that this MFC configuration can be used to improve charge transfer.

Biosensors **2024**, *14*(12), 572; **https://doi.org/10.3390/bios14120572**

biosensors

MDPI

Article

Polypyrrole-Modified *Saccharomyces cerevisiae* Used in Microbial Fuel Cell

Kasparas Kižys, Domas Pirštelis, Ingrida Bružaitė and Inga Morkvėnaitė *

Department of Nanotechnology, State Research Institute Center for Physical Sciences and Technology, Sauletekio 3, LT-10257 Vilnius, Lithuania
* Correspondence: inga.vilkonciene@ftmc.lt; Tel.: +370-6836-1345

Abstract

Microbial fuel cells (MFCs) are one of the contributors to the novel sustainable energy generation from organic waste. However, the application of MFCs is limited due to the slow charge transfer between cells and electrodes. This problem can be solved by modifying cells with conductive polymers, such as polypyrrole (PPy). We investigated the viability and electroactivity of modified cells at five different pyrrole concentrations, namely 8, 25, 50, 100, and 200 mM. The 100 mM concentration of PPy solution had the highest impact on yeast cells' proliferation and growth, with the CFU/mL of PPy-treated yeast cells being $0.6 \times 10^7 \pm 5 \times 10^{-2}$. The power density of the constructed MFC was evaluated by using an external load. The MFCs were analyzed using cyclic voltammetry (CV) and differential pulse voltammetry (DPV). Although CV results with different pyrrole concentrations were similar, DPV indicated that yeast modification with 50 mM pyrrole resulted in the most significant current density, which may be attributed to an increase in charge transfer due to the conductive properties of polypyrrole. The power density achieved with modified yeast in wastewater, 12 mW/m^2, reached levels similar to those in laboratory solutions, 45 mW/m^2.

Biosensors **2025**, *15*(8), 519; **https://doi.org/10.3390/bios15080519**

Assessment of redox activity of acetyltransferase and histone deacetylase activity in human dilated heart atrium-derived mesenchymal stem/stromal cells by scanning electrochemical microscopy

Rokas Miksiunas[1,2], Daiva Bironaite[1], Antanas Zinovicius[2,3], Kasparas Kizys[2], Katazyna Blazevic[4], Inga Morkvenaite-Vilkonciene[2,5], Sigita Bendinskaite[4], Arunas Ramanavicius[2,4*]

[1]Department of Regenerative medicine, State Research Institute Centre for Innovative Medicine, Vilnius, Lithuania
[2]Department of Nanotechnology, State Research Institute Centre for Physical Sciences and Technology, Vilnius, Lithuania
[3]Department of Mechatronics, Robotics, and Digital Manufacturing, Vilnius Gediminas Technical University, Vilnius, Lithuania
[4] Department of Physical Chemistry, Faculty of Chemistry, Vilnius University, Vilnius, Lithuania
[5]Department of Electrical Engineering, Vilnius Gediminas Technical University, Vilnius, Lithuania
*Corresponding author: Arunas Ramanavicius, e-mail: arunas.ramanavicius@chf.vu.lt, tel. +37060032332

Abstract

In this study, the acetylation level and intracellular redox state of human atrial myocardium-derived mesenchymal stem cells (hmMSCs) were investigated by flow cytometer and scanning electrochemical microscopy (SECM) in feedback mode, using cell impermeable ferrocene monocarboxylic acid (FcCOOH) as a redox mediator. The hmMSCs were isolated from the right atriums of human healthy/not dilated and dilated cardiomyopathy (DCM) hearts. SECM experiments were performed vertically approaching the surface of immobilized hmMSC treated/untreated by class I and II histone deacetylase (HDAC) inhibitor – suberoyl-aniline hydroxamic acid (SAHA). Data demonstrate that DCM cells were larger, had lower levels of acetylated proteins, and decreased intracellular redox capacity compared to the healthy hmMSCs. HDAC inhibitor SAHA improved both cell types' acetylation level and intracellular redox capacities, with a more pronounced effect on healthy hmMSCs. Based on the findings, it was concluded that SECM is a highly effective, noninvasive tool for assessing the intracellular redox activity of hmMSCs. SECM results are comparable with flow cytometry results and enable the distinction of redox levels of healthy and DCM cells, as well as the assessment of the influence of some biologically active compounds.

Upcoming publication, sent and being reviewed since 2025.05.17

NOTES

NOTES

Vilniaus universiteto leidykla
Saulėtekio al. 9, III rūmai, LT-10222 Vilnius
El. p. info@leidykla.vu.lt, www.leidykla.vu.lt
bookshop.vu.lt, journals.vu.lt
Tiražas 12 egz.